1

THE ONE-ELECTRON ATOM

One-electron atoms include the hydrogen atom, He(II), Li(III), Be(IV), and so on. The mass-energy and angular momentum of the electron are constant; this requires that the *equation of motion of the electron*[1] be temporally and spatially harmonic. Thus, the classical wave equation[2] applies and

$$\left[\nabla^2 - \frac{1}{v^2}\frac{\delta^2}{\delta t^2}\right]\rho(r,\theta,\phi,t) = 0 \tag{1.1}$$

where $\rho(r,\theta,\phi,t)$ is the function of the electron in time and space. (In each case, the nucleus contains Z protons and the atom has a net positive charge of $(Z-1)e$.) All forces are central and Special Relativity applies. Thus, the coordinates must be three-dimensional spherically harmonic coordinates plus time. The time, radial, and angular solutions of the wave equation are separable. The motion is time-harmonic with frequency ω_n. To be a harmonic solution of the wave equation in spherical coordinates, the angular functions must be spherical harmonic functions.

THE BOUNDARY CONDITION OF NONRADIATION AND THE RADIAL FUNCTION—THE CONCEPT OF THE "ORBITSPHERE"

A zero of the spacetime Fourier transform of the product function of two spherical harmonic angular functions, a time-harmonic function, and an unknown radial function is sought.

THE BOUNDARY CONDITION

The condition for radiation by a moving charge is derived from Maxwell's equations. To radiate, the spacetime Fourier transform of the current-density function must possess components synchronous with waves traveling at the speed of light [1]. Alternatively,

> *For non-radiative states, the current-density function must not possess spacetime Fourier components that are synchronous with waves traveling at the speed of light.*

---

1 The equation of motion of an extended electron is postulated based on first principles and should not be confused with the energy equation of a point-particle probability density wave such as the Schrödinger equation of quantum mechanics.

2 This is not to be confused with the Schrödinger equation which is not a proper wave equation.

DERIVATION OF THE CONDITION FOR NONRADIATION

The condition for radiation by a moving point charge given by Haus [1] is that its spacetime Fourier transform does possess components that are synchronous with waves traveling at the speed of light. Conversely, it is proposed that the condition for nonradiation by an ensemble of moving point charges that comprises a charge-density function is that its spacetime Fourier transform does NOT possess components that are synchronous with waves traveling at the speed of light. The Haus derivation applies to a moving charge-density function as well because charge obeys superposition. The Haus derivation is summarized below.

The Fourier components of the current produced by the moving charge are derived. The electric field is found from the vector equation in Fourier space (**k**, w-space). The inverse Fourier transform is carried over the magnitude of $\mathbf{k}$. The resulting expression demonstrates that the radiation field is proportional to $\mathbf{J}_\perp(\frac{\omega}{c}\mathbf{n},\omega)$ where $\mathbf{J}_\perp(\mathbf{k},\omega)$ is the spacetime Fourier transform of the current perpendicular to $\mathbf{k}$ and $\mathbf{n} \equiv \frac{\mathbf{k}}{|k|}$. Specifically,

$$\mathbf{E}_\perp(\mathbf{r},\omega)\frac{d\omega}{2\pi} = \frac{c}{2\pi}\int \rho(\omega,\Omega)d\omega d\Omega\sqrt{\frac{\mu_0}{\varepsilon_0}}\mathbf{n}\ X\ \left(\mathbf{n}\ X\ \mathbf{J}_\perp\left(\frac{\omega}{c}\mathbf{n},\omega\right)e^{i\left(\frac{\omega}{c}\right)\mathbf{n}\bullet\mathbf{r}}\right) \tag{1.2}$$

The field $\mathbf{E}_\perp(\mathbf{r},\omega)\frac{d\omega}{2\pi}$ is proportional to $\mathbf{J}_\perp\left(\frac{\omega}{c}\mathbf{n},\omega\right)$, namely, the Fourier component for which $\mathbf{k} = \frac{\omega}{c}$. Factors of ω that multiply the Fourier component of the current are due to the density of modes per unit volume and unit solid angle. An unaccelerated charge does not radiate in free space, not because it experiences no acceleration, but because it has no Fourier component $\mathbf{J}_\perp\left(\frac{\omega}{c}\mathbf{n},\omega\right)$.

DERIVATION OF THE BOUNDARY CONDITION

In general, radial solutions of the Helmholtz wave equation are spherical Bessel functions, Neumann functions, Hankel functions, and associated Laguerre functions. It was found that any radial solution with radial motion results in radiation. Thus, a solution of the two-dimensional wave equation plus time is the proper stable, nonradiative equation of motion of the bound electron. The corresponding radial function is the radial Dirac delta function. The Dirac delta function defines the elimination of the radial dependence which reduces the number of dimensions of the Helmholtz wave equation from four to three. Then, the solution for the radial electron function which satisfies the boundary condition is a delta function in spherical coordinates—a spherical shell [2]

$$f(r) = \frac{1}{r^2}\delta(r - r_n) \tag{1.3}$$

where r_n is an allowed radius. This function defines the charge density on a spherical shell of a fixed radius, not yet determined, and Eq. (1.1) becomes the two-dimensional wave equation plus time with separable time and angular functions. Given time harmonic motion with angular

velocity, ω, and a radial delta function, the relationship between an allowed radius and the electron wavelength is given by

$$2\pi r_n = \lambda_n \tag{1.4}$$

where the integer subscript n here and in Eq. (1.3) is *determined during photon absorption* as given in the Excited States of the One-Electron Atom (Quantization) section. It is shown in this section that the force balance between the electric fields of the electron and proton plus any resonantly absorbed photons gives the result that $r_n = nr_1$ wherein n is an integer in an excited state.

The Fourier transform of the radial Dirac delta function is a sinc function. Consider the radial wave vector of the sinc function when the radial projection of the velocity is c where Eq. (1.4) applies. In this case, the relativistically corrected wavelength is

$$\lambda = r \tag{1.5}$$

Substitution of Eq. (1.5) into the sinc function results in the vanishing of the entire Fourier transform of the current-density function.

SPACETIME FOURIER TRANSFORM OF THE ELECTRON FUNCTION

The electron charge-density (mass-density) function is the product of a radial delta function ($f(r) = \frac{1}{r^2}\delta(r - r_n)$), two angular functions (spherical harmonic functions), and a time-harmonic function. The spacetime Fourier transform in three dimensions in spherical coordinates plus time is given [3, 4] as follows:

$$M(s,\Theta,\Phi,\omega) = \int_0^{\infty}\int_0^{\infty}\int_0^{\pi}\int_0^{2\pi} \rho(r,\theta,\phi,t)\exp(-i2\pi sr[\cos\Theta\cos\theta + \sin\Theta\sin\theta\cos(\phi-\Phi)]) \tag{1.6}$$

$$\exp(-i\omega t)r^2\sin\theta\, dr\, d\theta\, d\phi\, dt$$

With circular symmetry [3]

$$M(s,\Theta,\omega) = 2\pi\int_0^{\infty}\int_0^{\infty}\int_0^{\pi} \rho(r,\theta,t)J_o\left(2\pi sr\sin\Theta\sin\theta\right)\exp\left(-i2\pi sr\cos\Theta\cos\theta\right)r^2\sin\theta\exp\left(-i\omega t\right)dr\,d\theta\,dt \tag{1.7}$$

With spherical symmetry [3],

$$M(s,\omega) = 4\pi\int_0^{\infty}\int_0^{\infty} \rho(r,t)\mathrm{sinc}(2sr)r^2\exp(-i\omega t)dr\,dt \tag{1.8}$$

The solutions of the classical wave equation are separable.

$$\rho(r,\theta,\phi,t) = f(r)g(\theta)h(\phi)k(t) \tag{1.9}$$

The orbitsphere function is separable into a product of functions of independent variables, $r, \theta, \phi,$ and t. The radial function which satisfies the boundary condition is a delta function. The time functions are of the form $e^{i\omega t}$, the angular functions are spherical harmonics, sine or cosine trigonometric functions or sums of these functions, each raised to various powers. The spacetime Fourier transform is derived of the separable variables for the angular space function of $\sin\phi$ and $\sin\theta$. It follows from the spacetime Fourier transform given below that other possible spherical harmonics angular functions give the same form of result as the transform of

$\sin\theta$ and $\sin\phi$. Using Eq. (1.8), $F(s)$, the space Fourier transform of $f(r)=\delta(r-r_n)$ is given as follows:

$$F(s)=4\pi\int_0^\infty \frac{1}{r^2}\delta(r-r_n)\mathrm{sinc}(2sr)r^2dr \tag{1.10}$$

$$F(s)=4\pi\mathrm{sinc}(2sr_n) \tag{1.11}$$

The subscript n is used hereafter; however, the quantization condition appears in the Excited States of the One-Electron Atom (Quantization) section. Quantization arises as "allowed" solutions of the wave equation corresponding to a resonance between the electron and a photon.

Using Eq. (1.7), $G(s,\Theta)$, the space Fourier transform of $g(\theta)=\sin\theta$ is given as follows where there is no dependence on ϕ:

$$G(s,\Theta)=2\pi\int_0^\infty\int_0^\pi \sin\theta J_o\left(2\pi sr\sin\Theta\sin\theta\right)\exp\left(-i2\pi sr\cos\Theta\cos\theta\right)\sin\theta r^2d\theta dr \tag{1.12}$$

$$G(s,\Theta)=2\pi\int_0^\infty\int_0^\pi r^2\sin^2\theta J_o\left(2\pi sr\sin\Theta\sin\theta\right)\cos\left(2\pi sr\cos\Theta\cos\theta\right)d\theta dr \tag{1.13}$$

From Luke [5] and [6]:

$$J_\upsilon(z)=\left(\frac{1}{2}z\right)^\nu\sum_{n=0}^\infty\frac{(-1)^n\left(\frac{z}{2}\right)^{2n}}{n!\Gamma(\nu+n+1)}=\left(\frac{1}{2}z\right)^\nu\sum_{n=0}^\infty\frac{(-1)^n\left(\frac{z}{2}\right)^{2n}}{n!(\nu+n)!} \tag{1.14}$$

Let

$$Z=2\pi sr\sin\Theta\sin\theta \tag{1.15}$$

With substitution of Eqs. (1.15) and (1.14) into Eq. (1.13),

$$G(s,\Theta)=2\pi\int_0^\infty\int_0^\pi r^2\sin^2\theta\left[\sum_{n=0}^\infty\frac{(-1)^n\left(\pi sr\sin\Theta\sin\theta\right)^{2n}}{n!n!}\right]\cos(2\pi sr\cos\Theta\cos\theta)d\theta dr \tag{1.16}$$

$$G(s,\Theta)=2\pi\int_0^\infty r^2\int_0^\pi\sum_{n=0}^\infty\frac{(-1)^n\left(\pi sr\sin\Theta\right)^{2n}}{n!n!}\sin^{2(n+1)}\theta\cos\left(2\pi sr\cos\Theta\cos\theta\right)d\theta dr \tag{1.17}$$

$$G(s,\Theta)=2\pi\int_0^\infty r^2\int_0^\pi\sum_{n=1}^\infty\frac{(-1)^{n-1}\left(\pi sr\sin\Theta\right)^{2(n-1)}}{(n-1)!(n-1)!}\sin^{2n}\theta\cos(2\pi sr\cos\Theta\cos\theta)d\theta dr \tag{1.18}$$

From Luke [7], with Re(u) > $-\frac{1}{2}$:

$$J_\upsilon(z)=\frac{\left(\frac{1}{2}z\right)^\upsilon}{\Gamma\left(\frac{1}{2}\right)\Gamma\left(\upsilon+\frac{1}{2}\right)}\int_0^\pi\cos\left(z\cos\theta\right)\sin^{2\upsilon}\theta d\theta \tag{1.19}$$

Let

$$z=2\pi sr\cos\theta \text{ and } n=\upsilon \tag{1.20}$$

Applying the relationship, the integral of a sum is equal to the sum of the integrals to Eq. (1.18), and transforming Eq. (1.18) into the form of Eq. (1.19) by multiplication by

$$1=\frac{\Gamma\left(\frac{1}{2}\right)\Gamma\left(\upsilon+\frac{1}{2}\right)\left(\pi sr\cos\Theta\right)^{\upsilon}}{\left(\pi sr\cos\Theta\right)^{\upsilon}\Gamma\left(\frac{1}{2}\right)\Gamma\left(\upsilon+\frac{1}{2}\right)} \tag{1.21}$$

and by moving the constant outside of the integral gives:

$$G(s,\Theta)=2\pi\int_0^{\infty}r^2\sum_{\upsilon=1}^{\infty}\int_0^{\pi}\frac{(-1)^{\upsilon-1}\left(\pi r\sin\Theta\right)^{2(\upsilon-1)}}{(\upsilon-1)!(\upsilon-1)!}$$
$$\frac{\Gamma\left(\frac{1}{2}\right)\Gamma\left(\upsilon+\frac{1}{2}\right)\left(\pi sr\cos\Theta\right)^{\upsilon}}{\left(\pi sr\cos\Theta\right)^{\upsilon}\Gamma\left(\frac{1}{2}\right)\Gamma\left(\upsilon+\frac{1}{2}\right)}\sin^{2\upsilon}\theta\cos(2\pi sr\cos\Theta\cos\theta)d\theta dr \tag{1.22}$$

$$G\left(s,\Theta\right)=2\pi\int_0^{\infty}r^2\sum_{\upsilon=1}^{\infty}\frac{(-1)^{\upsilon-1}\left(\pi r\sin\Theta\right)^{2(\upsilon-1)}}{(\upsilon-1)!(\upsilon-1)!}$$

$$\frac{\Gamma\left(\frac{1}{2}\right)\Gamma\left(\upsilon+\frac{1}{2}\right)\left(\pi sr\cos\Theta\right)^{\upsilon}}{\left(\pi sr\cos\Theta\right)^{\upsilon}\Gamma\left(\frac{1}{2}\right)\Gamma\left(\upsilon+\frac{1}{2}\right)}\int_0^{\pi}\sin^{2\upsilon}\theta\cos(2\pi sr\cos\Theta\cos\theta)d\theta dr \tag{1.23}$$

Applying Eq. (1.19),

$$G\left(s,\Theta\right)=2\pi\int_0^{\infty}r^2\sum_{\upsilon=1}^{\infty}\frac{(-1)^{\upsilon-1}\left(\pi r\sin\Theta\right)^{2(\upsilon-1)}}{(\upsilon-1)!(\upsilon-1)!}\frac{\Gamma\left(\frac{1}{2}\right)\Gamma\left(\upsilon+\frac{1}{2}\right)}{\left(\pi sr\cos\Theta\right)^{\upsilon}}J_{\upsilon}\left(2\pi sr\cos\Theta\right)dr \tag{1.24}$$

Using the Hankel transform formula from Bateman [8]:

$$\int_0^{\infty}r^{-\left(\frac{1}{2}\right)}\left(rs\right)^{\left(\frac{1}{2}\right)}J_{\upsilon}\left(rs\right)dr=s^{\left(\frac{1}{2}\right)} \tag{1.25}$$

and the Hankel transform relationship from Bateman [9], the general Eq. (1.31) is derived as follows:

$$f(x)\text{ <=======> }g(y;\upsilon)=\int_0^{\infty}f(x)\left(xy\right)^{\left(\frac{1}{2}\right)}J_{\upsilon}\left(xy\right)dx \tag{1.26}$$

$$x^m f(x),m=0,1,2...\text{ <=======> }y^{\left(\frac{1}{2}-\upsilon\right)}\left(\frac{d}{ydy}\right)^m\left[y^{\left(m+\upsilon-\frac{1}{2}\right)}g(y;m+\upsilon)\right] \tag{1.27}$$

$$\int_0^{\infty}r^{\upsilon}r^{-\left(\frac{1}{2}\right)}\left(rs\right)^{\left(\frac{1}{2}\right)}J_{\upsilon}\left(rs\right)dr=s^{\left(\frac{1}{2}-\upsilon\right)}\left(\frac{d}{sds}\right)^{\upsilon}\left[s^{\left(\upsilon+\upsilon-\frac{1}{2}\right)}s^{\left(\frac{1}{2}\right)}\right] \tag{1.28}$$

$$\int_0^{\infty}r^{\upsilon}s^{\left(\frac{1}{2}\right)}J_{\upsilon}\left(rs\right)dr=\frac{s^{\left(\frac{1}{2}-\upsilon\right)}}{s^{\upsilon}}\left(\frac{d}{ds}\right)^{\upsilon}\left[s^{(2\upsilon)}\right] \tag{1.29}$$

$$\int_0^\infty r^\upsilon s^{\left(\frac{1}{2}\right)} J_\upsilon(rs)dr = s^{\left(\frac{1}{2}-2\upsilon\right)} \frac{2\upsilon!}{(\upsilon-1)!} s^\upsilon = \frac{2\upsilon!}{(\upsilon-1)!} s^{\left(\frac{1}{2}-\upsilon\right)} \tag{1.30}$$

$$\int_0^\infty r^\upsilon s^{-\left(\frac{1}{2}\right)} s^{\left(\frac{1}{2}\right)} J_\upsilon(rs)dr = \frac{2\upsilon!}{(\upsilon-1)!} s^{-\upsilon} \tag{1.31}$$

Collecting the r raised to a power terms, Eq. (1.24) becomes,

$$G(s,\Theta) = 2\pi \sum_{\upsilon=1}^{\infty} \int_0^\infty \frac{(-1)^{\upsilon-1} (\pi \sin\Theta)^{2(\upsilon-1)}}{(\upsilon-1)!(\upsilon-1)!} \frac{\Gamma\left(\frac{1}{2}\right)\Gamma\left(\upsilon+\frac{1}{2}\right)}{(\pi s\cos\Theta)^\upsilon} r^\upsilon J_\upsilon(2\pi sr\cos\Theta)dr \tag{1.32}$$

Let $r = \frac{r'}{2\pi\cos\Theta}$; $dr = \frac{dr'}{2\pi\cos\Theta}$,

$$G(s,\Theta) = 2\pi \sum_{\upsilon=1}^{\infty} \int_0^\infty \frac{(-1)^{\upsilon-1} (\pi \sin\Theta)^{2(\upsilon-1)}}{(\upsilon-1)!(\upsilon-1)!} \frac{\Gamma\left(\frac{1}{2}\right)\Gamma\left(\upsilon+\frac{1}{2}\right)}{(\pi s\cos\Theta)^\upsilon} \frac{r^\upsilon}{(2\pi\cos\Theta)^{\upsilon+1}} J_\upsilon(sr')dr' \tag{1.33}$$

By applying Eq. (1.31), Eq. (1.33) becomes,

$$G(s,\Theta) = 2\pi \sum_{\upsilon=1}^{\infty} \frac{(-1)^{\upsilon-1} (\pi \sin\Theta)^{2(\upsilon-1)}}{(\upsilon-1)!(\upsilon-1)!} \frac{\Gamma\left(\frac{1}{2}\right)\Gamma\left(\upsilon+\frac{1}{2}\right)}{(\pi s\cos\Theta)^\upsilon (2\pi\cos\Theta)^{\upsilon+1}} \frac{2\upsilon!}{(\upsilon-1)!} s^{-\upsilon} \tag{1.34}$$

By collecting power terms of s, Eq. (1.34) becomes,

$$G(s,\Theta) = 2\pi \sum_{\upsilon=1}^{\infty} \frac{(-1)^{\upsilon-1} (\pi \sin\Theta)^{2(\upsilon-1)}}{(\upsilon-1)!(\upsilon-1)!} \frac{\Gamma\left(\frac{1}{2}\right)\Gamma\left(\upsilon+\frac{1}{2}\right)}{(\pi\cos\Theta)^{2\upsilon+1} 2^{\upsilon+1}} \frac{2\upsilon!}{(\upsilon-1)!} s^{-2\upsilon} \tag{1.35}$$

$H(s,\Phi)$, the space Fourier transform of $h(\phi) = \sin\phi$ is given as follows where there is no dependence on θ:

The spectrum of $\sin\phi$ and $\sin\theta$ are equivalent. Applying a change of variable to the Fourier transform of $g(\theta) = \sin\theta$.

θ ======> ϕ implies Θ =======> Φ

Therefore, $\hat{y}$ replaces Θ in Eq. (1.35),

$$H(s,\Phi) = 2\pi \sum_{\upsilon=1}^{\infty} \frac{(-1)^{\upsilon-1} (\pi \sin\Phi)^{2(\upsilon-1)}}{(\upsilon-1)!(\upsilon-1)!} \frac{\Gamma\left(\frac{1}{2}\right)\Gamma\left(\upsilon+\frac{1}{2}\right)}{(\pi\cos\Phi)^{2\upsilon+1} 2^{\upsilon+1}} \frac{2\upsilon!}{(\upsilon-1)!} s^{-2\upsilon} \tag{1.36}$$

The time Fourier transform of $K(t) = \mathrm{Re}\{\exp(i\omega_n t)\}$ where ω_n is the angular frequency is given [4] as follows:

$$\int_0^\infty \cos\omega_n t \exp(-i\omega t)dt = \frac{1}{2\pi}\frac{1}{2}[\delta(\omega-\omega_n) + \delta(\omega+\omega_n)] \tag{1.37}$$

A very important theorem of Fourier analysis states that the Fourier transform of a product is the convolution of the individual Fourier transforms [10]. By applying this theorem, the spacetime Fourier transform of an orbitsphere, $M(s,\Theta,\Phi,\omega)$ is of the following form:

$$M(s,\Theta,\Phi,\omega) = F(s) \otimes G(s,\Theta) \otimes H(s,\Phi) K(\omega) \tag{1.38}$$

Therefore, the spacetime Fourier transform, $M(s,\Theta,\Phi,\omega)$, is the convolution of Eqs. (1.11), (1.35), (1.36), and (1.37).

$$M(s,\Theta,\Phi,\omega) = 4\pi \mathrm{sinc}(2sr_n) \otimes 2\pi \sum_{\upsilon=1}^{\infty} \frac{(-1)^{\upsilon-1}\left(\pi \sin\Theta\right)^{2(\upsilon-1)}}{(\upsilon-1)!(\upsilon-1)!} \frac{\Gamma\left(\frac{1}{2}\right)\Gamma\left(\upsilon+\frac{1}{2}\right)}{\left(\pi\cos\Theta\right)^{2\upsilon+1} 2^{\upsilon+1}} \frac{2\upsilon!}{(\upsilon-1)!} s^{-2\upsilon}$$

$$\otimes 2\pi \sum_{\upsilon=1}^{\infty} \frac{(-1)^{\upsilon-1}\left(\pi \sin\Phi\right)^{2(\upsilon-1)}}{(\upsilon-1)!(\upsilon-1)!} \frac{\Gamma\left(\frac{1}{2}\right)\Gamma\left(\upsilon+\frac{1}{2}\right)}{\left(\pi\cos\Phi\right)^{2\upsilon+1} 2^{\upsilon+1}} \frac{2\upsilon!}{(\upsilon-1)!} s^{-2\upsilon} \frac{1}{4\pi}[\delta(\omega-\omega_n)+\delta(\omega+\omega_n)] \tag{1.39}$$

The condition for nonradiation of a moving charge-density function is that the spacetime Fourier transform of the current-density function must not have waves synchronous with waves traveling at the speed of light, that is synchronous with $\frac{\omega_n}{c}$ or synchronous with $\frac{\omega_n}{c}\sqrt{\frac{\varepsilon}{\varepsilon_o}}$ where $\mathbf{r}$ is the dielectric constant of the medium. The Fourier transform of the charge-density function of the orbitsphere (bubble of radius r) is given by Eq. (1.39). In the case of time-harmonic motion, the current-density function is given by the time derivative of the charge-density function. Thus, the current-density function is given by the product of the constant angular velocity and the charge-density function. The Fourier transform of the current-density function of the orbitsphere is given by the product of the constant angular velocity and Eq. (1.39). Consider the radial and time parts of, $K_{\perp}$, the Fourier transform of the current-density function where the angular transforms are not zero:

$$K(s,\Theta,\Phi,\omega) = 4\pi\omega_n \frac{\sin(2sr_n)}{2sr_n} \otimes 2\pi \sum_{\upsilon=1}^{\infty} \frac{(-1)^{\upsilon-1}\left(\pi \sin\Theta\right)^{2(\upsilon-1)}}{(\upsilon-1)!(\upsilon-1)!} \frac{\Gamma\left(\frac{1}{2}\right)\Gamma\left(\upsilon+\frac{1}{2}\right)}{\left(\pi\cos\Theta\right)^{2\upsilon+1} 2^{\upsilon+1}} \frac{2\upsilon!}{(\upsilon-1)!} s^{-2\upsilon}$$

$$\otimes 2\pi \sum_{\upsilon=1}^{\infty} \frac{(-1)^{\upsilon-1}\left(\pi \sin\Phi\right)^{2(\upsilon-1)}}{(\upsilon-1)!(\upsilon-1)!} \frac{\Gamma\left(\frac{1}{2}\right)\Gamma\left(\upsilon+\frac{1}{2}\right)}{\left(\pi\cos\Phi\right)^{2\upsilon+1} 2^{\upsilon+1}} \frac{2\upsilon!}{(\upsilon-1)!} s^{-2\upsilon} \frac{1}{4\pi}[\delta(\omega-\omega_n)+\delta(\omega+\omega_n)] \tag{1.40}$$

For the case that the current-density function is constant, the delta function of Eq. (1.40) is replaced by a constant. For time harmonic motion, with angular velocity, ω_n, Eq. (1.40) is nonzero only for $\omega = \omega_n$; thus, $-\infty < s < \infty$ becomes finite only for the corresponding wavenumber, s_n. The relationship between the radius and the wavelength is

$$v_n = \lambda_n f_n \tag{1.41}$$

$$v_n = 2\pi r_n f_n = \lambda_n f_n \tag{1.42}$$

$$2\pi r_n = \lambda_n \tag{1.43}$$

The motion on the orbitsphere is angular; however, a radial component exists due to Special

Relativistic effects. Consider the radial wave vector of the sinc function. When the radial projection of the velocity is c

$$\mathbf{s}_n \bullet \mathbf{v}_n = \mathbf{s}_n \bullet \mathbf{c} = \omega_n \tag{1.44}$$

the relativistically corrected wavelength given by Eq. (1.259) is[3]

$$\lambda_n = r_n \tag{1.45}$$

(i.e. the lab frame motion in the angular direction goes to zero as the velocity approaches the speed of light as given by Eq. (24.15)). The charge-density functions in spherical coordinates plus time are given by Eqs. (1.64-1.65). In the case of Eq. (1.64), the wavelength of Eq. (1.44) is independent of θ; whereas, in the case of Eq. (1.65), the wavelength in Eq. (1.44) is a function of $\sin\theta$. Thus, in the latter case, Eq. (1.45) holds wherein the relationship of wavelength and the radius as a function of θ are given by $r_n \sin\theta = \lambda_n \sin\theta$.

---

[3] The special relativistic length contraction relationship observed for a laboratory frame relative to an inertial frame moving at constant rectilinear velocity v in the direction of velocity v is

$$l = l_o \sqrt{1 - \frac{v^2}{c^2}} \tag{1}$$

Consider the distance on a great circle given by

$$\int_0^{2\pi} r d\theta = r\theta \Big|_0^{2\pi} = 2\pi r \tag{2}$$

In a gedanken experiment at a fixed position, the distance undergoes length contraction only in the θ direction as $v \to c$. Thus, as $v \to c$ the distance on a great circle approaches its radius which is the relativistically contracted electron wavelength. In the case of the charge motion, the components must be checked relative to waves traveling at the speed of light. In this case a contracted wavelength arises.

The charge motion may be visualized. From the visualization, the nonradiation condition becomes apparent. At light speed, there can be no motion transverse to the radius. The radial projection of the time harmonic motion of a point charge of a great circle becomes equivalent to a time harmonic oscillator moving along an axis of distance $2r_n$ in the direction of r. In spherical coordinates, the lab frame is at rest at the origin. Relativistic invariance of charge requires that all of the charge of a current loop be projected onto a line in the radial direction. For n=1, ℓ=0, the charge is uniformly distributed. Consider, the radial projection of a point charge on a great circle at $\phi = 0$ and a point charge at $\phi = \pi$. Both points move from opposite ends of a line of length $2r_n$ ($-r_n \le r \le +r_n$) and are at the origin in a quarter of a period which is time $t = \frac{r_n}{2c}$. The points then cross. (The crossing is equivalent to elastic scattering at the origin which results in a momentum reversal for both points.) The points interchange roles and travel to the opposite starting points in a half of a period which is time $t = \frac{2r_n}{2c}$. So, with respect to each position, a point left and a point reappeared in $t = \frac{2r_n}{2c}$. Since $T = \frac{2\pi}{\omega} = \frac{\lambda}{c}$, the wavelength is r_n. This situation applies for any ϕ. In the lab frame, the current is uniform and constant. In the frame synchronous with waves traveling at the speed of light, the motion is equivalent to no net current and no net charge motion. Thus, no radiation is possible.

When all positions of the orbitsphere are considered in the gedanken experiment, it is apparent that the lab-frame electron motion is on a sphere with a radius contracted by the factor 2π. The derivation is given in the Special Relativistic Correction to the Ionization Energies section. With the wavelength in the speed of light frame given by Eq. (1.45), the relativistic invariance of the angular momentum of the electron of $\hbar$ (Eq. (1.57) gives the corresponding electron mass in the mass density as $2\pi m_e$.

The equipotential, uniform or constant charge-density function (Eq. (1.64)) further comprises a current pattern given in the Orbitsphere Equation of Motion for $\ell = 0$ section and corresponds to the spin function of the electron. It also corresponds to the nonradiative $n = 1$, $\ell = 0$ state of atomic hydrogen. There is acceleration without radiation. In this case, centripetal acceleration. A static charge distribution exists even though each point on the surface is accelerating along a great circle. Haus' condition predicts no radiation for the entire ensemble.

In cases of orbitals of heavier elements and excited states of one-electron atoms and atoms or ions of heavier elements which are not constant as given by Eq. (1.65), the constant spin function is modulated by a time and spherical harmonic function. The modulation or traveling charge-density wave corresponds to an orbital angular momentum in addition to a spin angular momentum. These states are typically referred to as p, d, f, etc. orbitals and correspond to an $\hbar$ quantum number not equal to zero. Haus' condition also predicts nonradiation for a constant spin function modulated by a time and spherically harmonic orbital function. However, in the case that such a state arises as an excited state by photon absorption, it is radiative due to a radial dipole term in its current-density function since it possesses spacetime Fourier transform components synchronous with waves traveling at the speed of light as given in the Instability of Excited States section.

Substitution of Eq. (1.45) into the sinc function results in the vanishing of the entire Fourier transform of the current-density function. Thus, spacetime harmonics of $\frac{\omega_n}{c} = k$ or $\frac{\omega_n}{c}\sqrt{\frac{\varepsilon}{\varepsilon_o}} = k$ do not exist for which the Fourier transform of the current-density function is nonzero. Radiation due to charge motion does not occur in any medium when this boundary condition is met. Note that the boundary condition for the solution of the radial function of the hydrogen atom with the Schrödinger equation is $\Psi \to 0$ as $r \to \infty$. Here, however, the boundary condition is derived from Maxwell's equations: For non-radiative states, the current-density function must not possess spacetime Fourier components that are synchronous with waves traveling at the speed of light. An alternative derivation which provides acceleration without radiation is given by Abbott [11] Bound electrons are described by a charge-density (mass-density) function which is the product of a radial delta function, Eq. (1.3), two angular functions (spherical harmonic functions), and a time harmonic function. This is a solution of the classical wave equation. This radial function implies that allowed states are two-dimensional spherical shell (zero thickness [4]) of charge density (and mass density) at specific radii r_n. Thus, a bound electron is a constant two-dimensional spherical surface of charge (zero thickness, total charge = $-e$, and total mass=$\theta = 0$), called *an electron orbitsphere shown in Figure 1.1, that can exist in a bound state at only specified distances from the nucleus determined by an energy*

---

[4] The orbitsphere has zero thickness, but in order that the speed of light is a constant maximum in any frame including that of the gravitational field that propagates out as a light-wave front at particle production, it gives rise to a spacetime dilation equal to 2π times the Newtonian gravitational or Schwarzschild radius $r_g = \frac{2Gm_e}{c^2} = 1.3525\ X\ 10^{-57}\ m$ according to Eqs. (23.36) and (23.140b) and discussion at the footnote after Eq. (23.40). This corresponds to a spacetime dilation of $8.4980\ X\ 10^{-57}\ m$ or $2.8346\ X\ 10^{-65}\ s$. Although the orbitsphere does not occupy space in the third spatial dimension, its mass discontinuity effectively "displaces" spacetime wherein the spacetime dilation can be considered a "thickness" associated with its gravitational field.

minimum for the n=1 state and integer multiples of this radius due to the action of resonant photons as shown the Determination of Orbitsphere Radii section and the Equation of the Electric Field inside the Orbitsphere section, respectively.

Figure 1.1. A bound electron is a constant two-dimensional spherical surface of charge (zero thickness, total charge = $-e$, and total mass= m_e), called *an electron orbitsphere.* For the n=1 state of the hydrogen atom, the orbitsphere has the Bohr radius of the hydrogen atom, $r = a_H$. It is nonradiative, a minimum-energy surface, and extremely stable in that the balanced forces correspond to a pressure of twenty million atmospheres.

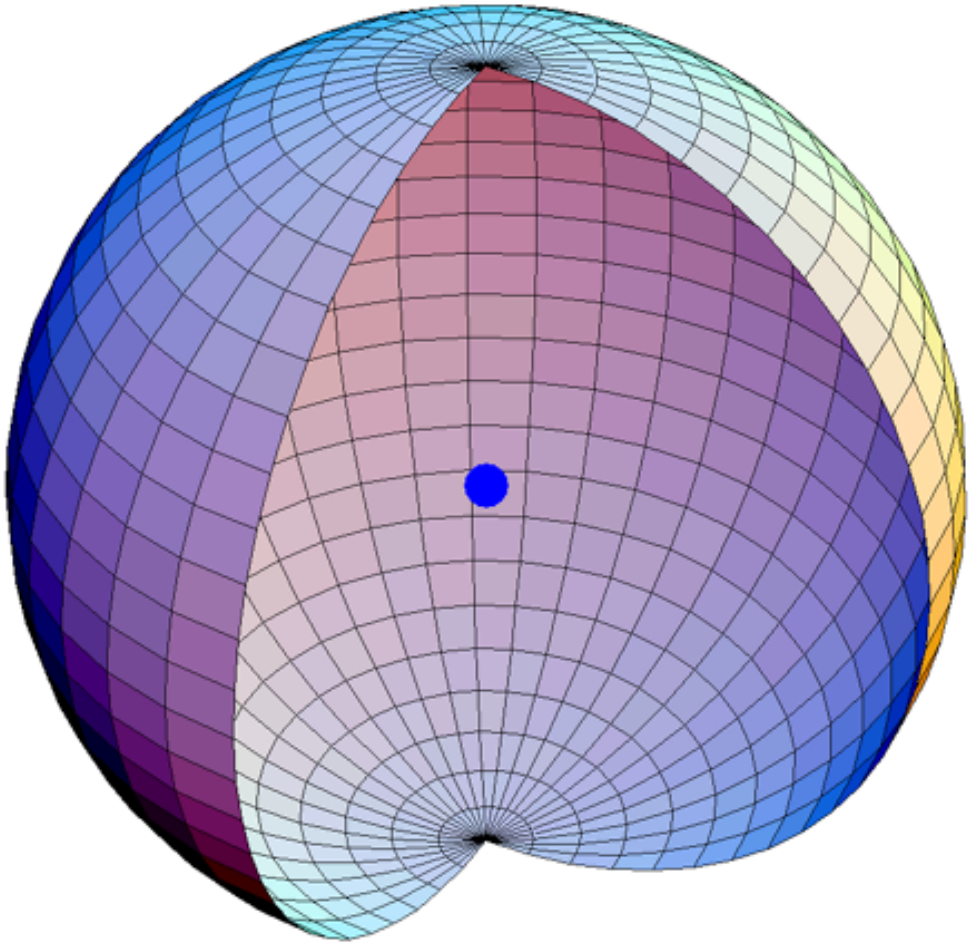

Given time-harmonic motion and a radial delta function, the relationship between an allowed radius and the electron wavelength is given by Eq. (1.43). Using the de Broglie relationship for the electron mass where the coordinates are spherical

$$\lambda_n = \frac{h}{p_n} = \frac{h}{m_e v_n} \tag{1.46}$$

the magnitude of the velocity for *every* point on the orbitsphere is

$$v_n = \frac{\hbar}{m_e r_n} \tag{1.47}$$

THE ANGULAR FUNCTION

By application of the nonradiation constraint, the electron equation of motion is a solution of the wave equation in two dimensions (plus time),wherein the radial function for the electron is a two-dimensional shell of zero thickness as given by Eq. (1.3). Therefore, the angular mass(charge)-density function of the electron, $A(\theta,\phi,t)$, must be a solution of

$$\left[\nabla^2 - \frac{1}{v^2}\frac{\partial^2}{\partial t^2}\right] A(\theta,\phi,t) = 0 \tag{1.48}$$

where $\rho(r,\theta,\phi,t) = f(r)A(\theta,\phi,t) = \frac{1}{r^2}\delta(r-r_n)A(\theta,\phi,t)$ *and* $A(\theta,\phi,t) = Y(\theta,\phi)k(t)$

$$\left[\frac{1}{r^2\sin\theta}\frac{\partial}{\partial\theta}\left(\sin\theta\frac{\partial}{\partial\theta}\right)_{r,\phi} + \frac{1}{r^2\sin^2\theta}\left(\frac{\partial^2}{\partial\phi^2}\right)_{r,\theta} - \frac{1}{v^2}\frac{\partial^2}{\partial t^2}\right] A(\theta,\phi,t) = 0 \tag{1.49}$$

where *v* is the linear velocity of the electron. (It is shown in the Special Relativistic Correction to the Ionization Energies section that the motion is azimuthal to the radius which constitutes an inertial frame that is relativistically invariant.) Conservation of momentum and energy allows the angular functions and time functions to be separated.

$$A(\theta,\phi,t) = Y(\theta,\phi)k(t) \tag{1.50}$$

Charge is conserved as well, and the charge of an electron is superimposable with its mass. That is, the angular mass-density function, $A(\theta,\phi,t)$, is also the angular charge-density function.

The electron orbitsphere experiences a constant potential energy because it is fixed at $r = r_n$. In general, the kinetic energy for an inverse squared electric force is half the potential energy. It is the rotation of the orbitsphere that causes spin angular momentum. The rotational energy of a rotating body, E_{rot}, is

$$E_{rot} = \frac{1}{2} I\omega^2 \tag{1.51}$$

where *I* is the moment of inertia and ω is the angular velocity. The angular velocity must be constant (at a given n) because r is constant and the energy and angular momentum are constant. The allowed angular velocities are related to the allowed frequencies by

$$\omega_n = 2\pi\nu_n \tag{1.52}$$

The allowed frequencies are related to allowed velocities by

$$v_n = \nu_n\lambda_n \tag{1.53}$$

The allowed velocities and angular frequencies are related to r_n by

$$v_n = r_n\omega_n \tag{1.54}$$

$$\omega_n = \frac{\hbar}{m_e r_n^2} \tag{1.55}$$

$$v_n = \frac{\hbar}{m_e r_n} \tag{1.56}$$

The scalar sum of the magnitude of the angular momentum of each infinitesimal point of the

orbitsphere $\mathbf{L}_i$ of mass m_i must be constant. The constant is $\hbar$.

$$\sum |\mathbf{L}_i| = \sum |\mathbf{r} \times m_i \mathbf{v}| = m_e r_n \frac{\hbar}{m_e r_n} = \hbar \tag{1.57}$$

where the velocity is given by Eq. (1.47). In the limit, the sum is replaced by a continuous integral over the surface wherein the point element masses and angular momenta are replaced by the corresponding densities. The integral of the magnitude of the angular momentum of the electron is $\hbar$ in any inertial frame and is ***relativistically invariant***. The vector projections of the orbitsphere spin angular momentum relative to the Cartesian coordinates are given in the Spin Angular Momentum of the Orbitsphere with $\ell = 0$ section.

In the case of an excited state, the charge-density function of the electron orbitsphere can be modulated by the corresponding "trapped" photon to give rise to orbital angular momentum about the z-axis. The "trapped photon" is a "standing electromagnetic wave" which actually is a circulating wave that propagates around the z-axis. Its source current superimposes with each great circle current-density element ("current loop") of the orbitsphere. In order to satisfy the boundary (phase) condition at the orbitsphere surface, the angular and time functions of the photon must match those of its source current which modulates the orbitsphere charge-density function as given in the Equation of the Electric Field Inside the Orbitsphere section. The time-function factor, *k(t)*, for the photon "standing wave" is identical to the time-function factor of the orbitsphere. Thus, the angular frequency of the "trapped photon" has to be identical to the angular frequency of the electron orbitsphere, ω_n given by Eq. (1.55). However, the linear velocity of the modulation component is not given by Eq. (1.54)—the orbital angular frequency is with respect to the z-axis; thus, the distance from the z-axis must be substituted for the orbitsphere radius of Eq. (1.54). The vector projections of the orbital angular momentum and the spin angular momentum of the orbitsphere are given in the Rotational Parameters of the Electron (Angular Momentum, Rotational Energy, and Moment of Inertia) section. Eq. (1.49) becomes

$$-\frac{\hbar^2}{2I}\left[\frac{1}{\sin\theta}\frac{\partial}{\partial\theta}\left(\sin\theta\frac{\partial}{\partial\theta}\right)_{r,\phi} + \frac{1}{\sin^2\theta}\left(\frac{\partial^2}{\partial\phi^2}\right)_{r,\theta}\right] A(\theta,\phi,t) = E_{rot} A(\theta,\phi,t) \tag{1.58}$$

The spacetime angular function, $A(\theta,\phi,t)$, is separated into an angular and a time function, $Y(\theta,\phi)k(t)$. The solution of the time harmonic function is $k(t) = e^{i\omega_n t}$. When the time harmonic function is eliminated,

$$-\frac{\hbar^2}{2I}\left[\frac{1}{\sin\theta}\frac{\partial}{\partial\theta}\left(\sin\theta\frac{\partial}{\partial\theta}\right)_{r,\phi} + \frac{1}{\sin^2\theta}\left(\frac{\partial^2}{\partial\phi^2}\right)_{r,\theta}\right] Y(\theta,\phi) = E_{rot} Y(\theta,\phi) \tag{1.59}$$

Eq. (1.59) is the equation for the rigid rotor. The angular function can be separated into a function of θ and a function of ϕ and the solutions are well known [12]. The energies are given by

$$E_{rot} = \frac{\hbar^2 \ell(\ell+1)}{2I} \quad \ell = 0,1,2,3,..., \tag{1.60}$$

where the moment of inertia, I, is derived in the Rotational Parameters of the Electron (Angular Momentum, Rotational Energy, and Moment of Inertia) section. The angular functions are the spherical harmonics, $Y_\ell^m(\theta,\phi) = P_\ell^m(\cos\theta)e^{im\phi}$. The spherical harmonic $Y_0^0(\theta,\phi) = 1$ is also a solution. The real parts of the spherical harmonics vary between -1 and 1. But the mass of the electron cannot be negative; and the charge cannot be positive. Thus, to insure that the function

is positive definite, the form of the angular solution must be a superposition:

$$Y_0^0(\theta,\phi)+Y_\ell^m(\theta,\phi) \tag{1.61}$$

(Note that $Y_\ell^m(\theta,\phi)=P_\ell^m(\cos\theta)e^{im\phi}$ are not normalized here as given by Eq. (3.53) of Jackson [13]; however, it is implicit that the magnitude is made to satisfy the boundary condition that the function is positive definite and Eq. (1.63) is satisfied.) $Y_0^0(\theta,\phi)$ is called the angular spin function corresponding to the quantum numbers $s=\frac{1}{2}$; $m_s=\pm\frac{1}{2}$ as given in the Spin Angular Momentum of the Orbitsphere with $\ell=0$ section. $Y_\ell^m(\theta,\phi)$ is called the angular orbital function corresponding to the quantum numbers $\ell=0, 1, 2, 3, 4,...$; $m_\ell = -\ell, -\ell+1, ..., 0, ..., +\ell$. 2π can be thought of as a modulation function. The charge density of the entire orbitsphere is the total charge divided by the total area, $\frac{-e}{4\pi r_n^2}$. The fraction of the charge of an electron in any area element is given by

$$N\left[Y_0^0(\theta,\phi)+Y_\ell^m(\theta,\phi)\right]r_n^2\sin\theta d\theta d\phi, \tag{1.62}$$

where N is the normalization constant. Therefore, the normalization constant is given by

$$-e=Nr_n^2\int_0^{\pi}\int_0^{2\pi}\left[Y_0^0(\theta,\phi)+Y_\ell^m(\theta,\phi)\right]\sin\theta d\theta d\phi \tag{1.63}$$

For $\ell=0$, $N=\frac{-e}{8\pi r_n^2}$. For $\ell\neq 0$, $N=\frac{-e}{4\pi r_n^2}$. The charge-density functions including the time-function factor are

$\ell=\mathbf{0}$

$$\rho(r,\theta,\phi,t)=\frac{e}{8\pi r^2}[\delta(r-r_n)]\left[Y_0^0(\theta,\phi)+Y_\ell^m(\theta,\phi)\right] \tag{1.64}$$

$\ell\neq\mathbf{0}$

$$\rho(r,\theta,\phi,t)=\frac{e}{4\pi r^2}[\delta(r-r_n)]\left[Y_0^0(\theta,\phi)+\mathrm{Re}\left\{Y_\ell^m(\theta,\phi)\left[1+e^{i\omega_n t}\right]\right\}\right] \tag{1.65a}$$

$$\rho(r,\theta,\phi,t)=\frac{e}{4\pi r^2}[\delta(r-r_n)]\left[Y_0^0(\theta,\phi)+\mathrm{Re}\left\{Y_\ell^m(\theta,\phi)e^{i\omega_n t}\right\}\right] \tag{1.65b}$$

where

$\mathrm{Re}\left\{Y_\ell^m(\theta,\phi)\left[1+e^{i\omega_n t}\right]\right\}=\mathrm{Re}\left[Y_\ell^m(\theta,\phi)+Y_\ell^m(\theta,\phi)e^{i\omega_n t}\right]=P_\ell^m(\cos\theta)\cos m\phi+P_\ell^m(\cos\theta)\cos\left(m\phi+\omega_n' t\right)$ or $\mathrm{Re}\left\{Y_\ell^m(\theta,\phi)e^{i\omega_n t}\right\}=P_\ell^m(\cos\theta)\cos\left(m\phi+\omega_n' t\right)$ and to keep the form of the spherical harmonic as a traveling wave about the z-axis, $\omega_n'=m\omega_n$ [5]. In the cases that $m\neq 0$, Eq. (1.65) represents a

---

[5] In Eq. (1.65a), $Y_0^0(\theta,\phi)$, a constant function, is added to a spherical harmonic function times $\left[1+e^{i\omega_n t}\right]$. Consider the term $\mathrm{Re}\left\{Y_\ell^m(\theta,\phi)\left[1+e^{i\omega_n t}\right]\right\}$. The first term corresponds to $Y_\ell^m(\theta,\phi)$ times one and has

traveling charge-density wave that moves on the surface of the orbitsphere about the z-axis with frequency ω_n and modulates the orbitsphere corresponding to $\ell = 0$. The latter gives rise to spin angular momentum as given in the Spin Angular Momentum of the Orbitsphere with $\ell = 0$ section. The spin and orbital angular momenta may couple as given in the Orbital and Spin Splitting section. In the cases that $Y_0^0(\phi,\theta) \neq 0$ and θ the charge is moving or rotating about the z-axis with frequency ω_n, but the charge density is not time dependent. The photon equations which correspond to the orbitsphere states, Eqs. (1.64) and (1.65), are given in the Excited States of the One-Electron Atom (Quantization) section. In addition to Haus' condition given by Eqs. (1.44-1.45), the orbitsphere states given by Eqs. (1.64-1.65) are shown to be nonradiative with the same condition as that of Eq. (1.45) applied to the vector potential as shown in Appendix I: Nonradiation Based on the Electromagnetic Fields and the Poynting Power Vector.

For $n = 1$, and $\ell = 0$, $m = 0$, and $s = 1/2$, the charge (and mass) distribution is spherically symmetric and $M_{1,0,0,1/2} = -4.552\ Cm^{-2}$ everywhere on the orbitsphere. Similarly, for $n = 2$, $\ell = 0$, $m = 0$, and $s = 1/2$, the charge distribution everywhere on the sphere is $M_{2,0,0,1/2} = -1.138\ Cm^{-2}$. For $n = 2$, $\ell = 1$, $m = 0$, and $s = 1/2$, the charge distribution varies with $\frac{\hbar}{4}$. $Y_1^0(\phi,\theta)$ is a maximum at $\theta = 0°$ and the charge density is also a maximum at this point, $M_{2,1,0,1/2}(\theta = 0°) = -2.276\ Cm^{-2}$. The charge density decreases as $\mathbf{S}$ increases; a minimum in the charge density is reached at $\theta = 180°$, $M_{2,1,0,1/2}(\theta = 180°) = 0\ Cm^{-2}$.

For $\ell = 1$ and $m = \pm 1$, the spherical harmonics are complex, and the angular functions comprise linear combinations of

$$Y_{1,x} = \sin\theta\cos\phi \tag{1.66}$$

$$Y_{1,y} = \sin\theta\sin\phi \tag{1.67}$$

Each of $Y_{1,x}$ and $Y_{1,y}$ is the component factor part of a phasor. They are not components of a vector; however, the x and y designation corresponds, respectively, to the historical p_x and p_y probability-density functions of quantum mechanics. $Y_{1,x}$ is a maximum at $\theta = 90°$ and $\phi = 0°$; $M_{2,1,x,1/2}(90°,0°) = -1.138\ Cm^{-2}$. Figure 1.2 gives pictorial representation of how the modulation function changes the electron density on the orbitsphere for several ℓ values[6]. Figure 1.3 gives a

---

$\omega_n = 0$; so, $m = 0$ and $\ell = 0$ is selected. This is equivalent to another constant function modulated by the spherical harmonic function (second term) which spins around the z-axis and comprises a traveling modulation wave. One rotation of the spherical harmonic function occurs in one period. Thus, Eq. (1.65a) can be rearranged to represent the electron as a superposition of a pure spin function plus a spin function that is modulated. Or, directly, Eq. (1.65a) represents the sum of a spin function and a modulation function times a time dependent function, $\left[1 + e^{i\omega_n t}\right]$. The latter can be considered a phasor corresponding to the modulation function spinning about the z-axis.

6 When the electron charge appears throughout this text in a function involving a linear combination of the spin and orbital functions, it is implicit that the charge is normalized. A constant times a solution to the wave equation such as a constant times a spherical harmonic function is a solution. The integral of the constant mass-density function corresponding to spin over the orbitsphere is the mass of the electron. The integral of any spherical harmonic modulation function corresponding to orbital angular momentum over the orbitsphere is zero. The modulated mass-density function has a lower limit of zero due to the trapped photon which is phase-locked to the modulation

pictorial representation of the charge-density wave of a p orbital that modulates the constant spin function and rotates around the z-axis. A single time point is shown for $\ell = 1$ and $m = \pm 1$ in Eq. (1.65).

function. And, the mass density can not be negative. Thus, the maximum magnitude of the unnormalized spherical harmonic function over all angles must be one. The summation of the constant function and the orbital function is normalized.

`Figure 1.2` The orbital function modulates the constant (spin) function. (shown for t = 0; three-dimensional view)

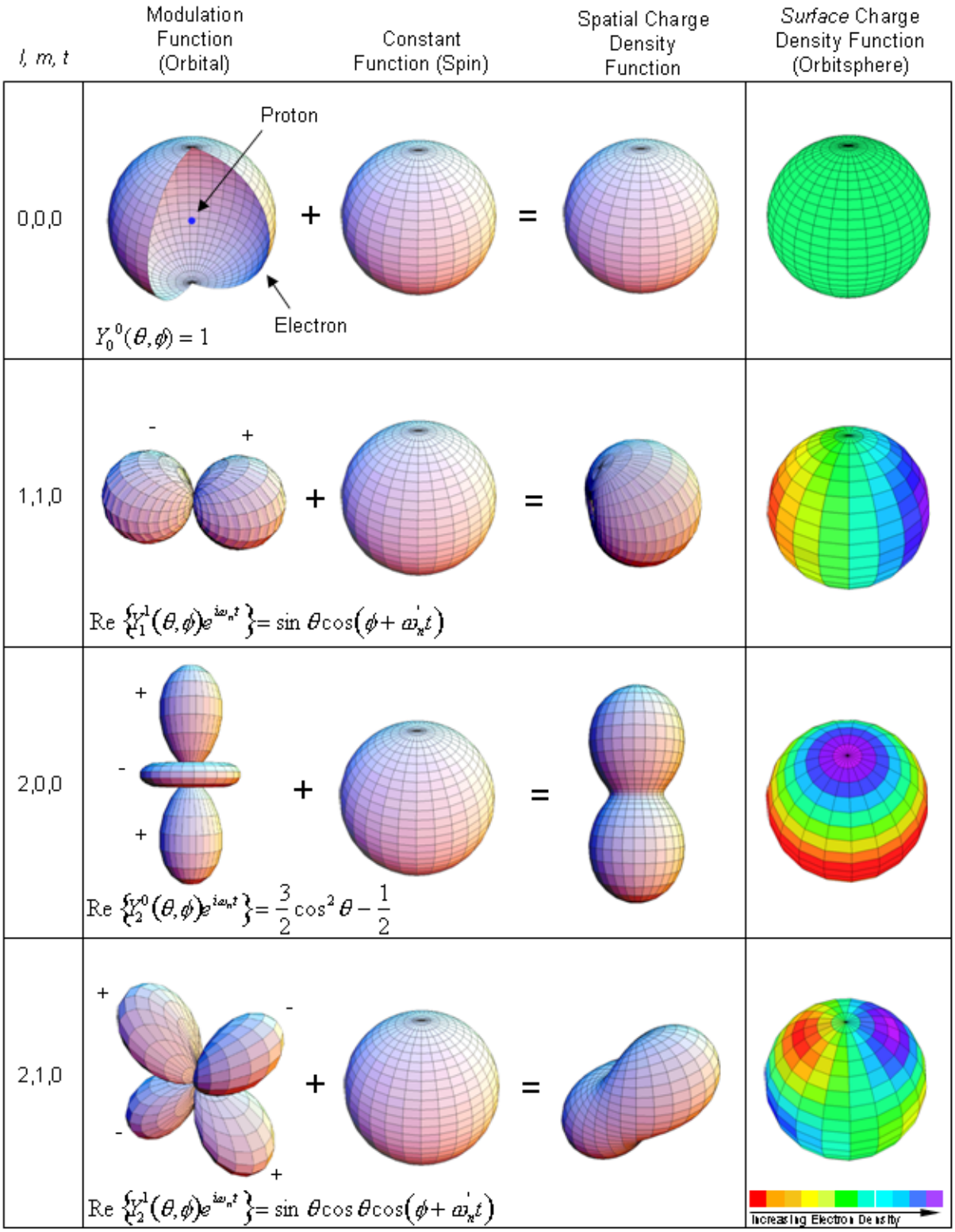

Figure 1.3. A pictorial representation of the charge-density wave of a p orbital that modulates the constant spin function and travels on the surface of the orbitsphere around the z-axis. A single time point is shown for $\ell = 1$ and $m = \pm 1$ in Eq. (1.65). The charge density increases from red to violet. The z-axis is the vertical axis.

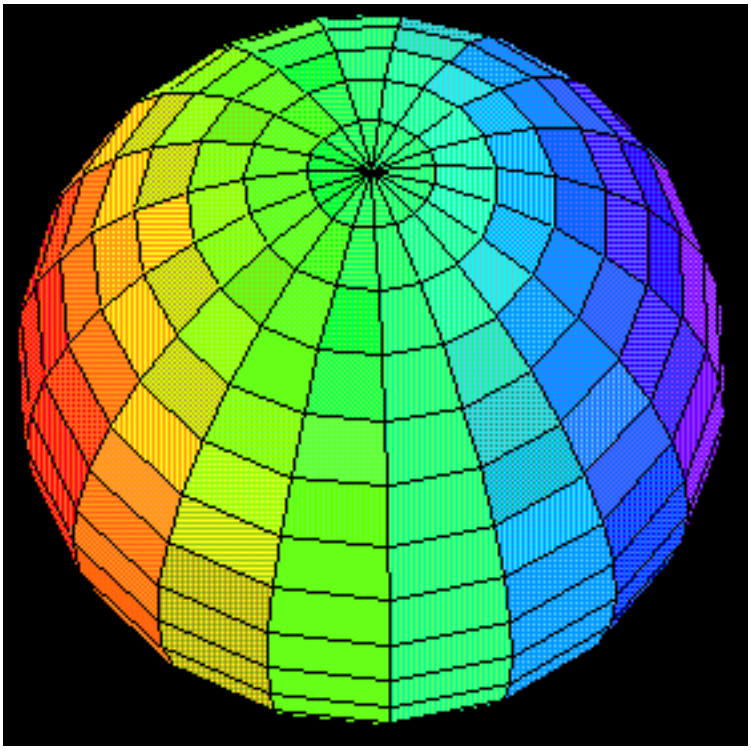

THE ORBITSPHERE EQUATION OF MOTION FOR ℓ = 0 BASED ON THE CURRENT VECTOR FIELD (CVF)

STERN-GERLACH-EXPERIMENT BOUNDARY CONDITIONS

It is known from the Stern-Gerlach experiment that a beam of silver atoms is split into two components when passed through an inhomogeneous magnetic field. This implies that the electron is a spin 1/2 particle with an intrinsic angular momentum in the direction of the applied field (spin axis) of $\pm\frac{\hbar}{2}$, and the magnitude of the angular momentum vector which precesses about the spin axis is $\sqrt{\frac{3}{4}}\hbar$. Furthermore, the magnitude of the splitting implies a magnetic moment of μ_B, a full Bohr magneton, given by Eq. (1.110) corresponding to $\hbar$ of total angular momentum on the axis of the applied field.

The algorithm to generate the spin function designated as $Y_0^0(\theta,\phi)$ (part of Eqs. (1.64-1.64)) and called the electron orbitsphere is developed in this section. It was shown in the Angular Function section that the integral of the magnitude of the angular momentum over the orbitsphere must be constant. The constant is $\hbar$ as given by Eq. (1.57). It is shown in this section that the projection of the intrinsic orbitsphere angular momentum onto the spin axis is

$\pm\frac{\hbar}{2}$, and the projection onto **S**, the axis which precesses about the spin axis, is $\hbar$ with a precessing component in the perpendicular plane of $\sqrt{\frac{3}{4}}\hbar$ and a component on the spin axis of $\pm\frac{\hbar}{2}$. Thus, the mystery of an intrinsic angular momentum of $\pm\frac{\hbar}{2}$ and a total angular momentum in a resonant RF experiment of $\mathbf{L}_z = \hbar$ is resolved since the sum of the intrinsic and spin-axis projection of the precessing component is $\hbar$. The Stern-Gerlach experiment implies a magnetic moment of one Bohr magneton and an associated angular momentum quantum number of 1/2. Historically, this quantum number is called the spin quantum number, s ($s = \frac{1}{2}$; $m_s = \pm\frac{1}{2}$), and that designation is maintained.

The electron has a measured magnetic field and corresponding magnetic moment of a Bohr magneton and behaves as a spin 1/2 particle or fermion. For any magnetic field, the solution for the corresponding current from Maxwell's equations is unique. Thus, the electron field requires a unique current according to Maxwell's equations. Several boundary conditions must be satisfied, and the orbitsphere equation of motion for $\ell = 0$ is solved as a boundary value problem. The boundary conditions are:

(1) each infinitesimal point (position) on the orbitsphere comprising a charge- (mass)-density element must have the same angular and linear velocity given by Eqs. (1.55) and (1.56), respectively;

(2) according to condition 1, every such infinitesimal point must move along a great circle and the current-density distribution must be uniform;

(3) the electron magnetic moment must align completely parallel or antiparallel with an applied magnetic field in agreement with the Stern-Gerlach experiment;

(4) according to condition 3, the projection of the intrinsic angular momentum of the orbitsphere onto the z-axis must be $\pm\frac{\hbar}{2}$, and the projection into the transverse plane must be $\pm\frac{\hbar}{4}$ to achieve the spin 1/2 aspect;

(5) the Larmor excitation of the electron in the applied magnetic field must give rise to a component of electron spin angular momentum that precesses about the applied magnetic field such that the contribution along the z-axis is $\pm\frac{\hbar}{2}$ and the projection onto the orthogonal axis which precesses about the z-axis must be $\pm\sqrt{\frac{3}{4}}\hbar$;

(6) due to conditions 4 and 5, the angular momentum components corresponding to the current of the orbitsphere and that due to the Larmor precession must rise to a total angular momentum on the applied-field axis of $\pm\hbar$;

(7) due to condition 6, the precessing electron has a magnetic moment of a Bohr magneton, and

(8) the energy of the transition of the alignment of the magnetic moment with an applied magnetic field must be given by Eqs. (1.205-1.206) wherein the g factor and Bohr magneton factors are due to the extended-nature of the electron such that it links flux in units of the magnetic flux quantum and has a total angular momentum on the applied-field axis of $\pm\hbar$.

Consider the derivation of Eqs. (1.58) and (1.59). The moment of inertia of a point particle orbiting an axis is mr^2, and that of a globe spinning about some axis is $I = \frac{2}{3}mr^2$. For ℓ = 0, the electron mass and charge are uniformly distributed over the orbitsphere, a two-dimensional, spherical shell, but the orbitsphere is *not* analogous to a globe. The velocity of a point mass on a spinning globe is a function of θ, but the magnitude of the velocity at each point of the orbitsphere is not a function of θ. To picture the distinction, it is a useful concept to consider that the orbitsphere is comprised of an infinite number of point elements that move on the spherical surface. Then, each point on the sphere with mass m_i has the same angular velocity, ω_n, the same magnitude of linear velocity, v_n, and the same moment of inertia, $m_i r_n^2$. The motion of each point of the orbitsphere is along a great circle, and the motion along each great circle is correlated with the motion on all other great circles such that the sum of all the contributions of the corresponding angular momenta is different from that of an orbiting point or a globe spinning about an axis. The orbitsphere angular momentum is uniquely directed disproportionately along two orthogonal axes.

The current-density function of the orbitsphere is generated from a basis set current-vector field defined as the orbitsphere current-vector field ("orbitsphere-cvf"). This in turn is generated from *orthogonal great circle current-density elements (one dimensional "current loops")* that serve as basis elements. As given in Appendix III, the *continuous* uniform electron current density function $Y_0^0(\theta,\phi)$ (part of Eqs. (1.64-1.65)) is then exactly generated from this orbitsphere-cvf as a basis element by a convolution operator comprising an autocorrelation-type function. The operator comprises the convolution of each great circle current loop of the orbitsphere-cvf designated as the primary orbitsphere-cvf with a second orbitsphere-cvf basis element designated as the secondary orbitsphere-cvf. Each secondary element is weighted according to the angular momentum of each great circle of a primary orbitsphere-cvf that it replaces by the convolution. The uniform, equipotential charge-density function of the orbitsphere having only a radial discontinuous field at the surface according to Eq. (3) of Appendix IV is constant in time due to the motion of the current along great circles. The current flowing into any given point of the orbitsphere equals the current flowing out to satisfy the current continuity condition, $\nabla \cdot J = 0$.

The current-vector field pattern of the orbitsphere-cvf is not spatially uniform. There is no coincidence or nonuniqueness of elements of the current-vector field. But, there are many

crossings among elements at single points on the two-dimensional surface of the electron, and the density of the crossings is nonuniform over the surface. *Thus, each element of the basis set to generate the current pattern, a great circle current loop, must be one-dimensional so that the crossings are zero-dimensional with no element interaction at their crossing.* (This is a logical and necessary geometric progression for the construction of a fundamental particle which is two-dimensional.) In the limit, the basis set generates a continuous two-dimensional current density with a constant charge (mass) density wherein the crossings have no effect on the vector fields. Each one-dimensional element is independent of the others, and its contribution to the angular momentum and magnetic field independently superimposes with that of the others.

This unique aspect of a fundamental particle has the same properties of the superposition properties of the electric and magnetic fields of a photon. As shown in the Excited States of the One-Electron Atom (Quantization), the Creation of Matter from Energy, Pair Production, and the Leptons sections, the angular momentum in the electric and magnetic fields is conserved in excited states and in the creation of an electron from a photon in agreement with Maxwell's equations. It is useful to regard an electron as a photon frozen in time. The particle-production conditions are given in the latter sections.

Thus, the electron as an indivisible fundamental particle is related to the concepts of current and momentum elements, but the great-circle-current-loop basis elements used in the Generation of the Orbitsphere-cvf in Two Steps section should be considered more fundamentally in terms of sources of electric and magnetic field and sources of momentum that in aggregates give the corresponding properties of the electron as a whole. In fact, as shown in the Gravity section, all physical observables including the laws of nature and the fundamental constants can ultimately only be related to others and have no independent meaning . Then, the basis elements of an electron are understood in terms of what they do. The nomenclature reflects the analogous macroscopic sources and is adopted for convenience.

GENERATION OF THE ORBITSPHERE-CVF IN TWO STEPS

The orbitsphere spin function comprises a constant charge (current) density function with moving charge confined to a two-dimensional spherical shell. The uniform magnetostatic current-density function $Y_0^0(\theta,\phi)$ of the orbitsphere spin function comprises a continuum of correlated orthogonal great circle current loops wherein each point charge (current) density element moves time harmonically with constant angular velocity ω_n given by Eq. (1.55). $Y_0^0(\theta,\phi)$ is generated from a basis set current-vector field defined as the orbitsphere current-vector field ("orbitsphere-cvf"). The current-density of the orbitsphere-cvf is *continuous*, but it may be modeled as a current pattern comprising a superposition of an infinite series of correlated orthogonal great circle current loops. The equation of motion for each charge-density element (and correspondingly for each mass-density element) which gives the current pattern of the orbitsphere-cvf is generated in two steps, STEP ONE and STEP TWO corresponding to two components which are superimposed. The *time-independent* current pattern is obtained by defining a basis set for generating the current distribution over the surface of a spherical shell of zero thickness. As such a basis set, consider that the electron current is evenly distributed within two orthogonally linked great-circle current loops for each STEP to generate each component. The current pattern comprising two components is generated over the surface by the two sets of rotations (STEP ONE and STEP TWO) of two orthogonal great circle current loops that serve as

basis elements about each of the $\left(\mathbf{i}_x, \mathbf{i}_y, 0\mathbf{i}_z\right)$ and $\left(-\frac{1}{\sqrt{2}}\mathbf{i}_x, \frac{1}{\sqrt{2}}\mathbf{i}_y, \mathbf{i}_z\right)$-axes, respectively, by π radians. Since the two sets of linked orthogonal basis-element current loops undergo independent rotations over the surface, the electron current is correspondingly divided by the number of basis loops, four, and then by the angular span of the rotations to form a normalized current density. Then, the physical properties are derived in the Spin Angular Momentum of the Orbitsphere with ℓ = 0 section and are shown to match the boundary conditions. The vector projection of the corresponding angular momentum at each point of each current element is integrated over the entire orbitsphere-cvf surface to give the electron angular momentum. The correct current pattern is confirmed by achieving the condition that the magnitude of the velocity at any point on the surface is given by Eq. (1.56) and by obtaining the required angular momentum projections of $\frac{\hbar}{2}$ and $\frac{\hbar}{4}$ along and the z-axis and along an axis in the xy-plane, respectively. In Appendix III, the *continuous* uniform electron current density function $Y_0^0(\theta,\phi)$ having the same angular momentum components of $\mathbf{L}_{xy} = \frac{\hbar}{4}$ and $\mathbf{L}_z = \frac{\hbar}{2}$ as that of the orbitsphere-cvf is then exactly generated from this orbitsphere-cvf as a basis element by a convolution operator comprising an autocorrelation-type function.

Next, consider two infinitesimal charge (mass)-density elements at two separate positions or points, one and two, of the first pair of orthogonal great circle current loops that serve as the basis set for STEP ONE as shown in Figure 1.4. In the basis-set reference frame at time zero, element one is at $x' = 0$, $y' = 0$, and $z' = r_n$ and element two is at $x' = r_n$, $y' = 0$, and $z' = 0$. Let element one move on a great circle counter clockwise toward the -y'-axis, and let element two move clockwise on a great circle toward the z'-axis, as shown in Figure 1.4. The equations of motion, in the sub-basis-set reference frame are given by

point one:

$$x_1' = 0 \qquad y_1' = -r_n \sin(\omega_n t) \qquad z_1' = r_n \cos(\omega_n t) \tag{1.68a}$$

point two:

$$x_2' = r_n \cos(\omega_n t) \qquad y_2' = 0 \qquad z_2' = r_n \sin(\omega_n t) \tag{1.68b}$$

Figure 1.4. Step One. The current on the great circle in the y'z'-plane moves counter clockwise and the current on the great circle in the x'z'-plane moves clockwise. Each point or coordinate position on the continuous two-dimensional electron orbitsphere-cvf defines an infinitesimal charge (mass)-density element which moves along a geodesic orbit comprising a great circle. Two such infinitesimal charges (masses) at points one (moving counter clockwise (arrow) on the great circle in the y'z'-plane) and two (moving clockwise (arrow) on the great circle in the x'z'-plane) of two orthogonal great circle current loops in the basis frame are considered as sub-basis elements to generate $Y_0^0(\theta,\phi)$. The xyz-system is the laboratory frame, and the orthogonal-current-loop basis set is rigid with respect to the x'y'z'-system that rotates about the $(\mathbf{i}_x,\mathbf{i}_y,0\mathbf{i}_z)$-axis by π radians to generate the elements of the first component of the orbitsphere-cvf. The angular momentum vector of the orthogonal great circle current loops in the x'y'-plane that is evenly distributed over the surface is $\frac{\hbar}{2\sqrt{2}}$.

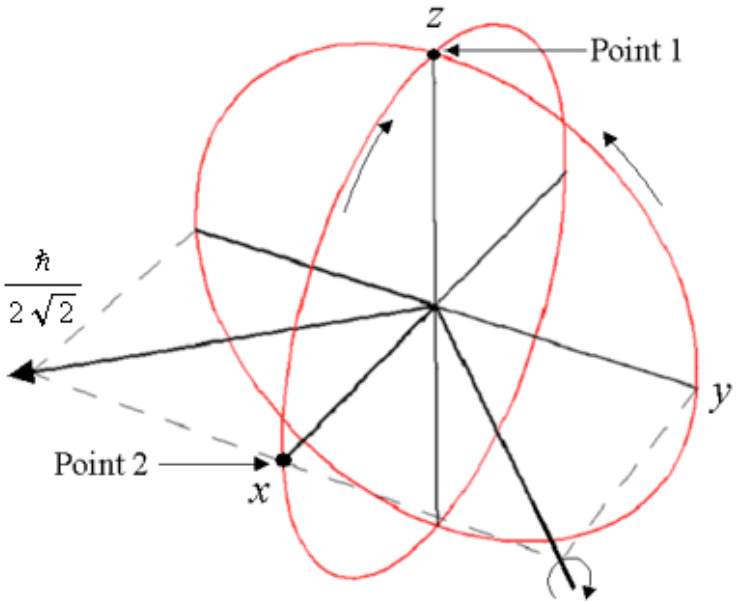

The orthogonal great circle basis set for STEP ONE is shown in Figure 1.4. One half of the orbitsphere-cvf, the orbitsphere-cvf component of STEP ONE, is generated by the rotation of two orthogonal great circles about the $(\mathbf{i}_x,\mathbf{i}_y,0\mathbf{i}_z)$-axis by π wherein one basis-element great circle initially is initially in the yz-plane and the other is in the xz-plane:

Step One

$$\begin{bmatrix} x' \\ y' \\ z' \end{bmatrix} = \begin{bmatrix} \frac{1}{2}+\frac{\cos\theta}{2} & \frac{1}{2}-\frac{\cos\theta}{2} & -\frac{\sin\theta}{\sqrt{2}} \\ \frac{1}{2}-\frac{\cos\theta}{2} & \frac{1}{2}+\frac{\cos\theta}{2} & \frac{\sin\theta}{\sqrt{2}} \\ \frac{\sin\theta}{\sqrt{2}} & -\frac{\sin\theta}{\sqrt{2}} & \cos\theta \end{bmatrix} \bullet \left(\begin{bmatrix} 0 \\ r_n\cos\phi \\ r_n\sin\phi \end{bmatrix} + \begin{bmatrix} r_n\cos\phi \\ 0 \\ r_n\sin\phi \end{bmatrix} \right) \tag{1.69}$$

The first component of the orbitsphere-cvf given by Eq. (17) can also be generated by each of rotating a great circle basis element initially in the yz or the xz-planes about the $\left(\mathbf{i}_x, \mathbf{i}_y, 0\mathbf{i}_z\right)$-axis by 2π radians as shown in Figures 1.5 and 1.6, respectively.

Figure 1.5. The current pattern of the orbitsphere-cvf component of STEP ONE shown with 6 degree increments of θ from the perspective of looking along the z-axis. The yz-plane great circle current loop that served as a basis element that was initially in the yz-plane is shown as red.

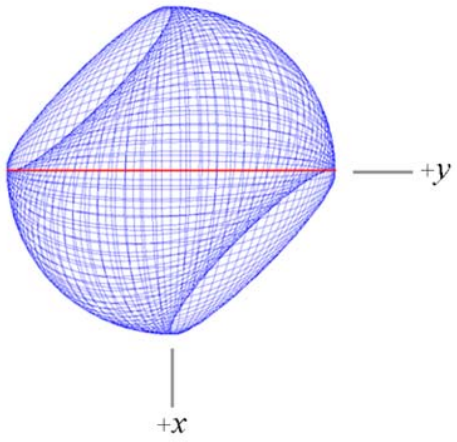

Figure 1.6. The current pattern of the orbitsphere-cvf component of STEP ONE shown with 6 degree increments of θ from the perspective of looking along the z-axis. The great circle current loop that served as a basis element that was initially in the xz-plane is shown as red.

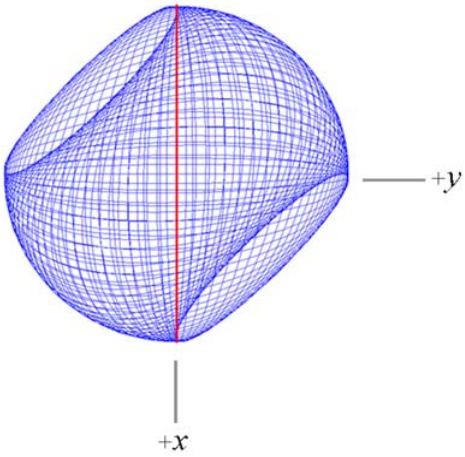

For Step Two, consider two charge (mass)-density elements, point one and two, in the basis-set reference frame at time zero. Element one is at $x' = 0$, $y' = r_n$, and $z' = 0$ and element two is at $x' = r_n$, $y' = 0$, and $z' = 0$. Let element one move clockwise on a great circle toward the -z'-axis, and let element two move counter clockwise on a great circle toward the y'-axis as shown in Figure 1.7. The equations of motion, in the basis-set reference frame are given by

point one:

$$x_1' = r_n \sin\left(\frac{\pi}{4}\right)\cos(\omega_n t) \qquad y_1' = r_n \cos\left(\frac{\pi}{4}\right)\cos(\omega_n t) \qquad z_1' = -r_n \sin(\omega_n t) \tag{1.70a}$$

point two:

$$x_2' = r_n \cos(\omega_n t) \qquad y_2' = r_n \sin(\omega_n t) \qquad z_2' = 0 \tag{1.70b}$$

Figure 1.7. Step Two. The current on the great circle in the plane that bisects the x'y'-quadrant and is parallel to the z'-axis moves clockwise, and the current on the great circle in the x'y'-plane moves counter clockwise. Rotation of the great circles about the $\left(-\frac{1}{\sqrt{2}}\mathbf{i}_x, \frac{1}{\sqrt{2}}\mathbf{i}_y, \mathbf{i}_z\right)$-axis by π radians generates the elements of the second component of the orbitsphere-cvf. The angular momentum vector of the orthogonal great circle current loops along the $\left(-\frac{1}{\sqrt{2}}\mathbf{i}_x, \frac{1}{\sqrt{2}}\mathbf{i}_y, \mathbf{i}_z\right)$-axis is $\frac{\hbar}{2\sqrt{2}}$ corresponding to each of the z and -xy-components of magnitude $\frac{\hbar}{4}$.

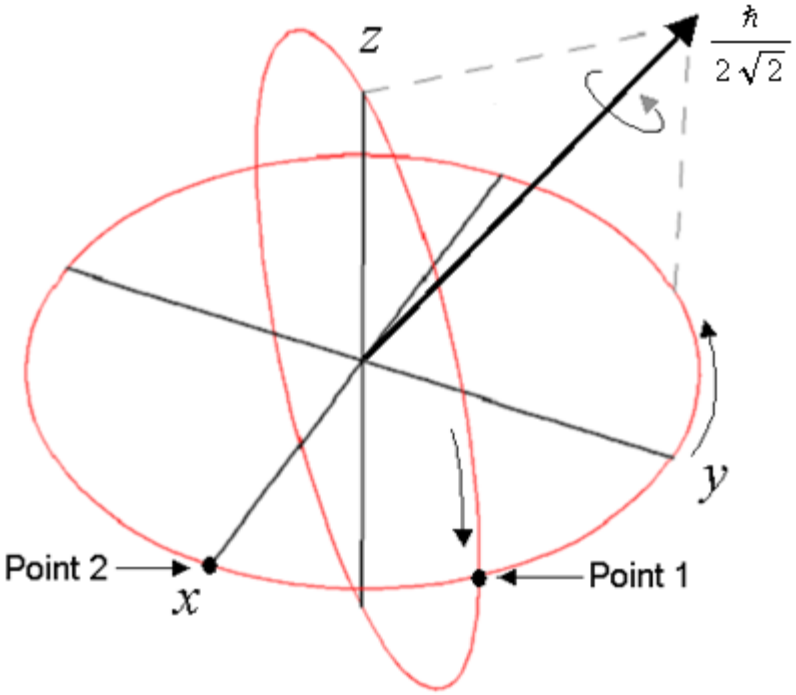

The orthogonal great circle basis set for STEP TWO is shown in Figure 1.7. The second half of the orbitsphere-cvf, the orbitsphere-cvf component of STEP TWO, is generated by the rotation of two orthogonal great circles about the $\left(-\frac{1}{\sqrt{2}}\mathbf{i}_x, \frac{1}{\sqrt{2}}\mathbf{i}_y, \mathbf{i}_z\right)$-axis by π wherein one basis-element great circle is initially in the plane that bisects the xy-quadrant and is parallel to the z-axis and the other is in the xy-plane:

Step Two

$$\begin{bmatrix} x' \\ y' \\ z' \end{bmatrix} = \begin{bmatrix} \frac{1}{4}\left(1+3\cos\theta\right) & \frac{1}{4}\left(-1+\cos\theta+2\sqrt{2}\sin\theta\right) & \frac{1}{4}\left(-\sqrt{2}+\sqrt{2}\cos\theta-2\sin\theta\right) \\ \frac{1}{4}\left(-1+\cos\theta-2\sqrt{2}\sin\theta\right) & \frac{1}{4}\left(1+3\cos\theta\right) & \frac{1}{4}\left(\sqrt{2}-\sqrt{2}\cos\theta-2\sin\theta\right) \\ \frac{1}{2}\left(\frac{-1+\cos\theta}{\sqrt{2}}+\sin\theta\right) & \frac{1}{4}\left(\sqrt{2}-\sqrt{2}\cos\theta+2\sin\theta\right) & \cos^2\frac{\theta}{2} \end{bmatrix} \bullet \left(\begin{bmatrix} \frac{r_n\cos\phi}{\sqrt{2}} \\ \frac{r_n\cos\phi}{\sqrt{2}} \\ r_n\sin\phi \end{bmatrix} + \begin{bmatrix} r_n\cos\phi \\ r_n\sin\phi \\ 0 \end{bmatrix} \right) \tag{1.71}$$

The second component of the orbitsphere-cvf given by Eq. (18) can also be generated by each of rotating a great circle basis element that is initially in the plane that bisects the xy-quadrant and is parallel to the z-axis or is in the xy-plane about the $\left(-\frac{1}{\sqrt{2}}\mathbf{i}_x, \frac{1}{\sqrt{2}}\mathbf{i}_y, \mathbf{i}_z\right)$-axis by 2π radians as shown in Figures 1.8 and 1.9, respectively.

Figure 1.8. The current pattern of the orbitsphere-cvf component of STEP TWO shown with 6 degree increments of θ from the perspective of looking along the z-axis. The great circle current loop that served as a basis element that was initially in the plane that bisects the xy-quadrant and was parallel to the z-axis is shown as red.

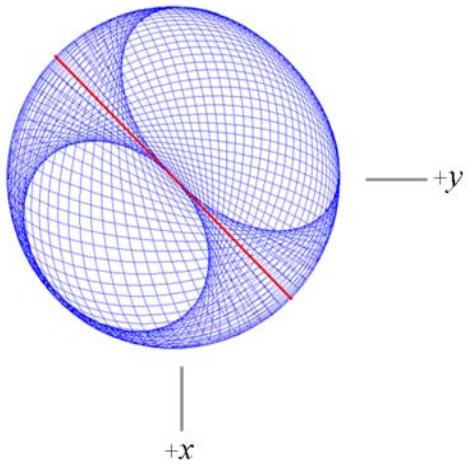

Figure 1.9. The current pattern of the orbitsphere-cvf component of STEP TWO shown with 6 degree increments of θ from the perspective of looking along the z-axis. The great circle current loop that served as a basis element that was initially in the xy-plane is shown as red.

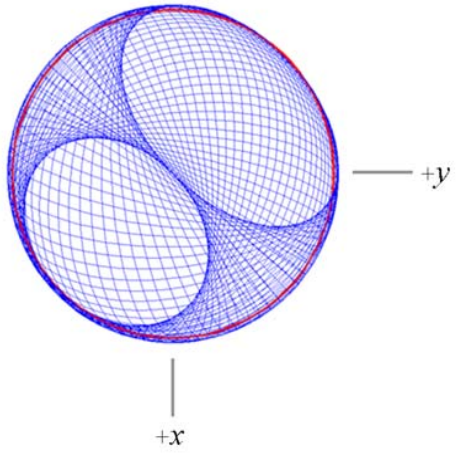

The orbitsphere-cvf is given by the superposition of the components from STEP ONE and from STEP TWO. Each STEP involves a unique combination of the initial and final directions of the primed coordinates and orientations of the angular momentum vectors due to the rotation of the basis-element great circles as summarized in Table 1.1. For example, the angular momentum vector of STEP ONE travels in the plane perpendicular to $\left(\mathbf{i}_x, \mathbf{i}_y, 0\mathbf{i}_z\right)$-axis; whereas, the angular momentum vector of STEP TWO is stationary since it is along the rotational axis, the $\left(-\frac{1}{\sqrt{2}}\mathbf{i}_x, \frac{1}{\sqrt{2}}\mathbf{i}_y, \mathbf{i}_z\right)$-axis.

Table 1.1. Summary of the results of the matrix rotations of the two sets of two orthogonal current loops to generate the orbitsphere-cvf.

Step	Initial Direction of Angular Momentum Components $(\hat{r}\times\hat{K})$[a]	Final Direction of Angular Momentum Components $(\hat{r}\times\hat{K})$[a]	Initial to Final Axis Transformation	$\mathbf{L}_{xy}$	$\mathbf{L}_z$
1	$\hat{x}$, $-\hat{y}$	$-\hat{x}$, $\hat{y}$	$+x'\rightarrow+y$ $+y'\rightarrow+x$ $+z'\rightarrow-z$	0	$\frac{\hbar}{4}$
2	$-\hat{x}$, $\hat{z}$	$-\hat{x}$, $\hat{z}$	$+z'\rightarrow-x$ $+x'\rightarrow-z$ $+y'\rightarrow-y$	$\frac{\hbar}{4}$	$\frac{\hbar}{4}$
Total				$\frac{\hbar}{4}$	$\frac{\hbar}{2}$

[a] $\mathbf{K}$ is the current density, $\mathbf{r}$ is the polar vector of the great circle, and "^" denotes the unit vectors $\hat{u}\equiv\frac{\mathbf{u}}{|\mathbf{u}|}$.

The current pattern of the orbitsphere-cvf generated by the rotations of the orthogonal great circle current loops is a continuous and total coverage of the spherical surface, but it is shown as visual representations using 6 degree increments θ of Eqs. (1.69) and (1.71) from seven perspectives in Figures 1.10A-G. In each case, the complete orbitsphere-cvf current pattern corresponds to all the correlated points, points one and two, of the orthogonal great circles shown in Figures 1.4 and 1.7 which are rotated according to Eqs. (1.69) and (1.71) where θ becomes continuous rather than discrete. The pattern also represents the momentum-vector field which is not equivalent to the mass (charge) density which for $Y_0^0(\phi,\theta)$ is uniform. Thus, the patterns represent the directions of the nonuniform flow of the uniform and constant mass and charge distribution of $Y_0^0(\theta,\phi)$. The orbitsphere-cvf serves as a basis element to exactly generate $Y_0^0(\theta,\phi)$ as given in Appendix III.

Figure 1.10A-C. The current pattern of the orbitsphere-cvf shown with 6 degree increments of θ from the perspective of looking along the z-axis, x-axis, and y-axis, respectively.

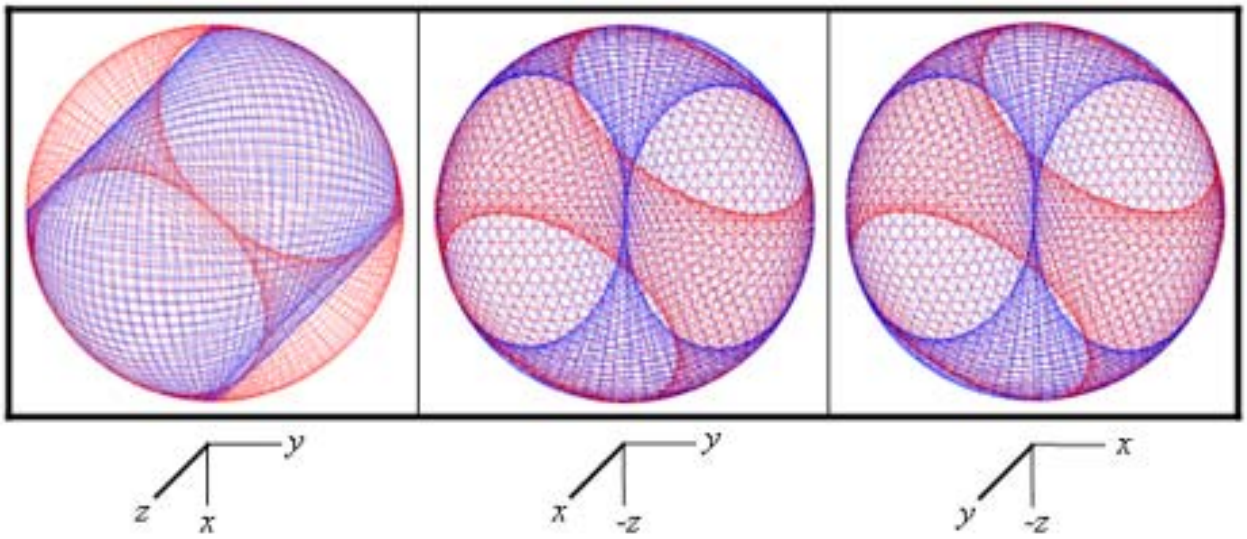

Figure 1.10D. The current pattern of the orbitsphere-cvf shown with 6 degree increments of θ from the perspective of looking along the direction of the spherical-coordinate angles $\theta = 0.838\ rad$, $\phi = 0.660\ rad$ which shows the "box view".

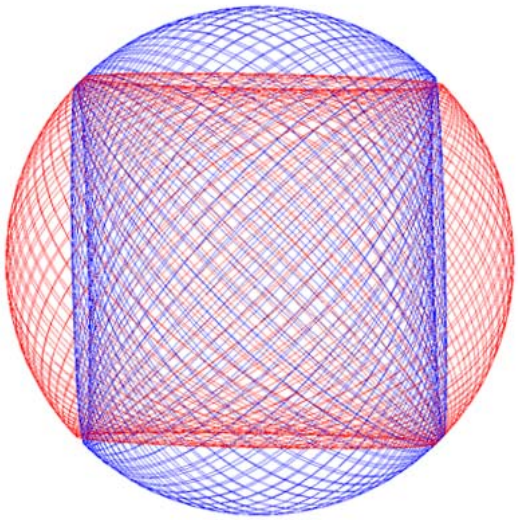

`Figure 1.10E.` The current pattern of the orbitsphere-cvf shown with 6 degree increments of θ from the perspective of looking along the direction of the spherical-coordinate angles $\theta = \frac{\pi}{2}$, $\phi = -0.0524\ rad$ which shows the "circle view".

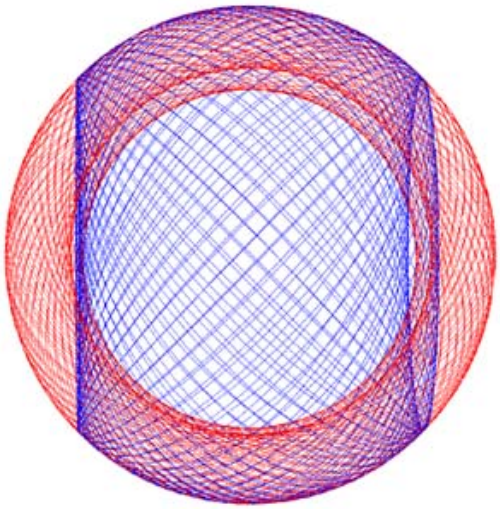

`Figure 1.10F.` The current pattern of the orbitsphere-cvf shown with 6 degree increments of θ from the perspective of looking along the direction of the spherical-coordinate angles $\theta = 0.620\ rad$, $\phi = -0.175\ rad$ which shows the "diamond view".

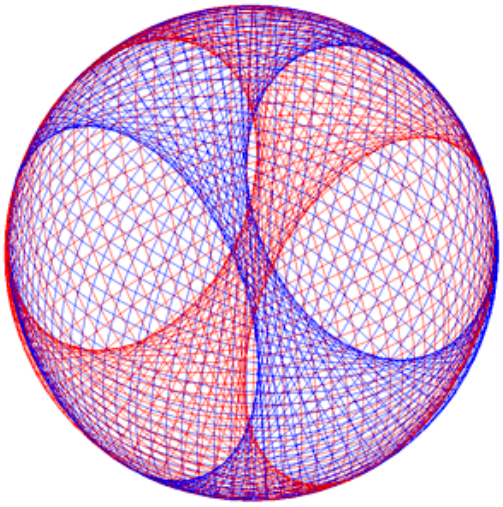

Figure 1.10G. The current pattern of the orbitsphere-cvf shown with 6 degree increments of θ from the perspective of looking along the z-axis onto which $\mathbf{L_R}$, the resultant angular momentum vector of the $\mathbf{L}_{xy}$ and $\mathbf{L}_z$ components, was aligned.

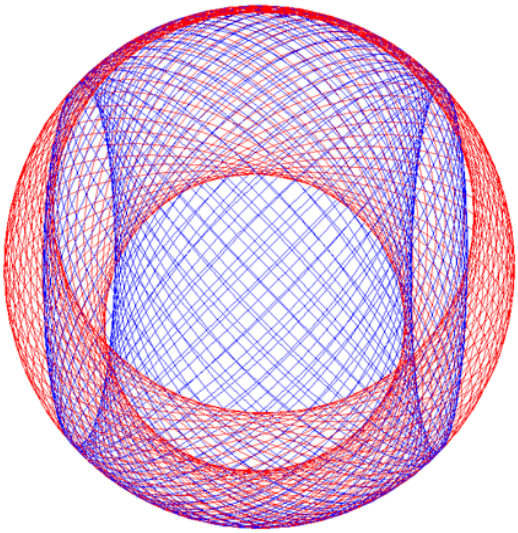

SPIN ANGULAR MOMENTUM OF THE ORBITSPHERE WITH ℓ = 0

As demonstrated in Figures 1.4-1.10, the orbitsphere-cvf comprising two components is generated over the surface by the two sets (STEP ONE and STEP TWO) of rotations of two orthogonal great circle current loops that serve as basis elements about each of the $\left(\mathbf{i_x}, \mathbf{i_y}, 0\mathbf{i_z}\right)$ and $\left(-\frac{1}{\sqrt{2}}\mathbf{i_x}, \frac{1}{\sqrt{2}}\mathbf{i_y}, \mathbf{i_z}\right)$-axes, respectively, by π radians. Next, consider two infinitesimal charge (mass)-density elements at two separate positions or points, one and two, of the two orthogonal great circle current loops that serve as the sub-basis set as shown in each of Figures 1.4 and 1.7. The vector projection of the corresponding angular momentum at each point of each current element is integrated over the entire orbitsphere-cvf surface to give the corresponding electron angular momentum. The correct current pattern is confirmed by achieving the condition that the magnitude of the velocity at any point on the surface is given by Eq. (1.56) and by obtaining the required angular momentum projections of $\frac{\hbar}{2}$ and $\frac{\hbar}{4}$ along and the z-axis and along an axis in the xy-plane, respectively, to satisfy the Stern-Gerlach-experimental boundary condition.

The mass density, $\frac{m_e}{4\pi r_1^2}$, of the orbitsphere of radius r_1 is uniform; however, the projections of the angular momenta of the great circle current loops of the orbitsphere onto the z-axis and onto the xy-plane are not. The resultant vectors can be derived by considering the contributions of the momenta corresponding to the two pairs of two orthogonal great circle current loops of Figures 1.4 and 1.7 as each basis set generates the current pattern of the corresponding component orbitsphere-cvf in STEP ONE and STEP TWO. The electron current, and thus, the momentum is evenly distributed within the two sets of orthogonally linked great-

circle current loops each with a mass of $\frac{m_e}{4}$. The total sum of the magnitude of the angular momentum from the contributions from all of the infinitesimal points on the orbitsphere is $\hbar$ (Eq. (1.57)). Thus, the angular momentum of each great circle is $\frac{\hbar}{4}$. The planes of the great circles are oriented at an angle of $\frac{\pi}{2}$ with respect to each other, and the resultant angular momentum is $\frac{\hbar}{2\sqrt{2}}$ along the $\left(\mathbf{i}_x, -\mathbf{i}_y, 0\mathbf{i}_z\right)$-axis and the $\left(-\frac{1}{\sqrt{2}}\mathbf{i}_x, \frac{1}{\sqrt{2}}\mathbf{i}_y, \mathbf{i}_z\right)$-axis for STEPS ONE and TWO, respectively. In the former case, the resultant vector rotates relative to the xyz-coordinate system about the $\left(\mathbf{i}_x, \mathbf{i}_y, 0\mathbf{i}_z\right)$-axis. Here, the angular momenta elements are then divided by the angular span of the rotation to form the normalized momentum density corresponding to the normalized current density. In the latter case, there is no angular renormalization in the determination of the projections of the resultant vector since the resultant vector is stationary. Half of the angular momentum is distributed over the orbitsphere-cvf in Step One and the other half is distributed in Step Two.

Consider the vector current directions shown in Figure 1.4. During Step One, the resultant angular momentum vector of magnitude $\frac{\hbar}{2\sqrt{2}}$ moves along a half a great circle in the plane that is parallel to the z-axis and bisects the +x-y-quadrant and the -x+y-quadrant. The trajectory of the resultant angular momentum vector from the xy-plane to the z-axis and back to the xy-plane is shown in Figure 1.11 where the angle θ of the resultant angular momentum vector from the initial xy-plane position varies from $\theta = 0$ to $\theta = \pi$. Here it can be appreciated that the vector projections onto the z-axis all add positively and the vector projections into the xy-plane sum to zero. With the initial direction defined as positive, the projection in the xy-plane varies from a maximum of $\frac{\hbar}{2\sqrt{2}}$ to zero to $\frac{\hbar}{2\sqrt{2}}$. The projection onto the z-axis varies from zero to a maximum of $\frac{\hbar}{2\sqrt{2}}$ to zero again. In each case, the projection of the angular momentum is periodic over the angular range of θ. The total of each projection, $\mathbf{L}_{xy}$ and $\mathbf{L}_z$, is the integral as a function of θ of the magnitude of the resultant vector of the two orthogonal angular momentum component vectors corresponding to the two orthogonal great circles. Alternatively, the projections may be obtained by using the root-mean square, or the projections may be obtained using the vector integral with the consideration that the incremental momentum density on the spherical surface follows the relationship $dz = R\sin\theta d\theta$ with respect to the z-axis, for example, as shown in Haus [14]. For the projection onto the axis in the xy-plane, $\cos\theta$ replaces $\sin\theta$. For any of these approaches, the angular momentum projection of each of the four basis-element-great-circle current loops onto the xy-plane and onto the z-axis is $\frac{\hbar}{4}\cos\theta$ and $\frac{\hbar}{4}\sin\theta$, respectively.

For Step One, the vector projection of the angular momentum onto the xy-plane is given by sum of the vector contributions from each great circle:

Magnitude and RMS Approach:

$$\mathbf{L}_{xy} = \sqrt{\frac{2}{\pi}\int_0^{\frac{\pi}{2}}\left[\frac{\hbar}{4}\cos\theta\right]^2 + \left[\frac{\hbar}{4}\cos\theta\right]^2 d\theta} - \sqrt{\frac{2}{\pi}\int_{\frac{\pi}{2}}^{\pi}\left[\frac{\hbar}{4}\cos\theta\right]^2 + \left[\frac{\hbar}{4}\cos\theta\right]^2 d\theta}$$

$$= \frac{\hbar}{2\sqrt{2}}\ \frac{1}{\sqrt{2}} - \frac{\hbar}{2\sqrt{2}}\ \frac{1}{\sqrt{2}} = 0 \tag{1.72}$$

Vector Integration Approach:

$$\mathbf{L}_{xy} = \frac{2}{\pi}\int_0^{\frac{\pi}{2}}\left(\frac{\hbar}{4}\cos\theta + \frac{\hbar}{4}\cos\theta\right)\cos\theta d\theta - \frac{2}{\pi}\int_{\frac{\pi}{2}}^{\pi}\left(\frac{\hbar}{4}\cos\theta + \frac{\hbar}{4}\cos\theta\right)\cos\theta d\theta$$

$$= \frac{\hbar}{4} - \frac{\hbar}{4} = 0$$

where each angular integral is normalized by, $\frac{\pi}{2}$, the angular range of θ. Similarly, the vector projection of the angular momentum onto the z-axis as shown in Figure 1.11 is

Magnitude and RMS Approach:

$$\mathbf{L}_z = \sqrt{\frac{1}{\pi}\int_0^{\pi}\left[\frac{\hbar}{4}\sin\theta\right]^2 + \left[\frac{\hbar}{4}\sin\theta\right]^2 d\theta} = \frac{\hbar}{2\sqrt{2}}\ \frac{1}{\sqrt{2}} = \frac{\hbar}{4} \tag{1.73}$$

Vector Integration Approach:

$$\mathbf{L}_z = \frac{1}{\pi}\int_0^{\pi}\left(\frac{\hbar}{4}\sin\theta + \frac{\hbar}{4}\sin\theta\right)\sin\theta d\theta = \frac{\hbar}{4}$$

where each angular integral is normalized by, π, the angular range of θ. Thus, from the initial $\frac{\hbar}{4}$ of angular momentum along each of the x and y-axes, $\frac{\hbar}{4}$ canceled in the xy-plane and $\frac{\hbar}{4}$ was projected onto the z-axis as the angular momentum was spread over one half of the surface of the sphere with Step One. This matches the condition of conservation of the scalar sum of the angular momentum which was merely distributed over the spherical surface in the generation of this component of the orbitsphere-cvf.

Figure 1.11. The trajectory of the resultant angular momentum vector of the orthogonal great circle current loops of magnitude $\frac{\hbar}{2\sqrt{2}}$ during Step One (gray vectors) gives $\mathbf{L}_z = \frac{\hbar}{4}$. The resultant angular momentum vector of the orthogonal great circle current loops of magnitude $\frac{\hbar}{2\sqrt{2}}$ of Step Two (black vector) is stationary with the projections of $\mathbf{L}_{xy} = \frac{\hbar}{4}$ and $\mathbf{L}_z = \frac{\hbar}{4}$.

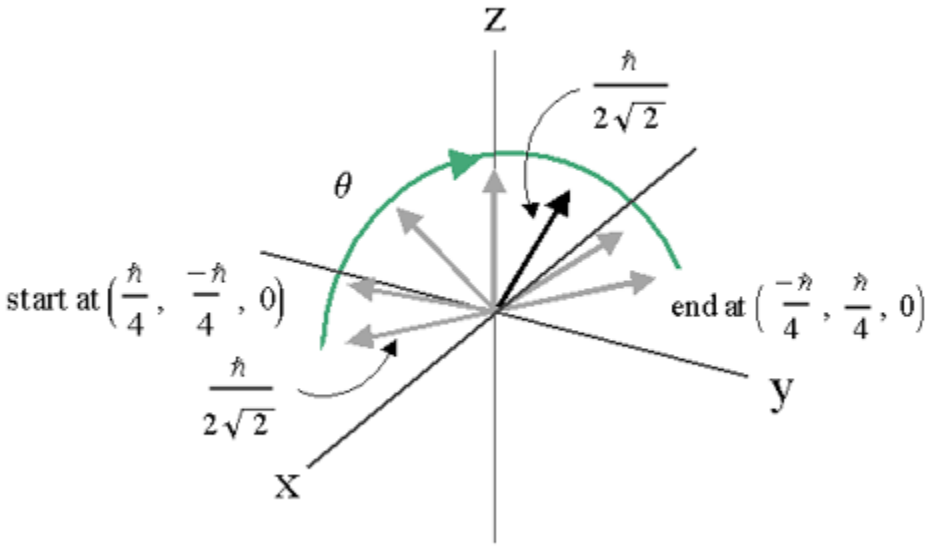

Consider the vector current directions shown in Figure 1.7. During Step Two, the orthogonal great-circle basis set are rotated about the $\left(-\frac{1}{\sqrt{2}}\mathbf{i}_x, \frac{1}{\sqrt{2}}\mathbf{i}_y, \mathbf{i}_z\right)$-axis. The resultant angular momentum vector is along this axis. Thus, the resultant angular momentum vector of magnitude $\frac{\hbar}{2\sqrt{2}}$ is stationary throughout the rotations that transform the axes as given in Table 1.1. The resultant angular momentum component of Step Two that is transverse to the z-axis, $\mathbf{L}_{xy}$, is in the direction of $\left(-\mathbf{i}_x, \mathbf{i}_y, 0\mathbf{i}_z\right)$ which is also the direction of the trajectory of the angular momentum component vectors of Step One as shown in Figure 1.11. The resultant angular momentum projections are the same as the initial projections given in Figure 1.7:

$$\mathbf{L}_{xy} = \frac{\hbar}{4} \tag{1.74}$$

$$\mathbf{L}_z = \frac{\hbar}{4} \tag{1.75}$$

The total vector projection of the angular momentum onto the xy-plane given by the sum of Eqs. (1.72) and (1.73) is

$$\mathbf{L}_{xy} = 0 + \frac{\hbar}{4} = \frac{\hbar}{4} \tag{1.76}$$

The total vector projection of the angular momentum into the z-axis given by the sum of Eqs. (1.72) and (1.73) is

$$\mathbf{L}_z = \frac{\hbar}{4} + \frac{\hbar}{4} = \frac{\hbar}{2} \tag{1.77}$$

The trajectories of the angular momenta and the resultant projections, $\mathbf{L}_{xy}$ and $\mathbf{L}_z$, given in Table 1.1 are visually demonstrated by computer simulations [15]. These results meet the boundary condition for the unique current having an angular velocity magnitude at each point on the surface given by Eq. (1.56) and give rise to the Stern Gerlach experiment as shown *infra.*, in

the Magnetic Parameters of the Electron (Bohr Magneton) section, and in the Electron g Factor section.

EXACT GENERATION OF $Y_0^0(\phi,\theta)$ FROM THE ORBITSPHERE-CVF

The further constraint that the current density is uniform such that the charge density is uniform, corresponding to an equipotential, minimum energy surface is satisfied by using the orbitsphere-cvf as a basis element to generate $Y_0^0(\theta,\phi)$ using a convolution operator as given in Appendix III. The orbitsphere-cvf comprises two components corresponding to each of STEP ONE and STEP TWO. The convolution operator comprises an autocorrelation-type function that that treats each component defined as a primary component corresponding to STEPS ONE and TWO separately and results in the replacement of each great circle of the primary component orbitsphere-cvf with a secondary component orbitsphere-cvf of matching angular momentum, orientation, and phase. The convolution is given by rotating a matched basis-element secondary about the same axis as that which generated the primary from the basis-element current loop to exactly give rise to a spherically-symmetric uniform current density. The superposition of the two resulting uniform densities gives $Y_0^0(\theta,\phi)$. The resulting exact uniform current distribution has the same angular momentum distribution, resultant, $\mathbf{L_R}$, and components of $\mathbf{L}_{xy}=\frac{\hbar}{4}$ and $\mathbf{L}_z=\frac{\hbar}{2}$ as those of the orbitsphere-cvf used as a primary basis element.

CONVOLUTION OPERATOR

As shown *supra* and in Appendix III, STEP TWO can also be generated by a 2π-rotation of a single basis-element current loop about the $\left(-\frac{1}{\sqrt{2}}\mathbf{i_x},\frac{1}{\sqrt{2}}\mathbf{i_y},\mathbf{i_z}\right)$-axis or a π-rotation of two orthogonal current loops such that the angular momentum vector is stationary on the $\left(-\frac{1}{\sqrt{2}}\mathbf{i_x},\frac{1}{\sqrt{2}}\mathbf{i_y},\mathbf{i_z}\right)$-axis as the component orbitsphere-cvf is generated. In the general case that the resultant angular momentum of each pair of orthogonal great circle current loops of the component orbitsphere-cvf is along the 2π-rotational axis (defined as the rotational axis which generates the component orbitsphere-cvf from a basis-element great circle), a secondary nth component orbitsphere-cvf can serve as a basis element to match the angular momentum of any given nth great circle of a primary component orbitsphere-cvf. The replacement of each great circle of the primary orbitsphere-cvf with a secondary orbitsphere-cvf of matching angular momentum, orientation, and phase comprises an autocorrelation-type function that exactly gives rise to the spherically-symmetric current density, $Y_0^0(\theta,\phi)$.

The orbitsphere-cvf comprises the superposition or sum of the components corresponding to STEPS ONE and STEP TWO. Thus, the convolution is performed on each component designated a primary component. The convolution of a secondary component orbitsphere-cvf element with the each great circle current loop of each primary orbitsphere-cvf is designated as the convolution operator, $A(\theta,\phi)$, given by

$$A(\theta,\phi)=\frac{1}{2r_n^2}\lim_{\Delta\theta_2\to 0}\sum_{m'=1}^{m'=\frac{2\pi}{|\Delta\theta_2|}}\lim_{\Delta\theta_1\to 0}\sum_{m=1}^{m=\frac{2\pi}{|\Delta\theta_1|}} 2°O(\theta,\phi)\otimes\begin{pmatrix}1°_1O(\theta,\phi)\delta(\theta-m\Delta\theta_1,\phi-\phi')\\ \\ +1°_2O(\theta,\phi)\delta(\theta-m'\Delta\theta_2,\phi-\phi'')\end{pmatrix} \tag{1.78}$$

$$=\frac{1}{2r_n^2}\lim_{\Delta\theta_2\to 0}\sum_{m'=1}^{m'=\frac{2\pi}{|\Delta\theta_2|}}\lim_{\Delta\theta_1\to 0}\sum_{m=1}^{m=\frac{2\pi}{|\Delta\theta_1|}} 2°O(\theta,\phi)\otimes\begin{pmatrix}GC_{STEPONE}(m\Delta\theta_1,\phi')\\ \\ +GC_{STEPTWO}(m'\Delta\theta_2,\phi'')\end{pmatrix}$$

wherein (1) the secondary component orbitsphere-cvf that is matched to the basis element of the primary is defined by the symbol $2°O(\theta,\phi)$, (2) the primary component orbitsphere-cvf of STEP M is defined by the symbol $1°_M O(\theta,\phi)$, (3) each rotated great circle of the primary component orbitsphere-cvf of STEP M is selected by the Dirac delta function $\delta(\theta-m\Delta\theta_M,\phi-\phi',)$; the product $1°_M O(\theta,\phi)\delta(\theta-m\Delta\theta_M,\phi-\phi')$ is zero except for the great circle at the angle $\theta=m\Delta\theta_M$ about the 2π-rotational axis; each selected great circle having $0\le\phi'\le 2\pi$ is defined by $GC_{STEPM}(m\Delta\theta_M,\phi')$, and (4) $\frac{1}{2r_n^2}$ is the normalization constant In Eq. (1.78), the angular momentum of each secondary component orbitsphere-cvf is equal in magnitude and direction as that of the current loop with which it is convolved. Furthermore, the orientations and phases of the convolved elements are matched by rotating the secondary component orbitsphere-cvf about the appropriate principle axis (axes) and about the C_∞-axis along its angular momentum vector, respectively. With the magnitude of the angular momentum of the secondary component orbitsphere-cvf matching that of the current loop which it replaces during the convolution and the loop then serving as a unit vector, the angular momentum resulting from the convolution operation is inherently normalized to that of the primary component orbitsphere-cvf.

The convolution of a sum is the sum of the convolutions. Thus, the convolution operation may be performed on each of STEP ONE and STEP TWO separately, and the result may be superposed in terms of the current densities and angular momenta.

$$A(\theta,\phi)=\frac{1}{2r_n^2}\begin{pmatrix}\lim_{\Delta\theta_2\to 0}\sum_{m'=1}^{m'=\frac{2\pi}{|\Delta\theta_2|}} 2°O(\theta,\phi)\otimes GC_{STEPONE}(m\Delta\theta_1,\phi')\\ \\ +\lim_{\Delta\theta_1\to 0}\sum_{m=1}^{m=\frac{2\pi}{|\Delta\theta_1|}} 2°O(\theta,\phi)\otimes GC_{STEPTWO}(m'\Delta\theta_2,\phi'')\end{pmatrix} \tag{1.79}$$

Factoring out the secondary component orbitsphere-cvf which is a constant at each position of $GC_{STEPM}(m\Delta\theta_M,\phi')$ gives

$$A(\phi,\theta)=\frac{1}{2r_n^2}2°O(\theta,\phi)\left(\begin{array}{l}\lim_{\Delta\theta_2\to 0}\sum_{m'=1}^{m'=\frac{2\pi}{|\Delta\theta_2|}} GC_{STEPONE}\left(m\Delta\theta_1,\phi'\right)\\ \\ +\lim_{\Delta\theta_1\to 0}\sum_{m=1}^{m=\frac{2\pi}{|\Delta\theta_1|}} GC_{STEPTWO}\left(m'\Delta\theta_2,\phi''\right)\end{array}\right) \tag{1.80}$$

The summation is the operator that generates the primary component orbitsphere-cvf of STEP M, $1°_M O(\theta,\phi)$. Thus, the current-density function is given by the dot product of each primary orbitsphere-cvf with itself. The result is the scalar sum of the square of each of the STEP ONE and STEP TWO primary component orbitsphere-cvfs:

$$A(\theta,\phi)=\frac{1}{2r_n^2}\left(\left(1°_1 O(\theta,\phi)\right)^2+\left(1°_2 O(\theta,\phi)\right)^2\right) \tag{1.81}$$

where the dot-product scalar is valid over the entire spherical surface. The orbitsphere-cvf squared given in Eq. (1.81) is the equation of a uniform sphere. The superposition of the uniform distributions from STEP ONE and STEP TWO is the exact uniform current density function $Y_0^0(\theta,\phi)$ that is an equipotential, minimum energy surface shown in Figure 1.12. The angular momentum is identically that of the superposition of the component orbitsphere-cvfs of the primary orbitsphere-cvf, $\mathbf{L}_{xy}=\frac{\hbar}{4}$ and $\mathbf{L}_z=\frac{\hbar}{2}$ given by Eqs. (1.76-1.77).

Figure 1.12. The orbitsphere is a two dimensional spherical shell of zero thickness with the Bohr radius of the hydrogen atom, $r=a_H$, having angular momentum components of $\mathbf{L}_{xy}=\frac{\hbar}{4}$ and $\mathbf{L}_z=\frac{\hbar}{2}$.

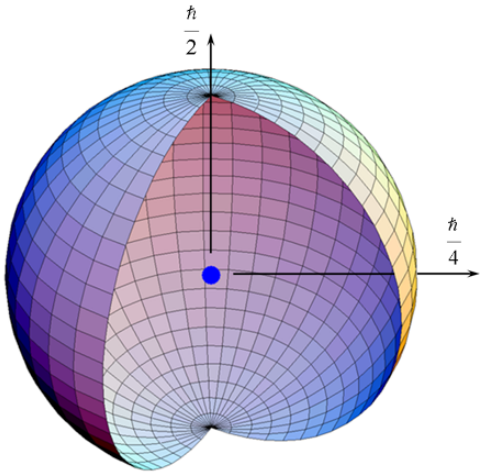

STEP-ONE MATRICES TO VISUALIZE THE CURRENTS OF $Y_0^0(\phi,\theta)$

Consider the case that the STEP-ONE primary component orbitsphere-cvf is given by Eq. (17). The yz-plane great circle current loop that served as a basis element that was initially in the yz-

plane is shown as red. The current is counterclockwise; thus, the angular momentum is along the x-axis. The secondary component orbitsphere-cvf shown in Figure 1.13 that is matched for angular momentum, orientation, and phase is given the matrix:

$$\begin{bmatrix} x' \\ y' \\ z' \end{bmatrix} = \begin{bmatrix} \cos\left(\frac{\pi}{4}\right) & -\sin\left(\frac{\pi}{4}\right) & 0 \\ \sin\left(\frac{\pi}{4}\right)\cos\theta & \cos\left(\frac{\pi}{4}\right)\cos\theta & \sin\theta \\ -\sin\left(\frac{\pi}{4}\right)\sin\theta & -\cos\left(\frac{\pi}{4}\right)\sin\theta & \cos\theta \end{bmatrix} \begin{bmatrix} 0 \\ r_n\cos\phi \\ r_n\sin\phi \end{bmatrix} \tag{1.82}$$

Figure 1.13. The current pattern of the secondary component orbitsphere-cvf given by Eq. (26) and shown with 6 degree increments of θ from the perspective of looking along the z-axis. The great circle current loop that served as a basis element that was initially in the yz-plane is shown as red.

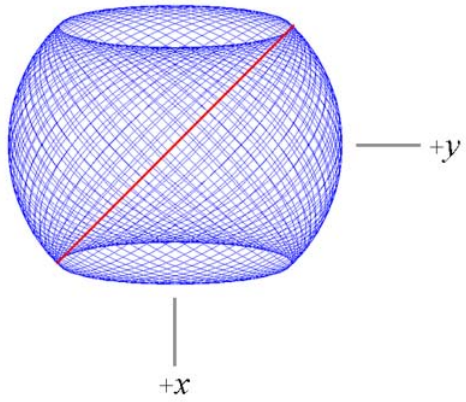

The secondary component orbitsphere-cvf is aligned on the yz-plane and the resultant angular momentum vector, $\mathbf{L_R}$, is also along the x-axis.

Then, the uniform current distribution is given from Eq. (23) as a infinite sum of the convolved elements comprising the secondary component orbitsphere-cvf given by Eq. (26) rotated according to Eq. (17), the matrix which generated the primary component orbitsphere-cvf. The resulting constant function is exact as given by Eq. (25). A representation (Figure 1.14) that shows the current elements can be generated by showing the basis-element secondary component orbitsphere-cvf as a sum of N great circles using Eq. (26) and by showing the continuous convolution as a sum of M discrete incremental rotations of the position of the secondary component orbitsphere-cvf about the $\left(\mathbf{i_x}, \mathbf{i_y}, 0\mathbf{i_z}\right)$-axis using Eq. (23):

$$\begin{bmatrix} x' \\ y' \\ z' \end{bmatrix} = \sum_{m=1}^{m=M} \begin{bmatrix} \frac{1}{2}+\frac{\cos\left(\frac{m2\pi}{M}\right)}{2} & \frac{1}{2}-\frac{\cos\left(\frac{m2\pi}{M}\right)}{2} & -\frac{\sin\left(\frac{m2\pi}{M}\right)}{\sqrt{2}} \\ \frac{1}{2}-\frac{\cos\left(\frac{m2\pi}{M}\right)}{2} & \frac{1}{2}+\frac{\cos\left(\frac{m2\pi}{M}\right)}{2} & \frac{\sin\left(\frac{m2\pi}{M}\right)}{\sqrt{2}} \\ \frac{\sin\left(\frac{m2\pi}{M}\right)}{\sqrt{2}} & -\frac{\sin\left(\frac{m2\pi}{M}\right)}{\sqrt{2}} & \cos\left(\frac{m2\pi}{M}\right) \end{bmatrix}$$
$$\bullet \sum_{n=1}^{n=N} \begin{bmatrix} \cos\left(\frac{\pi}{4}\right) & -\sin\left(\frac{\pi}{4}\right) & 0 \\ \sin\left(\frac{\pi}{4}\right)\cos\left(\frac{n2\pi}{N}\right) & \cos\left(\frac{\pi}{4}\right)\cos\left(\frac{n2\pi}{N}\right) & \sin\left(\frac{n2\pi}{N}\right) \\ -\sin\left(\frac{\pi}{4}\right)\sin\left(\frac{n2\pi}{N}\right) & -\cos\left(\frac{\pi}{4}\right)\sin\left(\frac{n2\pi}{N}\right) & \cos\left(\frac{n2\pi}{N}\right) \end{bmatrix} \begin{bmatrix} 0 \\ r_n\cos\phi \\ r_n\sin\phi \end{bmatrix} \tag{1.83}$$

Figure 1.14. A representation of the uniform current pattern of the $Y_0^0(\phi,\theta)$ orbitsphere shown with 30 degree increments ($N = M = 12$ in Eq. (27)) of the angle to generate the orbitsphere current-vector field corresponding to Eq. (26) and 30 degree increments of the rotation of this basis element about the $\left(\mathbf{i}_x, \mathbf{i}_y, 0\mathbf{i}_z\right)$-axis corresponding to Eq. (25). The great circle current loop that served as a basis element that was initially in the plane along the $\left(\mathbf{i}_x, -\mathbf{i}_y, 0\mathbf{i}_z\right)$- and z-axes of each secondary component orbitsphere-cvf is shown as red. The perspective is transverse to the z-axis.

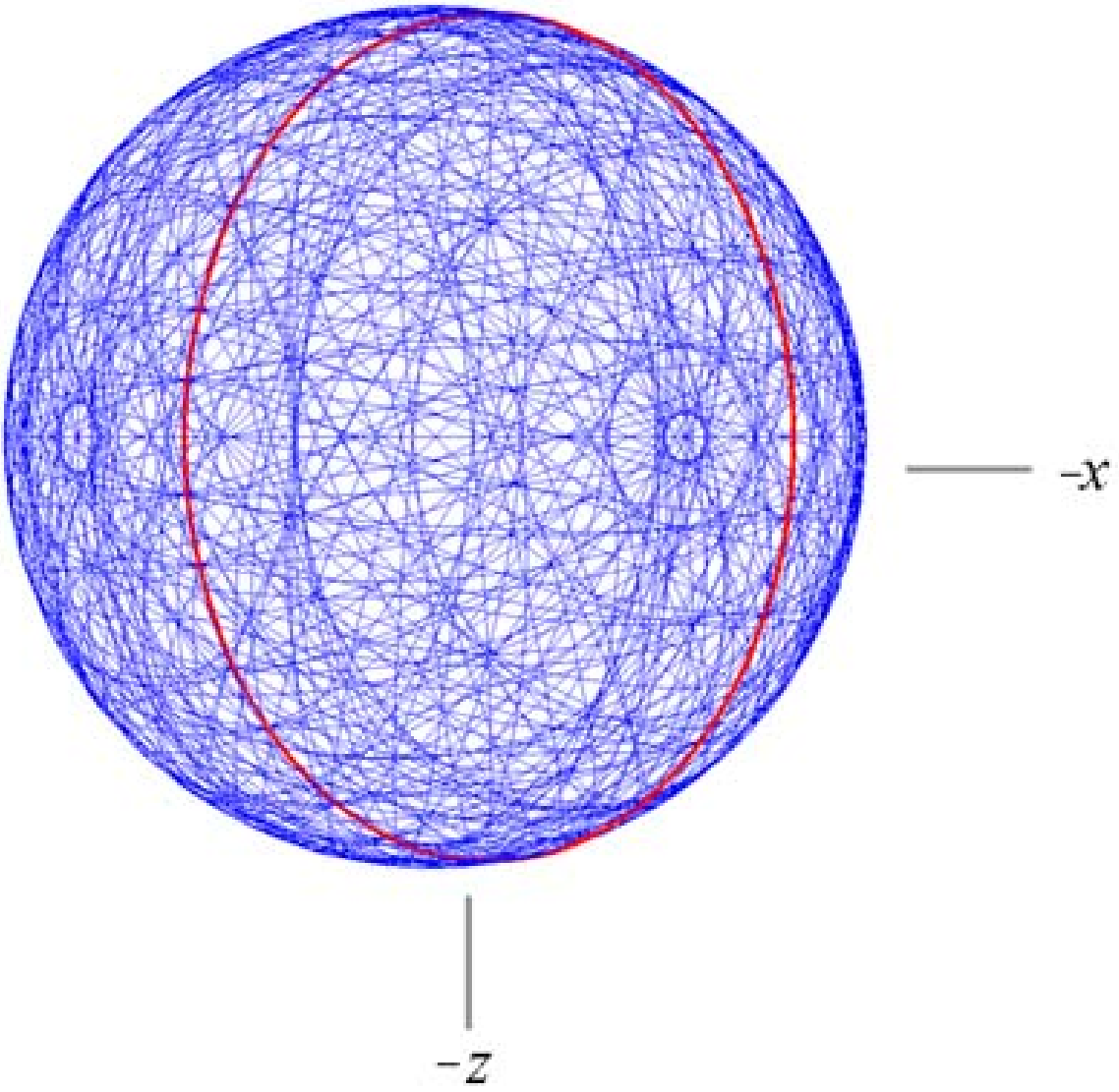

The similar result for STEP TWO is superimposed on that of STEP ONE wherein the uniform distribution is normalized as given in Appendix III.

RESONANT PRECESSION OF THE SPIN-1/2-CURRENT-DENSITY FUNCTION GIVES RISE TO THE BOHR MAGNETON

The Stern Gerlach experiment described below demonstrates that the magnetic moment of the electron can only be parallel or antiparallel to an applied magnetic field. In spherical coordinates, this implies a spin quantum number of 1/2 corresponding to an angular momentum on the z-axis of $\frac{\hbar}{2}$. However, the Zeeman splitting energy corresponds to a magnetic moment of μ_B and implies an electron angular momentum on the z-axis of $\hbar$—twice that given by Eq. (1.68-1.73). Consider the case of a magnetic field applied to the orbitsphere. The magnetic moment corresponding to the angular momentum along the z-axis results in the alignment of the z-axis of the orbitsphere with the magnetic field while the $\frac{\hbar}{4}$ resultant vector in the xy-plane causes precession about the applied field. The precession frequency is the Larmor frequency given by the product of the gyromagnetic ratio of the electron, $\frac{e}{2m}$, and the magnetic flux $\mathbf{B}$ [16]. The precessing electron can interact with a resonant photon that gives rise to Zeeman splitting—energy levels corresponding to parallel or antiparallel alignment of the electron magnetic moment with the magnetic field. The energy of the transition between these states is that of the resonant photon. The angular momentum of the precessing orbitsphere comprises the initial $\frac{\hbar}{2}$ projection on the z-axis and the initial $\frac{\hbar}{4}$ vector component in the xy-plane that then precesses about the z-axis. As shown in the Excited States of the One-Electron Atom (Quantization) section, conservation of the angular momentum of the photon of $\hbar$ gives rise to $\hbar$ of electron angular momentum. The parameters of the photon standing wave for the Zeeman effect are given in the Magnetic Parameters of the Electron (Bohr Magneton) section and Box 1.2.

The angular momentum of the orbitsphere in a magnetic field comprises the static $\frac{\hbar}{2}$ projection on the z-axis (Eq. (1.77)) and the $\frac{\hbar}{4}$ vector component in the xy-plane (Eq. (1.76)) that precesses about the z-axis at the Larmor frequency. A resonant excitation of the Larmor precession frequency gives rise to a trapped photon with $\hbar$ of angular momentum along a precessing $\mathbf{S}$-axis. In the coordinate system rotating at the Larmor frequency (denoted by the axes labeled X_R, Y_R, and Z_R in Figure 1.15), the X_R-component of magnitude $\frac{\hbar}{4}$ and $\mathbf{S}$ of magnitude $\hbar$ are stationary. The $\frac{\hbar}{4}$ angular momentum along X_R with a corresponding magnetic moment of $\frac{\mu_B}{4}$ (Eq. (28) of Box 1.2) causes $\mathbf{S}$ to rotate in the Y_R Z_R-plane to an angle of $\theta = \frac{\pi}{3}$ such that the torques due to the Z_R-component of $\frac{\hbar}{2}$ and the orthogonal X_R-component of $\frac{\hbar}{4}$ are balanced. Then the Z_R-component due to $\mathbf{S}$ is $\pm\hbar\cos\frac{\pi}{3} = \pm\frac{\hbar}{2}$. The

reduction of the magnitude of **S** along Z_R from $\hbar$ to $\frac{\hbar}{2}$ corresponds to the ratio of the X_R-component and the static Z_R-component of $\frac{\frac{\hbar}{4}}{\frac{\hbar}{2}}=\frac{1}{2}$ [7]. Since the X_R-component is $\frac{\hbar}{4}$, the Z_R-component of **S** is $\frac{\hbar}{2}$ which adds to the initial $\frac{\hbar}{2}$ component to give a total Z_R-component of $\hbar$.

---

[7] The torque balance can be appreciated by considering that **S** is aligned with Z_R if the X_R-component is zero, and the three vectors are mutually orthogonal if the X_R-component is $\frac{\hbar}{2}$. The balance can be shown by considering the magnetic energies resulting from the corresponding torques when they are balanced. Using Eqs. (23) and (25) of Box 1.2, the potential energy E_V due to the projection of **S**'s angular momentum of $\hbar$ along Z_R having $\frac{\hbar}{2}$ of angular momentum is

$$E_V = \mu_B B\cos\theta = \mu_B \frac{1}{2} B_{\mu_B} \cos\theta = \frac{1}{2}\hbar\omega_{\mu_B}\cos\theta \tag{1}$$

where B_{μ_B} is the flux due to a magnetic moment of a Bohr magneton and ω_{μ_B} is the corresponding gyromagnetic frequency. The application of a magnetic moment along the X_R-axis causes **S** to precess about the Z_R and X_R-axes. In the $X_R\,Y_R\,Z_R$-frame rotating at ω_{μ_B}, **S** precesses about the X_R-axis. The corresponding precession energy E_{X_R} of **S** about the X_R-component of $\frac{\hbar}{4}$ is the corresponding Larmor energy

$$E_{X_R} = -\frac{1}{4}\hbar\omega_{\mu_B} \tag{2}$$

The energy E_{Z_R} of the magnetic moment corresponding to **S** rotating about Z_R having $\frac{\hbar}{2}$ of angular momentum is the corresponding Larmor energy:

$$E_{Z_R} = \frac{1}{2}\hbar\omega_{\mu_B} \tag{3}$$

At torque balance, the potential energy is equal to the sum of the Larmor energies:

$$E_{Z_R} + E_{X_R} = \hbar\left(\frac{1}{2}-\frac{1}{4}\right)\omega_{\mu_B} = \frac{\hbar}{2}\left(1-\frac{\frac{1}{4}}{\frac{1}{2}}\right)\omega_{\mu_B} = \frac{1}{2}\hbar\omega_{\mu_B}\cos\theta \tag{4}$$

Balance occurs when $\theta=\frac{\pi}{3}$. Thus, the intrinsic torques are balanced. Furthermore, energy is conserved relative to the external field as well as the intrinsic, Z_R and X_R-components of the orbitsphere, and the Larmor relationships for both the gyromagnetic ratio and the potential energy of the resultant magnetic moment are satisfied as shown in Box 1.2.

`Figure 1.15.` The angular momentum components of the orbitsphere and $\mathbf{S}$ in the rotating coordinate system X_R, Y_R, and Z_R that precesses at the Larmor frequency about Z_R such that the vectors are stationary.

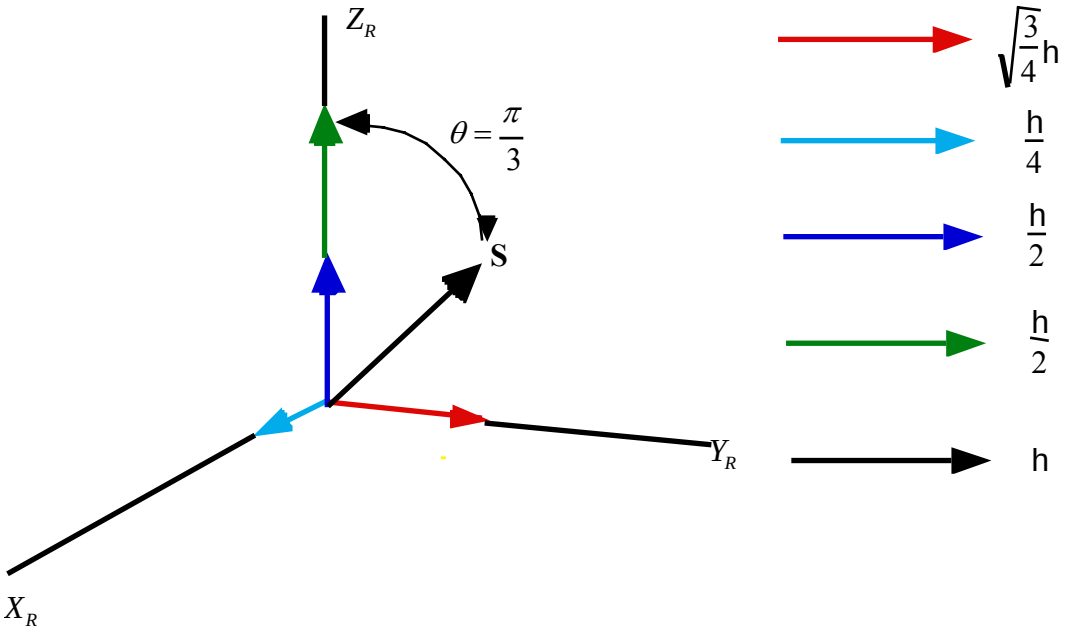

In summary, since the vector $\mathbf{S}$ that precesses about the z-axis at an angle of $\theta = \frac{\pi}{3}$ and an angle of $\phi = \frac{\pi}{2}$ with respect to $\mathbf{L}_{xy}$ given by Eq. (1.76) and has a magnitude of $\hbar$, the $\mathbf{S}$ projections in the X_R Y_R-plane and along the Z_R-axis are

$$\mathbf{S}_{\perp} = \hbar \sin\frac{\pi}{3} = \pm\sqrt{\frac{3}{4}}\hbar\,\mathbf{i}_{Y_R} \tag{1.84}$$

$$\mathbf{S}_{\parallel} = \pm\hbar\cos\frac{\pi}{3} = \pm\frac{\hbar}{2}\,\mathbf{i}_{Z_R} \tag{1.85}$$

The plus or minus sign of Eqs. (1.84) and (1.85) corresponds to the two possible vector orientations which are observed with the Stern-Gerlach experiment described below. The sum of the torques in the external magnetic field is balanced unless an RF field is applied to cause a Stern-Gerlach transition as discussed in Box 1.2.

Figure 1.16A. The angular momentum components of the orbitsphere and **S** in the stationary coordinate system. **S** and the components in the xy-plane precess at the Larmor frequency about the z-axis.

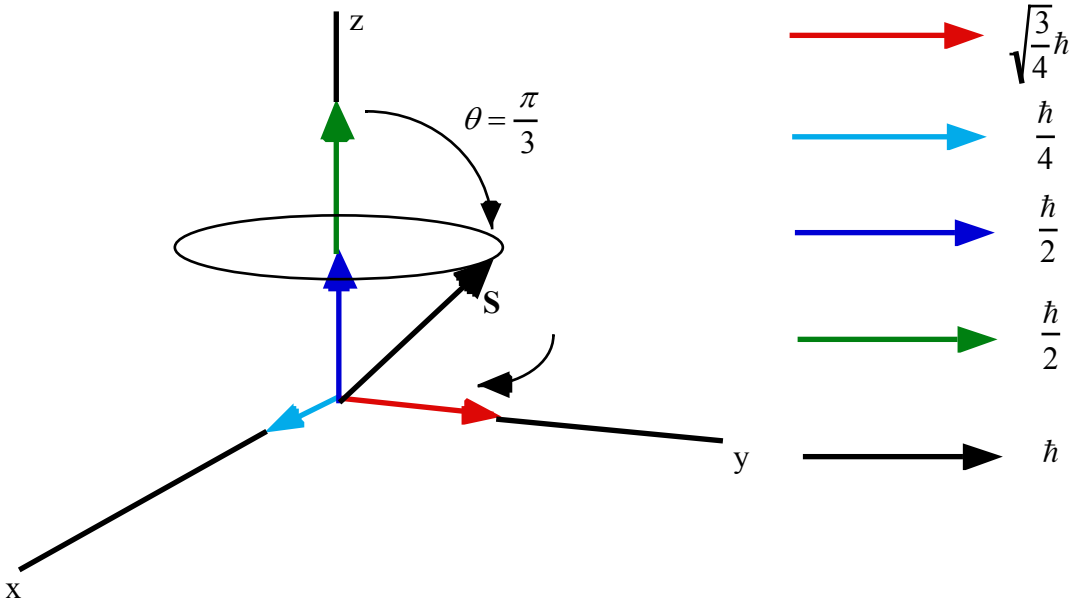

Figure 1.16B. The orientation of the orbitsphere and **S** that has the angular momentum components shown in Figure 1.16A. The applied magnetic field is in the z-axis direction. The dipole-current spins about the **S**-axis at angular velocity ω_n given by Eq. (1.55) and the orbitsphere and **S** precess at the Larmor frequency about the z-axis.

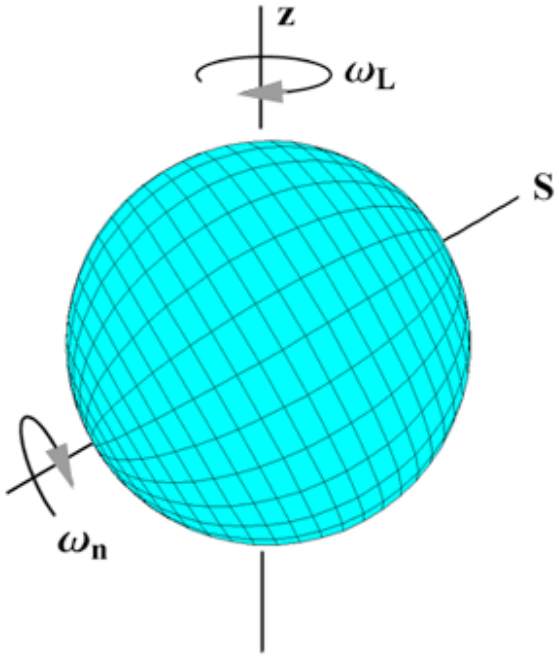

As shown in Figure 1.16, **S** forms a cone in time in the nonrotating laboratory frame with an angular momentum of $\hbar$ that is the source of the known magnetic moment of a Bohr magneton (Eq. (28) of Box 1.2) as shown in the Magnetic Parameters of the Electron (Bohr Magneton) section. The projection of this angular momentum onto the z-axis of $\frac{\hbar}{2}$ adds to the z-axis component before the magnetic field was applied to give a total of $\hbar$. Thus, in the absence of a resonant precession, the z-component of the angular momentum is $\frac{\hbar}{2}$, but the excitation of the precessing **S** component gives $\hbar$—twice the angular momentum on the z-axis. In addition, rather than a continuum of orientations with corresponding energies, the orientation of the magnetic moment must be only parallel or antiparallel to the magnetic field. This arises from conservation of angular momentum between the "static" and "dynamic" z-axis projections of the angular momentum with the additional constraint that the angular momentum has a "kinetic" as well as a "potential" or vector potential component. To conserve angular momentum, flux linkage by the electron is quantized in units of the magnetic flux quantum, $\Phi_0 = \frac{h}{2e}$, as shown in Box 1.2 and in the Electron g Factor section. Thus, the spin quantum number is $s = \frac{1}{2};\ m_s = \pm\frac{1}{2}$, but the observed Zeeman splitting corresponds to a full Bohr magneton due to $\hbar$ of angular momentum. This aspect was historically felt to be inexplicable in terms of classical physics and merely postulated in the past.

The demonstration that the boundary conditions of the electron in a magnetic field are met appears in Box 1.2. The observed electron parameters are explained physically. Classical laws give 1.) a gyromagnetic ratio of $\frac{e}{2m}$, 2.) a Larmor precession frequency of $\frac{e\mathbf{B}}{2m}$, 3.) the Stern-Gerlach experimental result of quantization of the angular momentum that implies a spin quantum number of 1/2 corresponding to an angular momentum of $\frac{\hbar}{2}$ on the z-axis, and 4.) the observed Zeeman splitting due to a magnetic moment of a Bohr magneton $\mu_B = \frac{e\hbar}{2m_e}$ corresponding to an angular momentum of $\hbar$ on the z-axis. Furthermore, the solution is relativistically invariant as shown in the Special Relativistic Correction to the Ionization Energies section. Dirac originally attempted to solve the bound electron physically with stability with respect to radiation according to Maxwell's equations with the further constraints that it was relativistically invariant and gave rise to electron spin [17]. He was unsuccessful and resorted to the current mathematical probability-wave model that has many problems as discussed in Appendix II: Quantum Electrodynamics (QED) is Purely Mathematical and Has No Basis in Reality.

ROTATIONAL PARAMETERS OF THE ELECTRON (ANGULAR MOMENTUM, ROTATIONAL ENERGY, AND MOMENT OF INERTIA)

One result of the correlated motion along great circles is that some of the kinetic energy is not counted in the rotational energy. That is, for any spin axis there will be an infinite number of great circles with planes passing through that axis with θ angles other than 90°. All points on

any one of these great circles will be moving, but not all of that motion will be part of the rotational energy; only that motion perpendicular to the spin axis will be part of the rotational energy. Thus, the rotational kinetic energy will always be less than the total kinetic energy. Furthermore, the following relationships must hold.

$$E_{rotational} = \frac{1}{2} I\omega^2 \le \frac{1}{2} m_e v^2 \tag{1.86}$$

$$I\omega \le \hbar \tag{1.87}$$

$$I \le m_e r^2 \tag{1.88}$$

Furthermore, it is known from the Stern-Gerlach experiment that a beam of silver atoms splits into two components when passed through an inhomogeneous magnetic field. This experiment implies a magnetic moment of one Bohr magneton and an associated angular momentum quantum number of 1/2. Historically, this quantum number is called the spin quantum number, and that designation will be retained. The angular momentum can be thought of arising from a spin component or equivalently an orbital component of the spin. The z-axis projection of the spin angular momentum was derived in the Spin Angular Momentum of the Orbitsphere with $\ell = 0$ section.

$$L_z = I\omega \mathbf{i}_z = \pm\frac{\hbar}{2} \tag{1.89}$$

where ω is given by Eq. (1.55); so, for $\ell = 0$

$$\left|L_z\right| = I\frac{\hbar}{m_e r^2} = \frac{\hbar}{2} \tag{1.90}$$

Thus,

$$I_z = I_{spin} = \frac{m_e r_n^{\,2}}{2} \tag{1.91}$$

From Eq. (1.51),

$$E_{rotational\ \ spin} = \frac{1}{2}\left[I_{spin}\omega^2\right] \tag{1.92}$$

From Eqs. (1.55) and (1.91),

$$E_{rotational} = E_{rotational\ \ spin} = \frac{1}{2}\left[I_{spin}\left(\frac{\hbar}{m_e r_n^{\,2}}\right)^2\right] = \frac{1}{2}\left[\frac{m_e r_n^{\,2}}{2}\left(\frac{\hbar}{m_e r_n^{\,2}}\right)^2\right] = \frac{1}{4}\left[\frac{\hbar^2}{2I_{spin}}\right] \tag{1.93}$$

When $\ell \neq 0$, the spherical harmonic is not a constant and the charge-density function is not uniform over the orbitsphere. Thus, the angular momentum can be thought of arising from a spin component and an orbital component.

DERIVATION OF THE ROTATIONAL PARAMETERS OF THE ELECTRON

In the derivation of Eq. (1.59) and its solution for $E_{rotational}$ (Eq. (1.60)), the moment of inertia, I, was assumed by McQuarrie [12] to be the moment of inertia of a point particle, mr_n^2. However, the correct equation of the electron is a two dimensional shell with a constant or a constant plus a spherical harmonic angular dependence. In that case, the relationships given by Eqs. (1.86) to (1.88) must hold.

The substitution of $C_1 I$ for I in the rigid rotor problem [12] where C_1 is a positive constant does not change the form of the previous solution given by Eq. (1.60). However, the result that

$$C_1 = \left[\frac{\ell(\ell+1)}{\ell^2+2\ell+1}\right]^{\frac{1}{2}} < 1 \tag{1.94}$$

derived below gives

$$E_{rotational} = \frac{\hbar^2 \ell(\ell+1)}{2I\left(\ell^2+2\ell+1\right)} \tag{1.95}$$

and gives the moment of inertia of the orbitsphere, $I_{orbital}$, where $\ell \neq 0$ as

$$C_1 I = I_{orbital} = m_e r_n^2 \left[\frac{\ell(\ell+1)}{\left(\ell^2+2\ell+1\right)}\right]^{\frac{1}{2}} \tag{1.96}$$

The solution of Eq. (1.59) for $|\mathbf{L}|$, the magnitude of the orbital angular momentum, is [12]

$$|\mathbf{L}| = \hbar\sqrt{\ell(\ell+1)} \tag{1.97}$$

where I of Eq. (1.59) is the moment of inertia of a point charge. It is demonstrated by Eq. (1.57) that the total sum of the magnitudes of the angular momenta of the infinitesimal points of the electron orbitsphere is $\hbar$; therefore, the magnitude of the angular momentum of an electron orbitsphere about the z-axis must be less than $\hbar$, and the corresponding moment of inertia must be less than that given by $m_e r_n^2$. For example, the moment of inertia of the uniform spherical shell, I_{RS}, is [18]

$$I_{RS} = \frac{2}{3} m r_n^2 \tag{1.98}$$

Thus, Eq. (1.97) must be multiplied by a constant, $0 < C_2 < 1$, to give the correct angular momentum. Given that generally $\mathbf{L}$ is

$$\mathbf{L} = I\omega\mathbf{i}_z \tag{1.99}$$

then

$$I_{orbital}\ \omega\mathbf{i}_z = \hbar C_2\sqrt{\ell(\ell+1)}\,, \tag{1.100}$$

where ω is given by Eq. (1.55). The orbital moment of inertia, $I_{orbital}$, is

$$I_{orbital} = m_e r_n^2 C_2\sqrt{\ell(\ell+1)} \tag{1.101}$$

The total kinetic energy, T, of the orbitsphere is

$$T = \frac{1}{2} m_e v_n^2 \tag{1.102}$$

Substitution of Eq. (1.56) gives

$$T = \frac{\hbar^2}{2m_e r_n^2} \tag{1.103}$$

$E_{rotational}$ of the rigid shell is given by Eq. (1.51) with I given by Eq. (1.98). $E_{rotational\ \text{orbital}}$ of the orbitsphere is given by Eq. (1.60) multiplied by C_2^2 so that Eqs. (1.86) to (1.88) hold with $I = m_e r_n^2$.

$$E_{rotational\ \text{orbital}} = C_2^2 \frac{\hbar^2}{2I} \ell(\ell+1) \tag{1.104}$$

Eq. (1.59) can be expressed in terms of the variable x which is substituted for $\cos\theta$. The resulting function $P(x)$ is called Legendre's equation and is a well-known equation in classical physics. It occurs in a variety of problems that are formulated in spherical coordinates. When the power series method of solution is applied to $P(x)$, the series must be truncated in order that the solutions be finite at $x = \pm 1$. The solution to Legendre's equation given by Eq. (1.60) is the maximum term of a series of solutions corresponding to the m and ℓ values [12, 19]. The rotational energy must be normalized by the total number of states—each corresponding to a set of quantum numbers of the power series solution. As demonstrated in the Excited States of the One-Electron Atom (Quantization) section, the quantum numbers of the excited states are

$n = 2, 3, 4, \ldots$

$\ell = 1, 2, \ldots, n-1$

$m = -\ell, -\ell+1, \ldots, 0, \ldots, +\ell$

In the case of an orbitsphere excited state, each rotational state solution of Eq. (1.59) (Legendre's equation) corresponds to a multipole moment of the charge-density function (Eq. (1.65)). $E_{rotational\ \text{orbital}}$ is normalized by $N_{\ell,s}$, the total number of multipole moments. $N_{\ell,s}$, the total number of multipole moments where each corresponds to an ℓ and mℓ quantum number of an energy level corresponding to a principal quantum number of n is

$$N_{\ell,s} = \sum_{\ell=0}^{n-1} \sum_{m_\ell=-\ell}^{+\ell} 1 = \sum_{\ell=0}^{n-1} 2\ell+1 = n^2 = (\ell+1)^2 = \ell^2 + 2\ell + 1 \tag{1.105}$$

Thus, C_2^2 is equal to $N_{\ell,s}^{-1}$ given by Eq. (1.105). Substitution of Eq. (1.105) into Eqs. (1.101) and (1.104) gives

$$E_{rotational\ \text{orbital}} = \frac{\hbar^2}{2I}\left[\frac{\ell(\ell+1)}{\ell^2+2\ell+1}\right] = \frac{\hbar^2}{2I}\left[\frac{\ell}{\ell+1}\right] = \frac{\hbar^2}{2m_e r_n^{\ 2}}\left[\frac{\ell}{\ell+1}\right] \tag{1.106}$$

Substitution of Eq. (1.105) into Eq. (1.101) with Eqs. (1.55) and (1.101) gives the orbital moment of inertia and angular momentum:

$$I_{orbital} = m_e r_n^{\ 2}\left[\frac{\ell(\ell+1)}{\ell^2+2\ell+1}\right]^{\frac{1}{2}} = m_e r_n^{\ 2}\sqrt{\frac{\ell}{\ell+1}} \tag{1.107a}$$

$$\mathbf{L} = I\omega\mathbf{i}_z = I_{orbital}\omega\mathbf{i}_z = m_e r_n^{\ 2}\left[\frac{\ell(\ell+1)}{\ell^2+2\ell+1}\right]^{\frac{1}{2}}\omega\mathbf{i}_z = m_e r_n^{\ 2}\frac{\hbar}{m_e r_n^{\ 2}}\sqrt{\frac{\ell}{\ell+1}} = \hbar\sqrt{\frac{\ell}{\ell+1}} \tag{1.107b}$$

In the case of the excited states, the orbitsphere charge-density function for $\ell \neq 0$, Eq. (1.65), is the sum of two functions of equal magnitude. $\mathbf{L}_z$, total is given by the sum of the spin and orbital angular momenta. The principal energy levels of the excited states are split when a

magnetic field is applied. The energy shifts due to spin and orbital angular momenta are given in the Spin and Orbital Splitting section.

$$\ell \neq \mathbf{0}$$

$$L_{z\ total} = L_{z\ spin} + L_{z\ orbital} \tag{1.108}$$

Similarly, the orbital rotational energy arises from a spin function (spin angular momentum) modulated by a spherical harmonic angular function (orbital angular momentum). The time-averaged mechanical angular momentum and rotational energy associated with the traveling charge-density wave on the orbitsphere is zero:

$$\left\langle L_{z\ orbital} \right\rangle = 0 \tag{1.109a}$$

$$\left\langle E_{rotational\ \text{orbital}} \right\rangle = 0 \tag{1.109b}$$

And, in the case of an excited state, the angular momentum of $\hbar$ is carried by the fields of the trapped photon. The energy and angular momentum amplitudes that couple to external magnetic and electromagnetic fields are given by Eq. (1.107b) and (1.106), respectively. The rotational energy due to spin is given by Eq. (1.93), and the total kinetic energy is given by Eq. (1.103). The demonstration that the modulated orbitsphere solutions are solutions of the wave equation appears in Box 1.1.

BOX 1.1 DERIVATION OF THE ROTATIONAL PARAMETERS OF THE ELECTRON FROM A SPECIAL CASE OF THE WAVE EQUATION—THE RIGID ROTOR EQUATION

For a time harmonic charge-density function, Eq. (1.49) becomes

$$\left[\frac{1}{r^2\sin\theta}\frac{\partial}{\partial\theta}\left(\sin\theta\frac{\partial}{\partial\theta}\right)_{r,\phi} + \frac{1}{r^2\sin^2\theta}\left(\frac{\partial^2}{\partial\phi^2}\right)_{r,\theta} + \frac{\omega^2}{v^2}\right]A(\theta,\phi) = 0 \tag{1}$$

Substitution of the velocity about a Cartesian coordinate axis, $v = \rho\omega$, into Eq. (1) gives

$$\left[\frac{1}{r^2\sin\theta}\frac{\partial}{\partial\theta}\left(\sin\theta\frac{\partial}{\partial\theta}\right)_{r,\phi} + \frac{1}{r^2\sin^2\theta}\left(\frac{\partial^2}{\partial\phi^2}\right)_{r,\theta} + \frac{\omega^2}{(\rho\omega)^2}\right]A(\theta,\phi) = 0 \tag{2}$$

Substitution of Eq. (1.55) into Eq. (1.2) gives

$$\left[\frac{1}{r^2\sin\theta}\frac{\delta}{\delta\theta}\left(\sin\theta\frac{\delta}{\delta\theta}\right)_{r,\phi} + \frac{1}{r^2\sin^2\theta}\left(\frac{\delta^2}{\delta\phi^2}\right)_{r,\theta} + \frac{\omega_n^2}{\left(\rho\frac{\hbar}{m_e r_n^2}\right)^2}\right]A(\theta,\phi) = 0 \tag{3}$$

Multiplication by the denominator of the second term in Eq. (3) gives

$$\left[\left(\rho\frac{\hbar}{m_e r_n^2}\right)^2\left[\frac{1}{r^2\sin\theta}\frac{\partial}{\partial\theta}\left(\sin\theta\frac{\partial}{\partial\theta}\right)_{r,\phi} + \frac{1}{r^2\sin^2\theta}\left(\frac{\partial^2}{\partial\phi^2}\right)_{r,\theta}\right] + \omega_n^2\right]A(\theta,\phi) = 0 \tag{4}$$

Substitution of Eq. (1.51) gives

$$\left[\left(\rho\frac{\hbar}{m_e r_n^2}\right)^2\left[\frac{1}{r^2\sin\theta}\frac{\partial}{\partial\theta}\left(\sin\theta\frac{\partial}{\partial\theta}\right)_{r,\phi} + \frac{1}{r^2\sin^2\theta}\left(\frac{\partial^2}{\partial\phi^2}\right)_{r,\theta}\right] + \frac{2E_{rot}}{I}\right]A(\theta,\phi) = 0 \tag{5}$$

The total rotational energy is given by the superposition of ℓ quantum states corresponding to a multipole expansion of total rotational energy of the orbitsphere. The total number, N, of multipole moments where each corresponds to an ℓ and mℓ quantum number of an energy level corresponding to a principal quantum number of n is

$$N = \sum_{\ell=0}^{n-1} \sum_{m_\ell=-\ell}^{+\ell} 1 = \sum_{\ell=0}^{n-1} 2\ell+1 = \ell^2+2\ell+1 = \left(\ell+1\right)^2 = n^2 \tag{6}$$

Summing over all quantum states gives

$$\left[\sum_{\ell=0}^{n-1} \sum_{m_\ell=-\ell}^{+\ell} \left(\rho\frac{\hbar}{m_e r_n^2}\right)^2 \left[\frac{1}{r^2\sin\theta}\frac{\partial}{\partial\theta}\left(\sin\theta\frac{\partial}{\partial\theta}\right)_{r,\phi} + \frac{1}{r^2\sin^2\theta}\left(\frac{\partial^2}{\partial\phi^2}\right)_{r,\theta}\right] + \sum_{\ell=0}^{n-1} \sum_{m_\ell=-\ell}^{+\ell} \frac{2E_{rot}}{I}\right] A(\theta,\phi) = 0 \tag{7}$$

Each of the orbital energy, orbital moment of inertia, and orbital angular momentum is a modulation of the orbitsphere function. Thus, the sum of ρ^2 over all ℓ quantum numbers is r_n^2. Substitution of $\rho_z = r_n\cos\theta;\ \rho_x = r_n\sin\theta\cos\phi;\ \rho_y = r_n\sin\theta\sin\phi$ into Eq. (7) gives

$$\left[\left(r_n\frac{\hbar}{m_e r_n^2}\right)^2 \left[\frac{1}{r_n^2\sin\theta}\frac{\partial}{\partial\theta}\left(\sin\theta\frac{\partial}{\partial\theta}\right)_{r,\phi} + \frac{1}{r_n^2\sin^2\theta}\left(\frac{\partial^2}{\partial\phi^2}\right)_{r,\theta}\right] + \left(\ell^2+2\ell+1\right)\frac{2E_{rot}}{I}\right] A(\theta,\phi) = 0 \tag{8}$$

where $\frac{2E_{rot}}{I}$ is the constant, ω_n given by Eq. (1.55), and $r = r_n$. Eq. (8) can be expressed in terms of the rotational energy of any given mode by dividing the denominator of the first term by, K^2, the factor corresponding to the vector projection of the rotational energy onto the z-axis.

$$\left[\frac{I\hbar^2}{2m_e^2 r_n^4\left(\ell^2+2\ell+1\right)}\left[\frac{1}{\sin\theta}\frac{\partial}{\partial\theta}\left(\sin\theta\frac{\partial}{\partial\theta}\right)_{r,\phi} + \frac{1}{\sin^2\theta}\left(\frac{\partial^2}{\partial\phi^2}\right)_{r,\theta}\right] + E_{rot}\right] A(\theta,\phi) = 0 \tag{9}$$

In the case that E_{rot} is the total rotational energy which is equal to the kinetic energy of the orbitsphere given by Eq. (1.103) and that the moment of inertia is given by

$$I = m_e r_n^2 \tag{10}$$

Eq. (9) becomes equivalent to Eq. (1.59).

$$\left[\frac{1}{N}\frac{\hbar^2}{2I}\left[\frac{1}{\sin\theta}\frac{\partial}{\partial\theta}\left(\sin\theta\frac{\partial}{\partial\theta}\right)_{r,\phi} + \frac{1}{\sin^2\theta}\left(\frac{\partial^2}{\partial\phi^2}\right)_{r,\theta}\right] + E_{rot\ \ total}\right] A(\theta,\phi) = 0 \tag{11}$$

where N is one. Eq. (11) applies to all of the multipole modes of the rotational energy with the appropriate moment of inertia, I, and factor N; thus, the rotational energy of each mode is given by Eq. (1.58) with these conditions. Eq. (9) can be expressed in terms of the rotational energy of any given mode by dividing the first term by, K^2, the factor corresponding to the vector projection of the rotational energy and the moment of inertia onto the z-axis.

$$\frac{I\hbar^2}{2m_e^2 r_n^4 K^2\left(\ell^2+2\ell+1\right)}\left[\frac{1}{\sin\theta}\frac{\partial}{\partial\theta}\left(\sin\theta\frac{\partial}{\partial\theta}\right)_{r,\phi} + \frac{1}{\sin^2\theta}\left(\frac{\partial^2}{\partial\phi^2}\right)_{r,\theta} + E_{rot}\right] A(\theta,\phi) = 0 \tag{12}$$

where in the case of the spherical harmonics, $N = \ell^2+2\ell+1$. From Eq. (1.51) and Eq. (1.99), Eq. (12) can be expressed as

$$\left[\frac{\hbar^2}{m_e^2 r_n^4 K^2\left(\ell^2+2\ell+1\right)}\left[\frac{1}{\sin\theta}\frac{\partial}{\partial\theta}\left(\sin\theta\frac{\partial}{\partial\theta}\right)_{r,\phi}+\frac{1}{\sin^2\theta}\left(\frac{\partial^2}{\partial\phi^2}\right)_{r,\theta}\right]+\frac{L^2}{I^2}\right]A(\theta,\phi)=0 \tag{13}$$

In the case of the spherical harmonic functions with Eq. (1.99) and Eq. (1.55), Eq. (12) gives

$$\sqrt{\frac{\hbar^2\left(\ell\left(\ell+1\right)\right)}{m_e^2 r_n^4 K^2\left(\ell^2+2\ell+1\right)}}=\frac{L}{I}=\frac{\hbar}{m_e r_n^2} \tag{14}$$

Thus,

$$\sqrt{\frac{\left(\ell\left(\ell+1\right)\right)}{\left(\ell^2+2\ell+1\right)}}=K \tag{15}$$

Eq. (12) becomes Eq. (11) where the rotational energy is given by Eq. (1.106).

$$E_{rotational\ \text{orbital}}=\frac{\hbar^2}{2I}\left[\frac{\ell\left(\ell+1\right)}{\ell^2+2\ell+1}\right] \tag{16}$$

and the orbital moment of inertia is given by Eq. (1.107).

$$I_{orbital}=m_e r_n{}^2\left[\frac{\ell(\ell+1)}{\ell^2+2\ell+1}\right]^{\frac{1}{2}} \tag{17}$$

The substitution of Eqs. (1.65), (6), and (16) into Eq. (11) gives

$$-\frac{\hbar^2}{2I}\left[\frac{\ell\left(\ell+1\right)}{\ell^2+2\ell+1}\right]+\frac{\hbar^2}{2m_e r_n^2}\sqrt{\frac{\ell\left(\ell+1\right)}{\ell^2+2\ell+1}}=0 \tag{18}$$

Substitution of Eq. (17) into Eq. (18) gives

$$-\frac{\hbar^2}{2m_e r_n^2\sqrt{\frac{\ell\left(\ell+1\right)}{\ell^2+2\ell+1}}}\left[\frac{\ell\left(\ell+1\right)}{\ell^2+2\ell+1}\right]+\frac{\hbar^2}{2m_e r_n^2}\sqrt{\frac{\ell\left(\ell+1\right)}{\ell^2+2\ell+1}}=0 \tag{19}$$

$$0=0 \tag{20}$$

Thus, the modulated orbitsphere solutions are shown to be solutions of the wave equation by their substitution into the wave equation (Eqs. (18-20). The present derivation of the rigid rotor equation given by the substitution of

$$E_{rot}=\frac{1}{2}I\omega_n^2$$

$$\omega_n=\frac{\hbar}{m_e r_n^2} \tag{21}$$

$$v=\rho\omega_n$$

is consistent with the wave equation relationship:

$$v=\lambda\frac{\omega}{2\pi} \tag{22}$$

Whereas, Schrödinger derivation from the Helmholtz equation [1] with the substitution of

$$\lambda = \frac{h}{m_e v} \tag{23}$$

gives the rigid rotor equation with the paradox that

$$v^2 = \frac{h}{m_e}\frac{\omega}{2\pi} \tag{24}$$

which is not the wave relationship,

$$v = \lambda\frac{\omega}{2\pi} \tag{25}$$

REFERENCES

1. D. A. McQuarrie, *Quantum Chemistry*, University Science Books, Mill Valley, CA, (1983), pp. 78-79.

MAGNETIC PARAMETERS OF THE ELECTRON (BOHR MAGNETON)

THE MAGNETIC FIELD OF AN ORBITSPHERE FROM SPIN

The orbitsphere with $\ell = 0$ is a shell of negative charge current comprising correlated charge motion along great circles. The superposition of the vector projection of the orbitsphere angular momentum on the z-axis is $\frac{\hbar}{2}$ with an orthogonal component of $\frac{\hbar}{4}$. As shown in the Orbitsphere Equation of Motion for $\ell = 0$ section, the application of a magnetic field to the orbitsphere gives rise to a precessing angular momentum vector $\mathbf{S}$ directed from the origin of the orbitsphere at an angle of $\theta = \frac{\pi}{3}$ relative to the applied magnetic field. The precession of $\mathbf{S}$ with an angular momentum of $\hbar$ forms a cone in the nonrotating laboratory frame to give a perpendicular projection of $\mathbf{S}_\perp = \pm\sqrt{\frac{3}{4}}\hbar$ (Eq. (1.84)) and a projection onto the axis of the applied magnetic field of $\mathbf{S}_\parallel = \pm\frac{\hbar}{2}$ (Eq. (1.85)). The superposition of the $\frac{\hbar}{2}$ z-axis component of the orbitsphere angular momentum and the $\frac{\hbar}{2}$ z-axis component of $\mathbf{S}$ gives $\hbar$ corresponding to the observed magnetostatic electron magnetic moment of a Bohr magneton. The $\hbar$ of angular momentum along $\mathbf{S}$ has a corresponding precessing magnetic moment of 1 Bohr magneton [20]:

$$\mu_B = \frac{e\hbar}{2m_e} = 9.274\ X\ 10^{-24}\ JT^{-1} \tag{1.110}$$

The rotating magnetic field of $\mathbf{S}$ is discussed in Box 1.2. The magnetostatic magnetic field corresponding to μ_B derived below is given by

$$\mathbf{H} = \frac{e\hbar}{m_e r_n^3}(\mathbf{i}_r \cos\theta - \mathbf{i}_\theta \sin\theta) \qquad \text{for } r < r_n \tag{1.111}$$

$$\mathbf{H} = \frac{e\hbar}{2m_e r^3}(\mathbf{i}_r 2\cos\theta + \mathbf{i}_\theta \sin\theta) \quad \text{for } r > r_n \tag{1.112}$$

It follows from Eq. (1.110), the relationship for the Bohr magneton, and relationship between the magnetic dipole field and the magnetic moment $\mathbf{m}$ [21] that Eqs. (1.111) and (1.112) are the equations for the magnetic field due to a magnetic moment of a Bohr magneton, $\mathbf{m} = \mu_B \mathbf{i}_\mathbf{z}$ where $\mathbf{i}_\mathbf{z} = \mathbf{i}_\mathbf{r}\cos\theta - \mathbf{i}_\theta \sin\theta$. Note that the magnetic field is a constant for $r < r_n$. See Figure 1.17. It is shown in the Magnetic Parameters of the Electron (Bohr Magneton) section that the energy stored in the magnetic field of the electron orbitsphere is

$$E_{mag,total} = \frac{\pi\mu_o e^2\hbar^2}{m_e{}^2 r_1^3} \tag{1.113}$$

Figure 1.17A. The two-dimensional cut-away representation of the magnetic field of an electron orbitsphere. The field is a dipole outside the orbitsphere and uniform inside the orbitsphere.

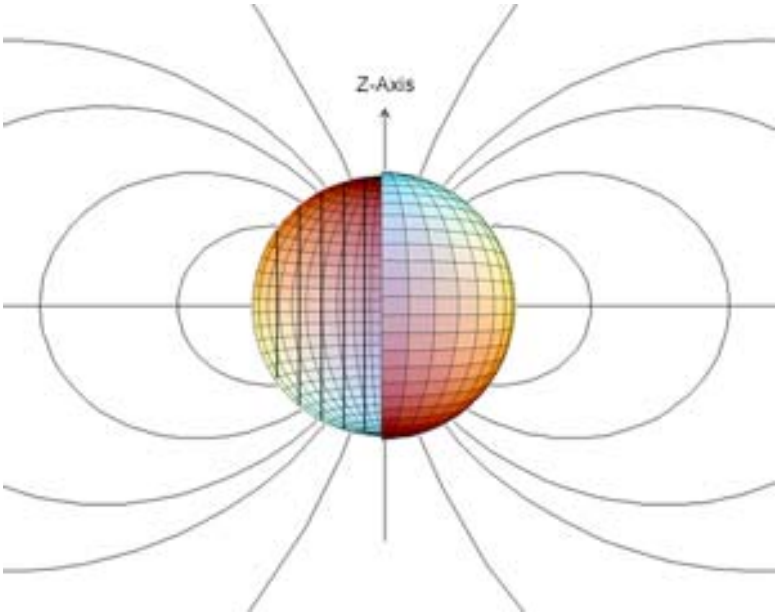

Figure 1.17B. The three-dimensional cut-away representation of the magnetic field of an electron orbitsphere. The field is a dipole outside the orbitsphere and uniform inside the orbitsphere.

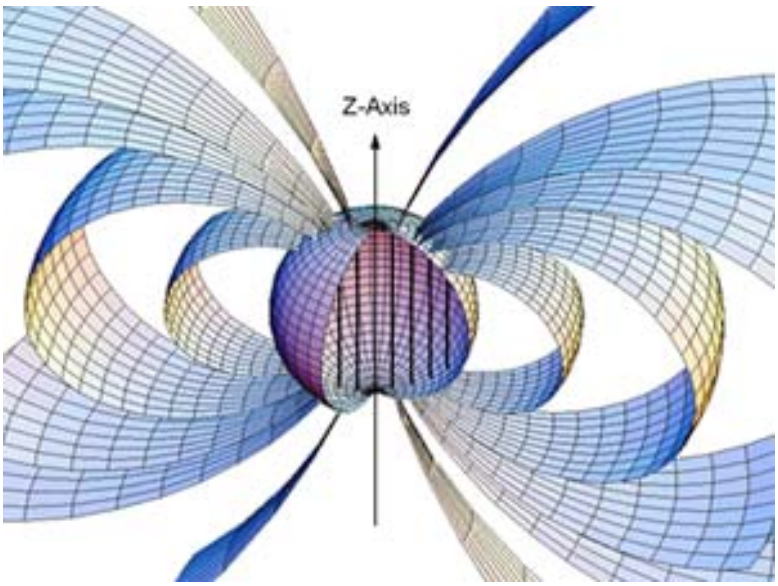

DERIVATION OF THE MAGNETIC FIELD

For convenience the angular moment vector with a magnitude in the stationary frame of $\hbar$ will be defined as the z-axis as shown in Figure 1.17[8] . The magnetic field must satisfy the following relationships:

$$\nabla \cdot \mathrm{H} = 0 \text{ } \textit{in free space} \tag{1.114}$$

$$\mathbf{n} \; X \; (\mathbf{H}_a - \mathbf{H}_b) = \mathbf{K} \tag{1.115}$$

$$\mathbf{n} \cdot (\mathbf{H}_a - \mathbf{H}_b) = 0 \tag{1.116}$$

$$\mathbf{H} = -\nabla \psi \tag{1.117}$$

Since the field is magnetostatic, the current is equivalent to current loops along the z-axis. Then, the z-component of the current, $|i|$, for a current loop of total charge, e, oriented at an angle θ with respect to the z-axis is given by the product of the charge, the angular velocity given by Eq. (1.55), and $\sin\theta$ where the projection of the current of the orbitsphere perpendicular to the z-axis which carries the incremental current, $\mathbf{i}i_\phi$, is a function of $\sin\theta$.

---

[8] As shown in Box 1.2, the angular momentum of $\hbar$ on the $\mathbf{S}$-axis is due to a photon standing wave that is phase-matched to a spherical harmonic source current, a spherical harmonic dipole $Y_\ell^m(\theta,\phi) = \sin\theta$ with respect to the $\mathbf{S}$-axis. The dipole spins about the $\mathbf{S}$-axis at the angular velocity given by Eq.(1.55). Since the field is magnetostatic in the RF rotating frame, the current is equivalent to current loops along the $\mathbf{S}$-axis. Thus, the derivation of the corresponding magnetic field is the same as that of the stationary field given in this section.

$$|i| = \frac{e\hbar}{m_e {r_n}^2} \sin\theta \tag{1.118}$$

The angular function of the current density of the orbitsphere is normalized by the geometrical factor N [18] given by

$$N = \frac{4\pi r_n^3}{2\pi \int_{-r_n}^{r_n} \left(r_n^2 - z^2\right) dz} = \frac{3}{2} \tag{1.119}$$

corresponding to the angular momentum of $\hbar$. (Eq. (1.119) can also be expressed in spherical coordinates for the density of a uniform shell divided by the integral in θ and ϕ of that of a spherical dipole squared [12]. The integration gives $\frac{8\pi}{3}$ which normalized by the uniform mass-density factor of 4π gives the geometrical factor of $\left(\frac{2}{3}\right)^{-1}$) The current density $\mathbf{K}i_\phi$ along the z-axis having a vector orientation perpendicular to the angular momentum vector is given by dividing the magnitude of $\mathbf{i}i_\phi$ (Eq. (1.118)) by the length r_n. The current density of the orbitsphere in the incremental length dz is

$$\mathbf{K}(\rho, \phi, z) = \mathbf{i}_\phi N \frac{e\hbar}{m_e {r_n}^3} = \mathbf{i}_\phi \frac{3}{2} \frac{e\hbar}{m_e {r_n}^3} \tag{1.120}$$

Because

$$z = r\cos\theta \tag{1.121}$$

the differential length is given by

$$dz = -\sin\theta r_n d\theta \tag{1.122}$$

and so the current density in the differential length $r_n d\theta$ as measured along the periphery of the orbitsphere is a function of $\sin\theta$ as given in Eq. (1.118). From Eq. (1.120), the surface current-density function of the orbitsphere about the z-axis ($\mathbf{S}$-axis) is given by

$$\mathbf{K}(r, \theta, \varphi) = \mathbf{i}_\phi \frac{3}{2} \frac{e\hbar}{m_e {r_n}^3} \sin\theta \tag{1.123}$$

Substitution of Eq. (1.123) into Eq. (1.115) gives

$$H_\theta^a - H_\theta^b = \frac{3}{2} \frac{e\hbar}{m_e {r_n}^3} \sin\theta \tag{1.124}$$

To obtain H_θ, the derivative of Y with respect to θ must be taken, and this suggests that the θ dependence of Y be taken as $\cos\theta$. The field is finite at the origin and is zero at infinity; so, solutions of Laplace's equation in spherical coordinates are selected because they are consistent with these conditions [22].

$$\Psi = C\left[\frac{r}{r_n}\right]\cos\theta \ ; \qquad r < r_n \tag{1.125}$$

$$\Psi = A\left[\frac{r_n}{r}\right]^2 \cos\theta \ ; \qquad r > r_n \tag{1.126}$$

The negative gradients of these potentials are

$$\mathbf{H} = \frac{-C}{r_n}(\mathbf{i}_r \cos\theta - \mathbf{i}_\theta \sin\theta) \quad \text{for } r < r_n \tag{1.127}$$

$$\mathbf{H} = \frac{A}{r_n}\left[\frac{r_n}{r}\right]^3 (\mathbf{i}_r 2\cos\theta + \mathbf{i}_\theta \sin\theta) \quad \text{for } r > r_n \tag{1.128}$$

The continuity conditions of Eqs. (1.115), (1.116), (1.123), and (1.124) are applied to obtain the following relationships among the variables

$$\frac{-C}{r_n} = \frac{2A}{r_n} \tag{1.129}$$

$$\frac{A}{r_n} - \frac{C}{r_n} = \frac{3}{2}\frac{e\hbar}{m_e {r_n}^3} \tag{1.130}$$

Solving the variables algebraically gives the magnetic fields of an electron:

$$\mathbf{H} = \frac{e\hbar}{m_e r_n^3}(\mathbf{i}_r \cos\theta - \mathbf{i}_\theta \sin\theta) \qquad \text{for } r < r_n \tag{1.131}$$

$$\mathbf{H} = \frac{e\hbar}{2m_e r^3}(\mathbf{i}_r 2\cos\theta + \mathbf{i}_\theta \sin\theta) \quad \text{for } r > r_n \tag{1.132}$$

The field is that of a Bohr magneton which matches the observed boundary conditions given in the Orbitsphere Equation of Motion for $\ell = 0$ section including the required spherical symmetry. The demonstration that the boundary conditions of the electron in a magnetic field are met appears in Box 1.2.

DERIVATION OF THE ENERGY

The energy stored in the magnetic field of the electron is

$$E_{mag} = \frac{1}{2}\mu_o \int_0^{2\pi}\int_0^{\pi}\int_0^{\infty} H^2 r^2 \sin\theta dr d\theta d\Phi \tag{1.133}$$

$$E_{mag\ \text{total}} = E_{mag\ \text{external}} + E_{mag\ \text{internal}} \tag{1.134}$$

$$E_{mag\ \text{internal}} = \frac{1}{2}\mu_o \int_0^{2\pi}\int_0^{\pi}\int_0^{r_1}\left[\frac{e\hbar}{m_e r_1^3}\right]^2 \left(\cos^2\theta + \sin^2\theta\right) r^2 \sin\theta dr d\theta d\Phi \tag{1.135}$$

$$E_{mag\ \text{internal}} = \frac{2\pi\mu_o e^2\hbar^2}{3{m_e}^2 r_1^3} \tag{1.136}$$

$$E_{mag\ \text{external}} = \frac{1}{2}\mu_o \int_0^{2\pi}\int_0^{\pi}\int_{r_1}^{\infty}\left[\frac{e\hbar}{2m_e r_1^3}\right]^2 \left(4\cos^2\theta + \sin^2\theta\right) r^2 \sin\theta dr d\theta d\Phi \tag{1.137}$$

$$E_{mag\ \text{external}} = \frac{\pi\mu_o e^2\hbar^2}{3{m_e}^2 r_1^3} \tag{1.138}$$

$$E_{mag\ \text{total}} = \frac{2\pi\mu_o e^2\hbar^2}{3m_e{}^2 r_1^3} + \frac{\pi\mu_o e^2\hbar^2}{3m_e{}^2 r_1^3} \tag{1.139}$$

$$E_{mag\ \text{total}} = \frac{\pi\mu_o e^2\hbar^2}{m_e{}^2 r_1^3} \tag{1.140}$$

$$E_{mag\ \text{total}} = \frac{4\pi\mu_o \mu_B^2}{r_1^3} \tag{1.141}$$

BOX 1.2. BOUNDARY CONDITIONS OF THE ELECTRON IN A MAGNETIC FIELD ARE MET

As shown in the Electron g Factor section, when a magnetic field with flux **B** is applied to an electron in a central field which comprises current loops, the orbital radius of each does not change due to the Lorentzian force provided by **B**, but the velocity changes as follows [1]:

$$\Delta v = \frac{erB}{2m_e} \tag{1}$$

corresponding to precession frequency of

$$\omega = \frac{\Delta v}{r} = \frac{eB}{2m_e} = \gamma_e B \tag{2}$$

where γ_e is the electron gyromagnetic ratio and ω is the Larmor frequency. Eq. (1) applies to the current perpendicular to the magnetic flux. In this case, the moment of inertia I of the orbitsphere which is a uniformly charged sphere [2] is

$$I = \frac{2}{3} m_e r_1^2 \tag{3}$$

From Eqs. (2) and (3), the corresponding angular momentum L and rotational energy E_{rot} are

$$L = I\omega = \frac{2}{3} m_e r_1^2 \gamma_e B \tag{4}$$

and

$$E_{rot} = \frac{1}{2} I\omega^2 = \frac{1}{3} m_e r_1^2 \left(\gamma_e B\right)^2 \tag{5}$$

respectively. The change in the magnetic moment corresponding to Eq. (1) is [1]:

$$\Delta\mathbf{m} = -\frac{e^2 r_1^2}{4m_e}\mathbf{B} \tag{6}$$

Using Eqs. (2-6), in the case of a very strong magnetic flux of 10 T applied to atomic hydrogen:

$$\omega = 8.794\ X\ 10^{11}\ rad \cdot \sec^{-1} \tag{7}$$

$$I = 1.701\ X\ 10^{-51}\ kg \cdot m^2 \tag{8}$$

$$L = 1.496\ X\ 10^{-39}\ J \cdot s \tag{9}$$

$$E_{rot} = 6.576\ X\ 10^{-28} J = 4.104\ X\ 10^{-9}\ eV \tag{10}$$

and

$$\Delta m = 1.315\ X\ 10^{-28} J \cdot T^{-1} \tag{11}$$

where the radius is given by Eq. (1.239) and $2/3$, the geometrical factor of a uniformly charged sphere [2], was used in the case of Eq. (11). Thus, these effects of the magnetic field are very small when they are compared to the intrinsic angular momentum of the electron of

$$L = \hbar = 1.055\ X\ 10^{-34}\ J \cdot s \tag{12}$$

The electronic angular frequency of hydrogen given by Eqs. (1.55) and (1.239)

$$\omega_1 = \frac{\hbar}{m_e r_1^2} = 4.134\ X\ 10^{16}\ rad \cdot \sec^{-1} \tag{13}$$

the total kinetic energy given by Eq. (1.241)

$$T = 13.606\ eV \tag{14}$$

and the magnetic moment of a Bohr magneton given by Eq. (1.110)

$$\mu_B = \frac{e\hbar}{2m_e} = 9.274\ X\ 10^{-24}\ JT^{-1} \tag{15}$$

E_{rot} is the energy that arises due to the application of the external flux $\mathbf{B}$. Thus, the external work required to apply the field is also given by Eq. (10). Since the orbitsphere is uniformly charged and is superconducting, this energy is conserved when the field is removed. It is also independent of the direction of the magnetic moment due to the intrinsic angular momentum of the orbitsphere of $\hbar$. The corresponding magnetic moment given by Eq. (6) does not change when the intrinsic magnetic moment of the electron changes orientation. Thus, it does not contribute to the energy of a spin-flip transition observed by the Stern Gerlach experiment. It always opposes the applied field and gives rise to the phenomenon of the diamagnetic susceptibility of materials which Eq. (6) predicts with very good agreement with observations [1]. Eq. (6) also predicts the absolute chemical shifts of hydride ions that match experimental observations as shown in the Hydrino Hydride Ion Nuclear Magnetic Resonance Shift section.

As shown in the Spin Angular Momentum of the Orbitsphere with $\ell = 0$ section, the angular momentum of the orbitsphere in a magnetic field comprises the initial $\frac{\hbar}{2}$ projection on the z-axis and the initial $\frac{\hbar}{4}$ vector component in the xy-plane that precesses about the z-axis. A resonant excitation of the Larmor precession frequency gives rise to an additional component of angular momentum which is consistent with Maxwell's equations. As shown in the Excited States of the One-Electron Atom (Quantization) section, conservation of the $\hbar$ of angular momentum of a trapped photon can give rise to $\hbar$ of electron angular momentum along the $\mathbf{S}$-axis. The photon standing waves of excited states are spherical harmonic functions which satisfy Laplace's equation in spherical coordinates and provide the force balance for the corresponding charge (mass)-density waves. Consider the photon in the case of the precessing electron with a Bohr magneton of magnetic moment along the $\mathbf{S}$-axis. The radius of the orbitsphere is unchanged, and the photon gives rise to current on the surface that satisfies the condition

$$\nabla \cdot J = 0 \tag{16}$$

corresponding to a rotating spherical harmonic dipole [3] that phase-matches the current (mass) density of Eq. (1.123). Thus, the electrostatic energy is constant, and only the magnetic energy need be considered as given by Eqs. (23-25). The corresponding central field at the orbitsphere surface given by the superposition of the central field of the proton and that of the photon follows from Eqs. (2.10-2.17):

$$\mathbf{E} = \frac{e}{4\pi\varepsilon_o r^2}\left[Y_0^0(\theta,\phi)\mathbf{i}_\mathbf{r} + \mathrm{Re}\left\{Y_\ell^m(\theta,\phi)e^{i\omega_n t}\right\}\mathbf{i}_\mathbf{y}\delta(r-r_1)\right] \quad (17)$$

where the spherical harmonic dipole $Y_\ell^m(\theta,\phi) = \sin\theta$ is with respect to the $\mathbf{S}$-axis. Force balance according to Eq. (1.232) is maintained by the equivalence of the harmonic modulation of the charge and the mass where e/m_e is invariant as given in the Special Relativistic Correction to the Ionization Energies section. The dipole spins about the $\mathbf{S}$-axis at the angular velocity given by Eq. (1.55). In the frame rotating about the $\mathbf{S}$ axis, the electric field of the dipole is

$$\mathbf{E} = \frac{e}{4\pi\varepsilon_o r^2}\sin\theta\sin\varphi\delta(r-r_1)\mathbf{i}_\mathbf{y} \quad (18)$$

$$\mathbf{E} = \frac{e}{4\pi\varepsilon_o r^2}\left(\sin\theta\sin\phi\mathbf{i}_\mathbf{r} + \cos\theta\sin\phi\mathbf{i}_\theta + \sin\theta\cos\phi\mathbf{i}_\phi\right)\delta(r-r_1) \quad (19)$$

The resulting current is nonradiative as shown by Eq. (1.39) and in Appendix I: Nonradiation Based on the Electromagnetic Fields and the Poynting Power Vector. Thus, the field in the RF rotating frame is magnetostatic as shown in Figure 1.17 but directed along the $\mathbf{S}$-axis. The time-averaged angular momentum and rotational energy due to the charge density wave are zero as given by Eqs. (1.109a) and (1.109b). However, the corresponding time-dependent surface charge density $\langle\sigma\rangle$ that gives rise to the dipole current of Eq. (1.123) as shown by Haus [4] is equivalent to the current due to a uniformly charged sphere rotating about the $\mathbf{S}$-axis at the constant angular velocity given by Eq. (1.55). The charge density is given by Gauss' law at the two-dimensional surface:

$$\sigma = -\varepsilon_0\mathbf{n}\cdot\nabla\Phi|_{r=r_n} = -\varepsilon_0\mathbf{n}\cdot\mathbf{E}|_{r=r_1} \quad (20)$$

From Eq. (19), $\langle\sigma\rangle$ is

$$\langle\sigma\rangle = \frac{e}{4\pi r_1^2}\frac{3}{2}\sin\theta \quad (21)$$

and the current (Eq. (1.123) is given by the product of Eq. (21) and the constant angular frequency (Eq. (1.55)). The precession of the magnetostatic dipole results in magnetic dipole radiation or absorption during a Stern-Gerlach transition. The application of a magnetic field causes alignment of the intrinsic electron magnetic moment of atoms of a material such that the population of electrons parallel versus antiparallel is a Boltzmann distribution which depends on the temperature of the material. Following the removal of the field, the original random-orientation distribution is restored as is the original temperature. The distribution may be altered by the application of an RF pulse at the Larmor frequency.

The application of a magnetic field with a resonant Larmor excitation gives rise to a precessing angular momentum vector $\mathbf{S}$ of magnitude $\hbar$ directed from the origin of the orbitsphere at an angle of $\theta = \frac{\pi}{3}$ relative to the applied magnetic field. $\mathbf{S}$ rotates about the axis of the applied field at the Larmor frequency. The magnitude of the components of $\mathbf{S}$ that are parallel and orthogonal to the applied field (Eqs (1.84-1.85)) are $\frac{\hbar}{2}$ and $\sqrt{\frac{3}{4}}\hbar$, respectively. Since both the RF field and the orthogonal components shown in Figure 1.15 rotate at the Larmor frequency, the RF field that causes a Stern Gerlach transition produces a stationary magnetic field with respect to these components as described by Patz [5].

The component of Eq. (1.85) adds to the initial $\frac{\hbar}{2}$ parallel component to give a total of $\hbar$ in the stationary frame corresponding to a Bohr magneton, μ_B, of magnetic moment. Eqs. (2) and (6) also hold in the case of the Stern Gerlach experiment. Superposition holds for Maxwell's equations, and only the angular momentum given by Eqs. (1.68-1.73) and the source current corresponding to Eq. (17) need be considered. Since it does not change, the diamagnetic component given from Eq. (1) does not contribute to the spin-flip transition as discussed *supra*. The potential energy of a magnetic moment $\mathbf{m}$ in the presence of flux $\mathbf{B}$ [6] is

$$E = \mathbf{m} \cdot \mathbf{B} \tag{22}$$

The angular momentum of the electron gives rise to a magnetic moment of μ_B. Thus, the energy ΔE_{mag}^{spin} to switch from parallel to antiparallel to the field is given by Eq. (1.147)

$$\Delta E_{mag}^{spin} = 2\mu_{\mathbf{B}}\, \mathbf{i}_{\mathbf{z}} \cdot \mathbf{B} = 2\mu_B B \cos\theta = 2\mu_B B \tag{23}$$

In the case of an applied flux of 10 T, Eq. (23) gives

$$\Delta E_{mag}^{spin} = 1.855\ X\ 10^{-22}\ J = 1.158 X\ 10^{-3}\ eV \tag{24}$$

ΔE_{mag}^{spin} is also given by Planck's equation. It can be shown from conservation of angular momentum considerations (Eqs. (26-32)) that the Zeeman splitting is given by Planck's equation and the Larmor frequency based on the gyromagnetic ratio (Eq. (2)). The electron's magnetic moment may only be parallel or antiparallel to the magnetic field rather than at a continuum of angles including perpendicular according to Eq. (22). No continuum of energies predicted by Eq. (22) for a pure magnetic dipole are possible. The energy difference for the magnetic moment to flip from parallel to antiparallel to the applied field is

$$\Delta E_{mag}^{spin} = 2\hbar\omega = 1.855\ X\ 10^{-22}\ J = 1.158 X\ 10^{-3}\ eV \tag{25}$$

corresponding to magnetic dipole radiation.

As demonstrated in the Orbitsphere Equation of Motion for $\ell = 0$ section, $\frac{\hbar}{2}$ of the orbitsphere angular momentum designated the static component is initially parallel to the field. An additional $\frac{\hbar}{2}$ parallel component designated the dynamic component comes from the $\hbar$ of angular momentum along $\mathbf{S}$. The angular momentum in the presence of an applied magnetic field is [7]

$$\mathbf{L} = \mathbf{r} \times (m_e \mathbf{v} + e\mathbf{A}) \tag{26}$$

where $\mathbf{A}$ is the vector potential evaluated at the location of the orbitsphere. The circular integral of $\mathbf{A}$ is the flux linked by the electron. During a Stern-Gerlach transition a resonant RF photon is absorbed or emitted, and the $\hbar$ component along $\mathbf{S}$ reverses direction. It is shown by Eqs. (29-32) that the dynamic parallel component of angular momentum corresponding to the vector potential due to the lightlike transition is equal to the "kinetic angular momentum" $(\mathbf{r} \times m\mathbf{v})$ of $\frac{\hbar}{2}$. Conservation of angular momentum of the orbitsphere requires that the static angular momentum component concomitantly flips. The static component of angular momentum undergoes a spin flip, and concomitantly the "potential angular momentum" $(\mathbf{r} \times e\mathbf{A})$ of the

dynamic component must change by $-\frac{\hbar}{2}$ due to the linkage of flux by the electron such that the total angular momentum is conserved.

In spherical coordinates, the relationship between the vector potential $\mathbf{A}$ and the flux $\mathbf{B}$ is

$$2\pi rA = \pi r^2 B \tag{27}$$

Eq. (27) can be substituted into Eq. (26) since the magnetic moment m is given [6] as

$$m = \frac{\text{charge} \cdot \text{angular momentum}}{2 \cdot \text{mass}} \tag{28}$$

and the corresponding energy is consistent with Eqs. (23) and (25) in this case as follows:

$$\Delta\mathbf{m} = -\frac{e(\mathbf{r} \times e\mathbf{A})}{2m_e} = \frac{e\frac{\hbar}{2}}{2m_e} = \frac{\mu_B}{2} \tag{29}$$

The boundary condition that the angular momentum is conserved is shown by Eqs. (1.144-1.146). It can be shown that Eq. (29) is also consistent with the vector potential along the axis of the applied field [8] given by

$$\mathbf{A} = \cos\frac{\pi}{3}\mu_0 \frac{e\hbar}{2m_e r^2}\sin\theta\mathbf{i}_\phi = \mu_0 \frac{1}{2}\frac{e\hbar}{2m_e r^2}\sin\theta\mathbf{i}_\phi \tag{30}$$

Substitution of Eq. (30) into Eq. (29) gives

$$\Delta\mathbf{m} = -\frac{e(\mathbf{r} \times e\mu_0 \frac{1}{2}\frac{e\hbar}{2m_e r^2}\sin\theta\mathbf{i}_\phi)}{2m_e} = -\frac{1}{2}\left[\frac{\mu_0 e^2}{2m_e r}\right]\frac{e\hbar}{2m_e} \tag{31}$$

with the geometrical factor of $2/3$ [2] and the current given by Eq. (1.123). Since k is the lightlike k^0, then $k = \omega_n / c$ corresponding to the RF photon field. The relativistic corrections of Eq. (31) are given by Eqs. (1.229) and (1.230) and the relativistic radius $r = \lambda\!\!\!^{-}_c$ given by Eq. (1.228). The relativistically corrected Eq. (31) is

$$\Delta\mathbf{m} = -\frac{1}{2}(2\pi\alpha)^{-1}\left[\frac{\mu_0 e^2}{2m_e \alpha a_0}\right]\frac{e\hbar}{2m_e} = \frac{\mu_B}{2} \tag{32}$$

The magnetic flux of the electron is given by

$$\nabla \times \mathbf{A} = \mathbf{B} \tag{33}$$

Substitution of Eq. (30) into Eq. (33) gives 1/2 the flux of Eq. (1.132).

From Eq. (28), the $\frac{\hbar}{2}$ of angular momentum before and after the field is applied corresponds to an initial magnetic moment on the applied-field-axis of $\frac{\mu_B}{2}$. After the field is applied, the contribution of $\frac{\mu_B}{2}$ from Eq. (29) with Eq. (27) gives a total magnetic moment along the applied-field-axis of μ_B, a Bohr magneton, wherein the additional contribution (Eq. (28)) arises from the angular momentum of $\hbar$ on the $\mathbf{S}$-axis. Thus, even though the magnitude of the vector projection of the angular momentum of the electron in the direction of the magnetic field

is $\frac{\hbar}{2}$, the magnetic moment corresponds to $\hbar$ due to the $\frac{\hbar}{2}$ contribution from the dynamic component, and the quantized transition is due to the requirement of angular momentum conservation as given by Eq. (28).

Eq. (22) implies a continuum of energies; whereas, Eq. (29) shows that the static-kinetic and dynamic vector potential components of the angular momentum are quantized at $\frac{\hbar}{2}$. Consequently, as shown in the Electron g Factor section, the flux linked during a spin transition is quantized as the magnetic flux quantum:

$$\Phi_0 = \frac{h}{2e} \tag{34}$$

Only the states corresponding to

$$m_s = \pm\frac{1}{2} \tag{35}$$

are possible due to conservation of angular momentum. It is further shown using the Poynting power vector with the requirement that flux is linked in units of the magnetic flux quantum, that the factor 2 of Eqs. (23) and (25) is replaced by the electron g factor.

Thus, in terms of flux linkage, the electron behaves as a superconductor with a weak link [9] as described in the Josephson Junction, Weak Link section and the Superconducting Quantum Interference Device (SQUID) section. Consider the case of a current loop with a weak link comprising a large number of superconducting electrons (e.g. 10^{10}). As the applied field increases, the Meissner current increases. In equilibrium, a dissipationless supercurrent can flow around the loop driven by the difference between the flux Φ that threads the loop and the external flux Φ_x applied to the loop. Based on the physics of the electrons carrying the supercurrent, when the current reaches the critical current, the kinetic angular momentum change of $\frac{\hbar}{2}$ equals the magnitude of the potential angular momentum change corresponding to the vector potential according to Eqs. (26) and (31). As a consequence, the flux is linked in units of the magnetic flux quantum as shown in the Electron g Factor section.

REFERENCES

1. E. M. Purcell, *Electricity and Magnetism*, McGraw-Hill, New York, (1965), pp. 370-379.
2. G. R. Fowles, *Analytical Mechanics*, Third Edition, Holt, Rinehart, and Winston, New York, (1977), p. 196.
3. J. D. Jackson, *Classical Electrodynamics*, Second Edition, John Wiley & Sons, New York, (1975), pp. 84-102; 752-763.
4. H. A. Haus, J. R. Melcher, "Electromagnetic Fields and Energy", Department of Electrical engineering and Computer Science, Massachusetts Institute of Technology, (1985), Sec. 8.6.
5. S. Patz, Cardiovasc. Interven. Radiol., (1986), 8:25, pp. 225-237.
6. D. A. McQuarrie, *Quantum Chemistry*, University Science Books, Mill Valley, CA, (1983), pp. 238-241.
7. E. M. Purcell, *Electricity and Magnetism*, McGraw-Hill, New York, (1965), p. 447.
8. E. M. Purcell, *Electricity and Magnetism*, McGraw-Hill, New York, (1965), pp. 361-367.
9. C. E. Gough, M. S. Colclough, E. M. Forgan, R. G. Jordan, M. Keene, C. M. Muirhead, A. I. M. Rae, N. Thomas, J. S. Abell, S. Sutton, Nature, Vol. 326, (1987), P. 855.

ELECTRON G FACTOR

As demonstrated by Purcell [16], when a magnetic field is applied to an electron in a central field which comprises a current loop, the orbital radius does not change, but the velocity changes as follows:

$$\Delta v = \frac{erB}{2m_e} \tag{1.142}$$

This corresponds to diamagnetism and gives rise to precession with a corresponding resonance as shown in Box 1.2. The angular momentum in the presence of an applied magnetic field is [16]

$$\mathbf{L} = \mathbf{r} \times (m_e \mathbf{v} + e\mathbf{A}) \tag{1.143}$$

where $\mathbf{A}$ is the vector potential evaluated at the location of the orbitsphere. Conservation of angular momentum of the orbitsphere permits a discrete change of its "kinetic angular momentum" $(\mathbf{r} \times m\mathbf{v})$ with respect to the field of $\frac{\hbar}{2}$, and concomitantly the "potential angular momentum" $(\mathbf{r} \times e\mathbf{A})$ must change by $-\frac{\hbar}{2}$. The flux change, ϕ, of the orbitsphere for $r < r_n$ is determined as follows [16]:

$$\Delta \mathbf{L} = \frac{\hbar}{2} - \mathbf{r} \times e\mathbf{A} \tag{1.144}$$

$$= \left[\frac{\hbar}{2} - \frac{e 2\pi r A}{2\pi} \right] \hat{z} \tag{1.145}$$

$$= \left[\frac{\hbar}{2} - \frac{e\phi}{2\pi} \right] \hat{z} \tag{1.146}$$

In order that the change in angular momentum, $\Delta \mathbf{L}$, equals zero, ϕ must be $\Phi_0 = \frac{h}{2e}$, the magnetic flux quantum. Thus, to conserve angular momentum in the presence of an applied magnetic field, the orbitsphere magnetic moment can be parallel or antiparallel to an applied field as observed with the Stern-Gerlach experiment, and the flip between orientations is accompanied by the "capture" of the magnetic flux quantum by the orbitsphere "coils" comprising infinitesimal loops of charge moving along geodesics (great circles). A superconducting loop with a weak link also demonstrates this effect [23].

The energy to flip the orientation of the orbitsphere due to its magnetic moment of a Bohr magneton, μ_B, is

$$\Delta E_{mag}^{spin} = 2\mu_B B \tag{1.147}$$

where

$$\mu_B = \frac{e\hbar}{2m_e} \tag{1.148}$$

During the spin-flip transition, power must be conserved. Power flow is governed by the Poynting power theorem,

$$\nabla \bullet (\mathbf{E} \times \mathbf{H}) = -\frac{\partial}{\partial t}\left[\frac{1}{2}\mu_o \mathbf{H} \bullet \mathbf{H} \right] - \frac{\partial}{\partial t}\left[\frac{1}{2}\varepsilon_o \mathbf{E} \bullet \mathbf{E} \right] - \mathbf{J} \bullet \mathbf{E} \tag{1.149}$$

STORED MAGNETIC ENERGY

Energy superimposes; thus, the calculation of the spin-flip energy is determined as a sum of contributions. The energy change corresponding to the "capture" of the magnetic flux quantum is derived below. From Eq. (1.140) for one electron,

$$\frac{1}{2}\mu_o \mathbf{H} \bullet \mathbf{H} = E_{mag}^{fluxon} = \frac{\pi \mu_0 e^2 \hbar^2}{(m_e)^2 r_n^3} \tag{1.150}$$

is the energy stored in the magnetic field of the electron. The orbitsphere is equivalent to a Josephson junction which can trap integer numbers of fluxons where the quantum of magnetic flux is $\Phi_0 = \frac{h}{2e}$. Consider Eq. (1.150). During the flip transition a fluxon treads the orbitsphere at the speed of light; therefore, the radius of the orbitsphere in the lab frame is 2π times the relativistic radius in the fluxon frame as shown in the Special Relativistic Correction to the Ionization Energies section. Thus, the energy of the transition corresponding to the "capture" of a fluxon by the orbitsphere, E_{mag}^{fluxon}, is

$$E_{mag}^{fluxon} = \frac{\pi \mu_o e^2 \hbar^2}{(m_e)^2 (2\pi r_n)^3} \tag{1.151}$$

$$= \frac{\mu_o e^2}{4\pi^2 m_e r_n}\left(\frac{e\hbar}{2m_e}\right)\left(\frac{h}{2e\pi r_n{}^2}\right) \tag{1.152}$$

$$= \frac{\mu_o e^2}{4\pi^2 m_e r_n}\mu_B\left(\frac{\Phi_0}{A}\right) \tag{1.153}$$

where A is the area and Φ_0 is the magnetic flux quantum.

$$E_{mag}^{fluxon} = 2\left[\frac{e^2\mu_o}{2m_e r_n}\right]\frac{1}{4\pi^2}\mu_B B \tag{1.154}$$

where the nth fluxon treading through the area of the orbitsphere is equivalent to the applied magnetic flux. Furthermore, the term in brackets can be expressed in terms of the fine structure constant, α, as follows:

$$\frac{e^2\mu_o}{2m_e r_n} = \frac{e^2\mu_o c v}{2m_e v r_n c} \tag{1.155}$$

Substitution of Eq. (1.47) gives

$$\frac{e^2\mu_o}{2m_e r_n} = \frac{e^2\mu_o c v}{2\hbar c} \tag{1.156}$$

Substitution of

$$c = \sqrt{\frac{1}{\varepsilon_o \mu_o}} \tag{1.157}$$

and

$$\alpha = \frac{\mu_o e^2 c}{2h} \tag{1.158}$$

gives

$$\frac{e^2\mu_o cv}{2\hbar c} = 2\pi\alpha\frac{v}{c} \tag{1.159}$$

The fluxon treads the orbitsphere at $v = c$ (k is the lightlike k^0, then $k = \omega_n / c$). Thus,

$$E_{mag}^{fluxon} = 2\frac{\alpha}{2\pi}\mu_B B \tag{1.160}$$

STORED ELECTRIC ENERGY

The superposition of the vector projection of the orbitsphere angular momentum on the z-axis is $\frac{\hbar}{2}$ with an orthogonal component of $\frac{\hbar}{4}$. Excitation of a resonant Larmor precession gives rise to $\hbar$ on an axis $\mathbf{S}$ that precesses about the spin axis at an angle of $\theta = \frac{\pi}{3}$. $\mathbf{S}$ rotates about the z-axis at the Larmor frequency. $\mathbf{S}_\perp$, the transverse projection, is $\pm\sqrt{\frac{3}{4}}\hbar$ (Eq. (1.84)), and $\mathbf{S}_\parallel$, the projection onto the axis of the applied magnetic field, is $\pm\frac{\hbar}{2}$ (Eq. (1.85)). As shown in the Spin Angular Momentum of the Orbitsphere with ℓ = 0 section, the superposition of the $\frac{\hbar}{2}$ z-axis component of the orbitsphere angular momentum and the $\frac{\hbar}{2}$ z-axis component of $\mathbf{S}$ gives $\hbar$ corresponding to the observed electron magnetic moment of a Bohr magneton, μ_B. The reorientation of $\mathbf{S}$ and the orbitsphere angular momentum from parallel to antiparallel to the magnetic field applied along the z-axis gives rise to a current. The current is acted on by the flux corresponding to Φ_0, the magnetic flux quantum, linked by the electron during the transition which gives rise to a Hall voltage. The electric field corresponding to the Hall voltage corresponds to the electric power term, $\frac{\delta}{\delta t}\left[\frac{1}{2}\varepsilon_o \mathbf{E}\bullet\mathbf{E}\right]$, of the Poynting power theorem (Eq. (1.149)).

Consider a conductor in a uniform magnetic field and assume that it carries a current driven by an electric field perpendicular to the magnetic field. The current in this case is not parallel to the electric field, but is deflected at an angle to it by the magnetic field. This is the Hall Effect, and it occurs in most conductors.

A spin-flip transition is analogous to Quantum Hall Effect given in the corresponding section wherein the applied magnetic field quantizes the Hall conductance. The current is then precisely perpendicular to the magnetic field, so that no dissipation (that is no ohmic loss) occurs. This is seen in two-dimensional systems, at cryogenic temperatures, in quite high magnetic fields. Furthermore, the ratio of the total electric potential drop to the total current, the Hall resistance, R_H, is precisely equal to

$$R_H = \frac{h}{ne^2} \tag{1.161}$$

The factor n is an integer in the case of the Integral Quantum Hall Effect, and n is a small rational fraction in the case of the Fractional Quantum Hall Effect. In an experimental plot [24]

as the function of the magnetic field, the Hall resistance exhibits flat steps precisely at these quantized resistance values; whereas, the regular resistance vanishes (or is very small) at these Hall steps. Thus, the quantized Hall resistance steps occur for a transverse superconducting state.

Consider the case that an external magnetic field is applied along the x-axis to a two dimensional superconductor in the yz-plane which exhibits the Integral Quantum Hall Effect. (See Figure 1.18.) Conduction electrons align with the applied field in the x direction as the field permeates the material. The normal current carrying electrons experience a Lorentzian force, $\mathbf{F}_L$, due to the magnetic flux. The y-directed Lorentzian force on an electron having a velocity $\mathbf{v}$ in the z direction by an x-directed applied flux, $\mathbf{B}$, is

$$\mathbf{F}_L = e\mathbf{v}\times\mathbf{B} \tag{1.162}$$

The electron motion is a cycloid where the center of mass experiences an $\mathbf{E}\times\mathbf{B}$ drift [25]. Consequently, the normal Hall Effect occurs. Conduction electron energy states are altered by the applied field and by the electric field corresponding to the Hall Effect. The electric force, $\mathbf{F}_H$, due to the Hall electric field, $\mathbf{E}_y$, is

$$\mathbf{F}_H = e\mathbf{E}_y \tag{1.163}$$

When these two forces are equal and opposite, conduction electrons propagate in the z direction alone. For this special case, it is demonstrated in Jackson [25] that the ratio of the corresponding Hall electric field E_H and the applied magnetic flux is

$$E_H / B = v \tag{1.164}$$

where v is the electron velocity. And, it is demonstrated in the Integral Quantum Hall Effect section that the Hall resistance, R_H, in the superconducting state is given by

$$R_H = \frac{h}{ne^2} \tag{1.165}$$

where n is an integer.

Figure 1.18. Coordinate system of crossed electric field, $\mathbf{E}_y$, corresponding to the Hall voltage, magnetic flux, $\mathbf{B}_x$, due to applied field, and superconducting current $\mathbf{i}_z$.

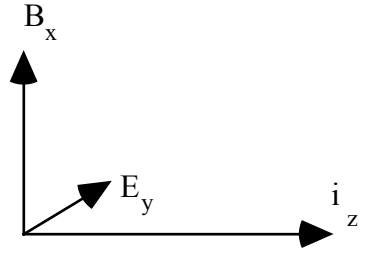

Consider the case of the spin-flip transition of the electron. In the case of an exact balance between the Lorentzian force (Eq. (1.162)) and the electric force corresponding to the Hall voltage (Eq. (1.163)), each superconducting point mass of the electron propagates along a great circle where

$$E/B = v \tag{1.166}$$

where v is given by Eq. (1.47). Substitution of Eq. (1.47) into Eq. (1.166) gives

$$E/B = \frac{\hbar}{m_e r} \tag{1.167}$$

Eq. (1.157) is the condition for superconductivity in the presence of crossed electric and magnetic fields. The electric field corresponding to the Hall voltage corresponds to the electric energy term, E_{ele}, of the Poynting power theorem (Eq. (1.149)).

$$E_{ele} = \frac{1}{2}\int_0^{2\pi}\int_0^{\pi}\int_0^{r_1} \varepsilon_o \mathbf{E} \bullet \mathbf{E} r^2 \sin\theta dr d\theta d\phi \tag{1.168}$$

The electric term for this superconducting state is derived as follows using the coordinate system shown in Figure 1.19.

Figure 1.19. Coordinate system of crossed electric field, $\mathbf{E}_r$, corresponding to the Hall voltage, magnetic flux, $\mathbf{B}_\theta$, due to applied field, and superconducting current $\mathbf{i}_\phi$.

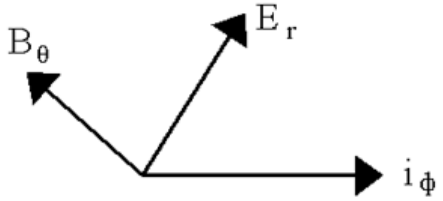

The current is perpendicular to $\mathbf{E}_r$, thus there is no dissipation. This occurs when

$$e\mathbf{E} = e\mathbf{v} \times \mathbf{B} \tag{1.169}$$

or

$$E/B = v \tag{1.170}$$

The electric field corresponding to the Hall voltage is

$$\mathbf{E} = \mathbf{v} \times \mathbf{B} \tag{1.171}$$

Substitution of Eq. (1.171) into Eq. (1.168) gives

$$E_{ele} = \frac{1}{2}\varepsilon_o \int_0^{2\pi}\int_0^{\pi}\int_0^{r_1} (vB)^2 r^2 \sin\theta dr d\theta d\phi \tag{1.172}$$

The spin flip transition may be induced by the absorption of a resonant photon. The velocity is determined from the distance traversed by each point and the time of the transition due to capture of a photon resonant with the spin-flip transition energy. The current $\mathbf{i}_\phi$ corresponding to the Hall voltage and $\mathbf{E}_r$ is given by the product of the electron charge and the frequency f of the photon where the correspondence principle holds as given in the Photon Absorption section.

$$i = ef \tag{1.173}$$

The resistance of free space for the propagation of a photon is the radiation resistance of free space, η.

$$\eta = \sqrt{\frac{\mu_0}{\varepsilon_0}} \tag{1.174}$$

The power P_r of the electron current induced by the photon as it transitions from free space to being captured by the electron is given by the product of the corresponding current and the resistance R which is given by Eq. (1.174).

$$P_r = i^2 R \tag{1.175}$$

Substitution of Eq. (1.173) and Eq. (1.174) gives

$$P_r = e^2 f^2 \sqrt{\frac{\mu_0}{\varepsilon_0}} \tag{1.176}$$

It follows from the Poynting power theorem (Eq. (1.149)) with spherical radiation that the transition time τ is given by the ratio of the energy and the power of the transition [26].

$$\tau = \frac{energy}{power} \tag{1.177}$$

The energy of the transition which is equal to the energy of the resonant photon is given by Planck's equation.

$$E = \hbar\omega = hf \tag{1.178}$$

Substitution of Eq. (1.176) and Eq. (1.178) into Eq. (1.177) gives

$$\tau = \frac{hf}{e^2 f^2 \sqrt{\frac{\mu_0}{\varepsilon_0}}} \tag{1.179}$$

The distance ℓ traversed by the electron with an kinetic angular momentum change of $\frac{\hbar}{2}$ is

$$\ell = \frac{2\pi r}{2} = \frac{\lambda}{2} \tag{1.180}$$

where the wavelength is given by Eq. (1.43). The velocity is given by the distance traversed divided by the transition time. Eq. (1.179) and Eq. (1.180) give

$$v = \frac{\lambda/2}{\tau} = \frac{\lambda/2}{\frac{hf}{e^2 f^2 \sqrt{\frac{\mu_0}{\varepsilon_0}}}} = \frac{\sqrt{\frac{\mu_0}{\varepsilon_0}} e^2}{2h} \lambda f \tag{1.181}$$

The relationship for a photon in free space is

$$c = \lambda f \tag{1.182}$$

As shown in the Unification of Spacetime, the Forces, Matter, and Energy section, the fine structure constant given by Eq. (1.158) is the dimensionless factor that corresponds to the relativistic invariance of charge.

$$\alpha = \frac{1}{4\pi} \sqrt{\frac{\mu_0}{\varepsilon_0}} \frac{e^2}{\hbar} = \frac{1}{2} \frac{\sqrt{\frac{\mu_0}{\varepsilon_0}}}{\frac{h}{e^2}} = \frac{\mu_0 e^2 c}{2h} \tag{1.183}$$

It is equivalent to one half the ratio of the radiation resistance of free space, $\sqrt{\frac{\mu_0}{\varepsilon_0}}$, and the hall resistance, $\frac{h}{e^2}$. The radiation resistance of free space is equal to the ratio of the electric field and

the magnetic field of the photon (Eq. (4.10)). Substitution of Eq. (1.182) and Eq. (1.183) into Eq. (1.181) gives

$$v = \alpha c \tag{1.184}$$

Substitution of Eq. (1.184) into Eq. (1.172) gives

$$E_{ele} = \frac{1}{2}\varepsilon_o \int_0^{2\pi}\int_0^{\pi}\int_0^{r_1} \left(\alpha c \mu_0 H\right)^2 r^2 \sin\theta dr d\theta d\phi \tag{1.185}$$

where

$$B = \mu_0 H \tag{1.186}$$

The relationship between the speed of light, c, and the permittivity of free space, ε_0, and the permeability of free space, μ_0, is

$$c = \frac{1}{\sqrt{\mu_0 \varepsilon_0}} \tag{1.187}$$

Thus, Eq. (1.185) may be written as

$$E_{ele} = \frac{1}{2}\alpha^2 \int_0^{2\pi}\int_0^{\pi}\int_0^{r_1} \mu_0 H^2 r^2 \sin\theta dr d\theta d\phi \tag{1.188}$$

Substitution of Eq. (1.136) gives

$$E_{ele} = \alpha^2 \frac{2\pi\mu_0 e^2 \hbar^2}{3 m_e^2 r_1^3} \tag{1.189}$$

The magnetic flux, $\mathbf{B}$, is quantized in terms of the Bohr magneton because the electron links flux in units of the magnetic flux quantum,

$$\Phi_0 = \frac{h}{2e} \tag{1.190}$$

Substitution of Eqs. (1.150-1.160) gives

$$E_{ele} = 2\left(\frac{2}{3}\alpha^2 \frac{\alpha}{2\pi}\mu_B B\right) \tag{1.191}$$

DISSIPATED ENERGY

The $\mathbf{J} \bullet \mathbf{E}$ energy over time is derived from the electron current corresponding to the Larmor excitation and the electric field given by Faraday's law due to the linkage of the magnetic flux of the fluxon during the spin-flip. Consider the electron current due the external field. The application of a magnetic field with a resonant Larmor excitation gives rise to a precessing angular momentum vector $\mathbf{S}$ of magnitude $\hbar$ directed from the origin of the orbitsphere at an angle of $\theta = \frac{\pi}{3}$ relative to the applied magnetic field. As given in the Spin Angular Momentum of the Orbitsphere with $\ell = 0$ section, $\mathbf{S}$ rotates about the axis of the applied field at the Larmor frequency. The magnitude of the components of $\mathbf{S}$ that are parallel and orthogonal to the applied field (Eqs (1.84-1.85)) are $\frac{\hbar}{2}$ and $\sqrt{\frac{3}{4}}\hbar$, respectively. Since both the RF field and the orthogonal components shown in Figure 1.15 rotate at the Larmor frequency, the RF field that causes a Stern Gerlach transition produces a stationary magnetic field with respect to these components as described in Box 1.2. The corresponding central field at the orbitsphere surface

given by the superposition of the central field of the proton and that of the photon follows from Eqs. (2.10-2.17) and Eq. (17) of Box 1.2:

$$\mathbf{E} = \frac{e}{4\pi\varepsilon_o r^2}\left[Y_0^0(\theta,\phi)\mathbf{i}_\mathbf{r} + \mathrm{Re}\left\{Y_\ell^m(\theta,\phi)e^{i\omega_n t}\right\}\mathbf{i}_\mathbf{y}\delta(r-r_1)\right] \tag{1.192}$$

where the spherical harmonic dipole $Y_\ell^m(\theta,\phi) = \sin\theta$ is with respect to the $\mathbf{S}$-axis. The dipole spins about the $\mathbf{S}$-axis at the angular velocity given by Eq. (1.55). The resulting current is nonradiative as shown by Eq. (1.39) and in Appendix I: Nonradiation Based on the Electromagnetic Fields and the Poynting Power Vector. Thus, the field in the RF rotating frame is magnetostatic as shown in Figure 1.17 but directed along the $\mathbf{S}$-axis. Thus, the corresponding current given by Eq. (1.123) is

$$\mathbf{K}(\rho,\phi,z) = \frac{3}{2}\frac{e\hbar}{m_e r_n^3}\sin\theta\mathbf{i}_\phi \tag{1.193}$$

Next consider the Faraday's equation for the electric field

$$\oint_C \mathbf{E}\bullet d\mathbf{s} = -\frac{d}{dt}\int_S \mu_0\mathbf{H}\bullet d\mathbf{a} \tag{1.194}$$

As demonstrated by Purcell [16], the velocity of the electron changes according to Lenz's law, but the change in centrifugal force is balanced by the change in the central field due to the applied field. The magnetic flux of the electron given by Eq. (1.131) is

$$\mathbf{B} = \mu_0\mathbf{H} = \frac{\mu_0 e\hbar}{m_e r_1^3}(\mathbf{i}_r\cos\theta - \mathbf{i}_\theta\sin\theta) \qquad \text{for } r < r_n \tag{1.195}$$

From Eq. (1.160), the magnetic flux $B_{\mathbf{J}\bullet\mathbf{E}}$ of the fluxon is

$$\mathbf{B}_{\mathbf{J}\bullet\mathbf{E}} = \frac{\alpha}{2\pi}\frac{\mu_0 e\hbar}{m_e r_1^3}(\mathbf{i}_r\cos\theta - \mathbf{i}_\theta\sin\theta) = \frac{\alpha}{2\pi}\frac{\mu_0 e\hbar}{m_e r_1^3}\mathbf{i}_z \tag{1.196}$$

The electric field $\mathbf{E}$ is constant about the line integral of the orbitsphere. Using Eq. (1.194) with the change in flux in units of fluxons along the z-axis given by Eq. (1.196) gives

$$\int_{-r_1}^{+r_1}\oint_C \mathbf{E}\bullet d\mathbf{s}dz = \int_{-r_1}^{+r_1} -\pi r^2\frac{dB}{dt}dz\mathbf{i}_\phi \tag{1.197}$$

$$\begin{aligned} 2\pi\ \mathbf{E}\int_0^\pi r_1\sin^2\theta\mathrm{d}\theta\ &= -\pi\frac{\Delta B}{\Delta t}r_1^2\sin^3\theta\mathrm{d}\theta\mathbf{i}_\phi \\ &= -\pi r_1^2\frac{2\Delta B}{3\Delta t}\mathbf{i}_\phi \end{aligned} \tag{1.198}$$

Substitution of Eq. (1.196) into Eq. (1.198) gives

$$\pi r_1\ \mathbf{E} = -\pi r_1^2\frac{2}{3}\frac{\alpha}{2\pi}\frac{\mu_0 e\hbar}{m_e r_1^3\Delta t}\mathbf{i}_\phi \tag{1.199}$$

$$\pi r_1\ \mathbf{E} = -\pi\frac{2}{3}\frac{\alpha}{2\pi}\frac{\mu_0 e\hbar}{m_e r_1\Delta t}\mathbf{i}_\phi \tag{1.200}$$

Thus,

$$\mathbf{E} = -\frac{2}{3}\frac{\alpha}{2\pi}\frac{\mu_0 e\hbar}{m_e r_1^2 \Delta t}\mathbf{i}_\phi \tag{1.201}$$

The dissipative power density $\mathbf{E} \bullet \mathbf{J}$ can be expressed in terms of the surface current density $\mathbf{K}$ as

$$\int_V (\mathbf{E} \bullet \mathbf{J}) \Delta t dv = \int_S (\mathbf{E} \bullet \mathbf{K}) \Delta t da \tag{1.202}$$

Using the electric field from Eq. (1.201) and the current density from Eq. (1.193) gives

$$\int_V (\mathbf{E} \bullet \mathbf{J}) \Delta t dv = \int_0^{2\pi}\int_0^{\pi}\left(\frac{2}{3}\frac{\alpha}{2\pi}\frac{\mu_0 e\hbar}{m_e r_1^2 \Delta t}\frac{3}{2}\frac{e\hbar}{m_e r_1^3}\sin^2\theta\right)\Delta t r_1^2 \sin\theta d\theta d\varphi \tag{1.203}$$

$$= \frac{4}{3}\frac{\alpha}{2\pi}\frac{\pi\mu_0 e^2\hbar^2}{m_e^2 r_1^3}$$

Substitution of Eqs. (1.150-1.160) into Eq. (1.203) gives

$$\int_V (\mathbf{E} \bullet \mathbf{J}) \Delta t dv = 2\left(\frac{4}{3}\right)\left(\frac{\alpha}{2\pi}\right)^2 \mu_B B \tag{1.204}$$

TOTAL ENERGY OF SPIN-FLIP TRANSITION

The principal energy of the transition corresponding to a reorientation of the orbitsphere is given by Eq. (1.147). And, the total energy of the flip transition is the sum of Eq. (1.147), and Eqs. (1.160), (1.191), and (1.204) corresponding to the electric energy, the magnetic energy, and the dissipated energy of a fluxon treading the orbitsphere, respectively.

$$\Delta E_{mag}^{spin} = 2\left(1 + \frac{\alpha}{2\pi} + \frac{2}{3}\alpha^2\left(\frac{\alpha}{2\pi}\right) - \frac{4}{3}\left(\frac{\alpha}{2\pi}\right)^2\right)\mu_B B \tag{1.205}$$

$$\Delta E_{mag}^{spin} = g\mu_B B \tag{1.206}$$

where the stored magnetic energy corresponding to the $\frac{\partial}{\partial t}\left[\frac{1}{2}\mu_o \mathbf{H} \bullet \mathbf{H}\right]$ term increases, the stored electric energy corresponding to the $\frac{\partial}{\partial t}\left[\frac{1}{2}\varepsilon_o \mathbf{E} \bullet \mathbf{E}\right]$ term increases, and the $\mathbf{J} \bullet \mathbf{E}$ term is dissipative. The magnetic moment of Eq. (1.147) is twice that from the gyromagnetic ratio as given by Eq. (28) of Box 1.2. The magnetic moment of the electron is the sum of the component corresponding to the kinetic angular momentum, $\frac{\hbar}{2}$, and the component corresponding to the vector potential angular momentum, $\frac{\hbar}{2}$, (Eq. (1.143). The spin-flip transition can be considered as involving a magnetic moment of g times that of a Bohr magneton. The g factor is redesignated the fluxon g factor as opposed to the anomalous g factor, and it is given by Eq. (1.205).

$$\frac{g}{2} = 1 + \frac{\alpha}{2\pi} + \frac{2}{3}\alpha^2\left(\frac{\alpha}{2\pi}\right) - \frac{4}{3}\left(\frac{\alpha}{2\pi}\right)^2 \tag{1.207}$$

For $\alpha^{-1} = 137.03604(11)$ [27]

$$\frac{g}{2} = 1.001\ 159\ 652\ 120 \tag{1.208}$$

The experimental value [28] is

$$\frac{g}{2} = 1.001\ 159\ 652\ 188(4) \tag{1.209}$$

The calculated and experimental values are within the propagated error of the fine structure constant. Different values of the fine structure constant have been recorded from different experimental techniques, and α^{-1} depends on a circular argument between theory and experiment [29]. One measurement of the fine structure constant based on the electron g factor is $\alpha_{g_e}^{-1} = 137.036006(20)$ [30]. This value can be contrasted with equally precise measurements employing solid state techniques such as those based on the Josephson effect [31] ($\alpha_J^{-1} = 137.035963(15)$) or the quantized Hall effect [32] ($\alpha_H^{-1} = 137.035300(400)$). A method of the determination of α^{-1} that depends on the circular methodology between theory and experiment to a lesser extent is the substitution of the independently measured fundamental constants μ_0, e, c, and h into Eq. (1.183). The following values of the fundamental constants are given by Weast [27]

$$\mu_o = 4\pi\ X\ 10^{-7}\ Hm^{-1} \tag{1.210}$$

$$e = 1.6021892(46)\ X\ 10^{-19}\ C \tag{1.211}$$

$$c = 2.99792458(12)\ X\ 10^{8}\ ms^{-1} \tag{1.212}$$

$$h = 6.626176(36)\ X\ 10^{-34}\ JHz^{-1} \tag{1.213}$$

For these constants,

$$\alpha^{-1} = 137.03603(82) \tag{1.214}$$

Substitution of the α^{-1} from Eq. (1.214) into Eq. (1.207) gives

$$\frac{g}{2} = 1.001\ 159\ 652\ 137 \tag{1.215}$$

The experimental value [28] is

$$\frac{g}{2} = 1.001\ 159\ 652\ 188(4) \tag{1.216}$$

Conversely, the fine structure calculated for the experimental $\frac{g}{2}$ and Eq. (1.207) is $\alpha^{-1} = 137.036\ 032\ 081$.

The *postulated* QED theory of $\frac{g}{2}$ is based on the determination of the terms of a *postulated* power series in α/π where each *postulated* virtual particle is a source of *postulated* vacuum polarization that gives rise to a *postulated* term. The algorithm involves scores of *postulated* Feynman diagrams corresponding to thousands of matrices with thousands of integrations per matrix requiring decades to reach a consensus on the "appropriate" *postulated* algorithm to remove the intrinsic infinities. The solution so obtained using the perturbation series further requires a *postulated* truncation since the series **diverges**. The remarkable

agreement between Eqs. (1.215) and (1.216) demonstrates that $\frac{g}{2}$ may be derived in closed form from Maxwell's equations in a simple straightforward manner that yields a result with eleven figure agreement with experiment—the limit of the experimental capability of the measurement of the fundamental constants that determine α. In Appendix II: Quantum Electrodynamics is Purely Mathematical and Has No Basis in Reality, the Maxwellian result is contrasted with the QED algorithm of invoking virtual particles, zero point fluctuations of the vacuum, and negative energy states of the vacuum. Rather than an infinity of radically different QED models, an essential feature is that *Maxwellian solutions are unique*.

The muon, like the electron, is a lepton with $\hbar$ of angular momentum. The magnetic moment of the muon is given by Eq. (1.147) with the electron mass replaced by the muon mass. It is twice that from the gyromagnetic ratio as given by Eq. (2.65) of the Orbital and Spin Splitting section corresponding to the muon mass. As is the case with the electron, the magnetic moment of the muon is the sum of the component corresponding to the kinetic angular momentum, $\frac{\hbar}{2}$, and the component corresponding to the vector potential angular momentum, $\frac{\hbar}{2}$, (Eq. (1.143). The spin-flip transition can be considered as involving a magnetic moment of g times that of a Bohr magneton of the muon. The g factor is equivalent to that of the electron given by Eq. (1.207).

The muon anomalous magnetic moment has been measured in a new experiment at Brookhaven National Laboratory (BNL) [33]. Polarized muons were stored in a superferric ring, and the angular frequency difference ω_a between the spin precession and orbital frequencies was determined by measuring the time distribution of high-energy decay positrons. The dependence of ω_a on the magnetic and electric fields is given by BMT equation which is the relativistic equation of motion for spin in uniform or slowly varying external fields [34]. The dependence on the electric field is eliminated by storing muons with the "magic" $\gamma = 29.3$, which corresponds to a muon momentum $p = 3.09\ GeV/c$. Hence measurement of ω_a and of B determines the anomalous magnetic moment.

The "magic" γ wherein the contribution to the change of the longitudinal polarization by the electric quadrupole focusing fields are eliminated occurs when

$$\frac{g_\mu \beta}{2} - \frac{1}{\beta} = 0 \tag{1.217}$$

where g_μ is the muon g factor which is required to be different from the electron g factor in the standard model due to the dependence of the mass dependent interaction of each lepton with vacuum polarizations due to virtual particles. For example, the muon is much heavier than the electron, and so high energy (short distance) effects due to strong and weak interactions are more important here [30]. The BNL Muon (g-2) Collaboration [33] used a "magic" $\gamma = 29.3$ which satisfied Eq. (1.217) identically for $\frac{g_\mu}{2}$; however, their assumption that this condition eliminated the affect of the electrostatic field on ω_a is flawed as shown in Appendix IV: Muon g Factor. Internal consistency was achieved during the determination of $\frac{g_\mu}{2}$ using the BMT equation with

the flawed assumption that $\frac{g_\mu}{2} \neq \frac{g_e}{2}$. The parameter measured by Carey et al. [33] corresponding to $\frac{g_\mu}{2}$ was the sum of a finite electric term as well as a magnetic term. The calculated result based on the equivalence of the muon and electron g factors

$$\frac{g_\mu}{2} = 1.001\ \ 165\ \ 923 \tag{1.218}$$

is in agreement with the result of Carey et al. [33]:

$$\frac{g_\mu}{2} = 1.001\ \ 165\ \ 925\ \ (15) \tag{1.219}$$

Rather than indicating an expanded plethora of postulated super-symmetry virtual particles which make contributions such as smuon-neutralino and sneutrino-chargino loops as suggested by Brown et al. [35], the deviation of the experimental value of $\frac{g_\mu}{2}$ from that of the standard model prediction simply indicates that the muon g factor is equivalent to the electron g factor.

DETERMINATION OF ORBITSPHERE RADII

The one-electron orbitsphere is a spherical shell of negative charge (total charge = $-e$) of zero thickness at a distance r_n from the nucleus of charge $+Ze$. It is well known that the field of a spherical shell of charge is zero inside the shell and that of a point charge at the origin outside the shell [36]. See Figure 1.20.

Figure 1.20. The electric fields of a proton, a bound electron, and a hydrogen atom corresponding to a minimum energy and no electron self interaction where the bubble-like geometry of the orbitsphere requires the central field of the proton.

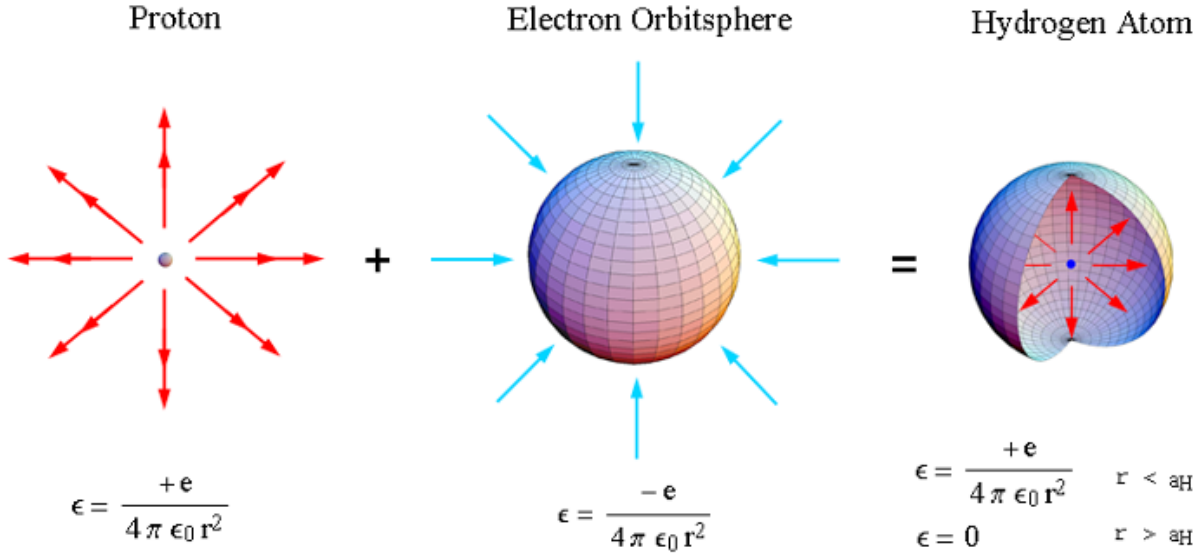

Thus, for a nucleus of charge Z, the force balance equation for the electron orbitsphere is

obtained by equating the forces on the mass and charge densities. For the ground state, $n=1$, the centrifugal force of the electron is given by

$$\mathbf{F}_{centrifugal} = \frac{m_e}{4\pi r_1^2}\frac{\mathbf{v}_1^2}{r_1} \tag{1.220}$$

where $\frac{m_e}{4\pi r_1^2}$ is the mass density of the orbitsphere. The centripetal force is the electric force, $\mathbf{F}_{ele}$, between the electron and the nucleus.

$$\mathbf{F}_{ele} = \frac{e}{4\pi r_1^2}\frac{Ze}{4\pi\varepsilon_o r_1^2} \tag{1.221}$$

where ε_o is the permittivity of free-space.

The second centripetal force is an electrodynamic force or radiation reaction force, a force dependent on the second derivative of charge position which respect to time, which arises between the electron and the nucleus. This force given in Sections 6.6, 12.10, and 17.3 of Jackson [37] achieves the condition that the sum of the mechanical momentum and electromagnetic momentum is conserved. The motion of each point in the magnetic field of the nucleus will cause a relativistic central force, $\mathbf{F}_{mag}$, which acts on each point mass. The magnetic central force is derived as follows from the Lorentzian force which is relativistically corrected. Each infinitesimal point of the orbitsphere moves on a great circle, and each point charge has the charge density $\frac{e}{4\pi r_n^2}$. As given in the Proton and Neutron section, the proton is comprised of a linear combination of three constant functions and three orthogonal spherical harmonic quark/gluon functions. The magnetic field front due to the motion of the electron propagates at the speed of light. From the photon inertial reference frame at the radius of each infinitesimal point of the electron orbitsphere, the proton charge distribution is given as the product of the quark and gluon functions which gives rise to a uniform distribution. The magnetic flux of the proton in the $v=c$ inertial frame at the electron radius follows from McQuarrie [20]:

$$\mathbf{B} = \frac{\mu_o e\hbar}{2m_p r_n^3} \tag{1.222}$$

And, the magnetic flux due to a nucleus of charge Z and mass m is

$$\mathbf{B} = \frac{\mu_o Ze\hbar}{2mr_n^3} \tag{1.223}$$

The motion of each point will cause a relativistic central force, $\mathbf{F}_{i\ mag}$, which acts on each point mass. The magnetic central force is derived as follows from the Lorentzian force which is relativistically corrected. The Lorentzian force density on each point moving at velocity $\mathbf{v}$ is

$$\mathbf{F}_{mag} = \frac{e}{4\pi r_n^2}\mathbf{v}\times\mathbf{B} \tag{1.224}$$

For the hydrogen atom with $Z=1$ and $m=m_p$, substitution of Eq. (1.47) for $\mathbf{v}$ and Eq. (1.223) for $\mathbf{B}$ gives

$$\mathbf{F}_{mag} = \frac{1}{4\pi r_1^2}\left[\frac{e^2\mu_o}{2m_e r_n}\right]\frac{\hbar^2}{mr_n^3}\hat{r} \tag{1.225}$$

The term in brackets can be expressed in terms the fine structure constant α wherein the radius of the electron relative to the $v = c$ frame (k is the lightlike k^0, then $k = \omega_n / c$), r_α^*, is the corresponding relativistic radius. From Eq. (1.43), the relationship between the radius and the electron wavelength is

$$2\pi r = \lambda \tag{1.226}$$

Using the de Broglie Eq. (1.46) with $v = c$

$$\lambda = \frac{h}{mv} = \frac{h}{mc} \tag{1.227}$$

With substitution of Eq. (1.227) into Eq. (1.226)

$$r_\alpha^* = \frac{\hbar}{mc} = \lambda\!\!\!^{-}_c = \alpha a_o \tag{1.228}$$

The radius of the electron orbitsphere in the $v = c$ frame is $\lambda\!\!\!^{-}_C$, where $v = c$ corresponds to the magnetic field front propagation velocity which is the same in all inertial frames, independent of the electron velocity as shown by the velocity addition formula of special relativity [38]. From Eqs. (1.158) and (1.228),

$$\frac{e^2\mu_o}{2m_e r_n} = 2\pi\alpha \tag{1.229}$$

where $\lambda\!\!\!^{-}_C$ is the Compton wavelength bar substituted for r_n, and a_o is the Bohr radius.

From Lorentz transformations with the electron's invariant angular momentum of $\hbar$ (Eq. (1.57), it can be shown that the relativistic correction to Eq. (1.225) is the reciprocal of Eq. (1.229). Consider an inertial frame following a great circle of radius r_n with $v = c$. The motion is tangential to the radius; thus, r_n is Lorentzian invariant. But, as shown in the Spacetime Fourier Transform of the Electron Function section and the Special Relativistic Correction to the Ionization Energies section, the tangential distance along a great circle is $2\pi r_n$ in the laboratory frame and r_n in the $v = c$ frame (k is the lightlike k^0, then $k = \omega_n / c$). In addition, the corresponding radius is reduced by α for the light speed radial field. Thus, the term in brackets in Eq. (1.225) is the inverse of the relativistic correction γ' for the electrodynamic central force.

The electron's magnetic moment of a Bohr magneton μ_B given by Eq. (1.110) is also invariant as well as its angular momentum of $\hbar$. The electron is nonradiative due to its angular motion as shown in Spacetime Fourier Transform of the Electron Function, Appendix I, and the Stability of Atoms and Hydrinos section. Furthermore, the angular momentum of the photon given in the Equation of the Photon section is $\mathbf{m} = \int \frac{1}{8\pi c}\mathrm{Re}\left[\mathbf{r}\times(\mathbf{E}\times\mathbf{B}^*)\right]dx^4 = \hbar$. It is conserved for the solutions for the resonant photons and excited state electron functions given in the Excited States of the One-Electron Atom (Quantization) section and the Equation of the Photon section. Thus, the electrodynamic angular momentum and the inertial angular momentum are matched such that the correspondence principle holds. It follows from the principle of conservation of angular momentum that $\frac{e}{m_e}$ of Eq. (1.110) is invariant. The same applies for the

intrinsic magnetic moment μ_B and angular momentum $\hbar$ of the free electron since it is given by the projection of the bound electron into a plane as shown in the Electron in Free Space section. However, special relativity must be applied to physics relative to the electron's center of mass due to the invariance of charge and the invariant four momentum as given by Purcell [38].

The correction to the term in brackets of Eq. (1.225) also follows from the Lorentz transformation of the electron's invariant magnetic moment as well as its invariant angular momentum of $\hbar$. Consider a great circle of the electron orbitsphere. As shown in the Spacetime Fourier Transform of the Electron Function section, the tangential distance along a great circle is $2\pi r_n$ in the laboratory frame and r_n in the $v = c$ frame; thus, electron mass density along each great circle can be considered to contract to a point with an increase of the relativistic mass density by a factor of 2π. Furthermore, due to invariance of charge under Gauss' Integral Law, with the radius given by (1.228), the charge corresponding to the source current of the magnetic field must be corrected by α^{-1}. Thus, from the perspective of the invariance of μ_B, the term in brackets in Eq. (1.225) is inverse of the relativistic correction for the electrodynamic central force.

$$\frac{\alpha^{-1}e^2\mu_o}{2(2\pi m_e)r_n} = \frac{\alpha^{-1}e^2\mu_o}{2(2\pi m_e)\lambda\!\!\!^{-}} = \frac{2\pi\alpha^{-1}e^2\mu_o}{2(2\pi m_e)\frac{h}{m_e c}} = 1 \tag{1.230}$$

Therefore, the force is given by

$$\mathbf{F}_{mag} = -\frac{1}{4\pi r_1^2}\frac{\hbar^2}{mr_1^3}\hat{r} \tag{1.231}$$

The force balance equation is given by equating the centrifugal and centripetal force densities:

$$\frac{m_e}{4\pi r_1^2}\frac{v_1^2}{r_1} = \frac{1}{4\pi r_1^2}\frac{\hbar^2}{m_e r_1^3} = \frac{e}{4\pi r_1^2}\frac{Ze}{4\pi\varepsilon_o r_1^2} - \frac{1}{4\pi r_1^2}\frac{\hbar^2}{mr_1^3} \tag{1.232}$$

where $Z = 1$ and $m = m_p$ for the hydrogen atom and the velocity is given by Eq. (1.47). (Since the surface-area factor cancels in all cases, this factor will be left out in subsequent force calculations throughout this book). From the force balance equation:

$$r_1 = \frac{4\pi\varepsilon_o\hbar^2}{Ze^2\mu_e} \tag{1.233}$$

where the reduced electron mass, μ_e, is

$$\mu_e = \frac{m_e m}{m_e + m} \tag{1.234}$$

The Bohr radius is

$$a_o = \frac{4\pi\varepsilon_o\hbar^2}{e^2 m_e} \tag{1.235}$$

And, the radius given by force balance between the centrifugal force and central electrostatic force alone is

$$r_1 = \frac{4\pi\varepsilon_o\hbar^2}{Ze^2 m_e} = \frac{a_0}{Z} \tag{1.236}$$

And, for hydrogen, m of Eq. (1.234) is

$$m = m_p \tag{1.237}$$

Substitution of the reduced electron mass for the electron mass gives, a_H, the Bohr radius of the hydrogen atom.

$$a_H = \frac{4\pi\varepsilon_o\hbar^2}{e^2\mu_e} \tag{1.238}$$

Thus, Eq. (1.233) becomes

$$r_1 = \frac{a_H}{Z} \tag{1.239}$$

where $Z = 1$ for the hydrogen atom. The results can also be arrived at by the familiar minimization of the energy.

ENERGY CALCULATIONS

The potential energy V between the electron and the nucleus separated by the radial distance radius r_1 considering the force balance between the centrifugal force and central electrostatic force alone is

$$V = \frac{-Ze^2}{4\pi\varepsilon_o r_1} = \frac{-Z^2e^2}{4\pi\varepsilon_o a_0} = -Z^2\ X\ 4.3598\ X\ 10^{-18}\ J = -Z^2\ X\ 27.212\ eV \tag{1.240}$$

Because this is a central force problem, the kinetic energy, T, is $-\frac{1}{2}V$.

$$T = \frac{Z^2e^2}{8\pi\varepsilon_o a_0} = Z^2\ X\ 13.606\ eV \tag{1.241}$$

The same result can be obtained from $T = \frac{1}{2}m_e v_1^2$ and Eq. (1.47). Alternatively, the kinetic energy T and the binding energy E_B, which are each equal to the change in stored electric energy, ΔE_{ele}, can be calculated from

$$T = \Delta E_{ele} = -\frac{1}{2}\varepsilon_o Z\int_{\infty}^{r_1}\mathbf{E}^2 d\mathcal{V} \text{ where } \mathbf{E} = -\frac{e}{4\pi\varepsilon_o r^2}\mathbf{i}_\mathbf{r} \tag{1.242}$$

Thus, as the orbitsphere shrinks from ∞ *to* r_1,

$$E_B = -\frac{Ze^2}{8\pi\varepsilon_o r_1} = -\frac{Z^2e^2}{8\pi\varepsilon_o a_0} = -Z^2\ X\ 2.1799\ X\ 10^{-18}\ J = -Z^2\ X\ 13.606\ eV \tag{1.243}$$

The calculated Rydberg constant R using Eq. (1.238) in Eqs. (1.240-1.243) which includes the relativistic correction corresponding to the magnetic force given by Eq. (1.231) is $10,967,758\ m^{-1}$. The experimental Rydberg constant is $10,967,758\ m^{-1}$. Furthermore, a host of parameters can be calculated for the hydrogen atom, as shown in Table 1.2.

Table 1.2. Some calculated parameters for the hydrogen atom ($n=1$).

radius	$r_1 = a_H$	$5.2947\ X\ 10^{-11}\ m$
potential energy	$V = \frac{-e^2}{4\pi\varepsilon_o a_H}$	$-27.196\ eV$
kinetic energy	$T = \frac{e^2}{8\pi\varepsilon_o a_H}$	$13.598\ eV$
angular velocity (spin)	$\omega_1 = \frac{\hbar}{m_e r_1^2}$	$4.1296\ X\ 10^{16}\ rads^{-1}$
linear velocity	$v_1 = r_1\omega_1$	$2.1865\ X\ 10^{6}\ ms^{-1}$
wavelength	$\lambda_1 = 2\pi r_1$	$3.325\ X\ 10^{-10}\ m$
spin quantum number	$s = \frac{1}{2}$	$\frac{1}{2}$
moment of Inertia	$I = \frac{m_e r_1^2}{2}$	$1.277\ X\ 10^{-51}\ kgm^2$
angular kinetic energy	$E_{angular} = \frac{1}{2} I\omega_1^2$	$6.795\ eV$
magnitude of the angular momentum	$\hbar$	$1.0545\ X\ 10^{-34}\ Js$
projection of the angular momentum onto the transverse-axis	$\frac{\hbar}{4}$	$2.636\ X\ 10^{-35}\ Js$
projection of the angular momentum onto the z-axis	$S_z = \frac{\hbar}{2}$	$5.273\ X\ 10^{-35}\ Js$
mass density	$\frac{m_e}{4\pi r_1^2}$	$2.589\ X\ 10^{-11}\ kgm^{-2}$
charge density	$\frac{e}{4\pi r_1^2}$	$4.553\ Cm^{-2}$

Table 1.3 gives the radii and energies for some one-electron atoms. In addition to the energies, the wavelength, angular frequency, and the linear velocity can be calculated for any one-electron atom from Eqs. (1.46), (1.55), and (1.56). Values are given in Table 1.4.

Table 1.3. Calculated energies (non-relativistic) and calculated ionization energies for some one-electron atoms.

Atom	Calculated r_1 [a] (a_0)	Calculated Kinetic Energy[b] (eV)	Calculated Potential Energy[c] (eV)	Calculated Ionization Energy[d] (eV)	Experimental Ionization Energy[e] (eV)
H	1.000	13.61	–27.21	13.61	13.59
He^+	0.500	54.42	–108.85	54.42	54.42
Li^{2+}	0.333	122.45	–244.90	122.45	122.45
Be^{3+}	0.250	217.69	–435.39	217.69	217.71
B^{4+}	0.200	340.15	–680.29	340.15	340.22
C^{5+}	0.167	489.81	–979.62	489.81	489.98
N^{6+}	0.143	666.68	–1333.37	666.68	667.03
O^{7+}	0.125	870.77	–1741.54	870.77	871.39

[a] from Equation (1.236)
[b] from Equation (1.241)
[c] from Equation (1.240)
[d] from Equation (1.243)
[e] experimental

It is noteworthy that the potential energy is a constant (at a given n) because the electron is at a fixed distance, r_n, from the nucleus. And, the kinetic energy and velocity squared are constant because the atom does not radiate at r_n and the potential energy is constant.

Table 1.4. Calculated radii, angular frequencies, linear velocities, and wavelengths for the $n=1$ state of some one-electron atoms (non-relativistic).

Atom	r_1 [a] (a_0)	angular[b] velocity ($10^{17} rad\ s^{-1}$)	linear[c] velocity ($10^6\ ms^{-1}$)	wavelength[d] ($10^{-10}\ m$)
H 1.000	0.413	2.19	3.325	
He^+	0.500	1.65	4.38	1.663
Li^{2+}	0.333	3.72	6.56	1.108
Be^{3+}	0.250	6.61	8.75	0.831
B^{4+}	0.200	10.3	10.9	0.665
C^{5+}	0.167	14.9	13.1	0.554
N^{6+}	0.143	20.3	15.3	0.475
O^{7+}	0.125	26.5	17.5	0.416

[a] from Equation (1.236)
[b] from Equation (1.55)
[c] from Equation (1.56)
[d] from Equation (1.46)

It should be noted that the linear velocity is an appreciable percentage of the velocity of light for some of the atoms in Table 1.3—5.9% for O^{7+} for example. Relativistic corrections must be applied before a comparison between the total energy and ionization energy (Table 1.3) is made.

SPECIAL RELATIVISTIC CORRECTION TO THE IONIZATION ENERGIES

The electron moves in an orbit relative to the laboratory frame. Muons and electrons are both leptons. Time dilation of muonic decay due to relativistic motion in a cyclotron orbit relative to a stationary laboratory frame provides strong confirmation of special relativity and confirms that the electron's frame is an inertial frame. eB/m bunching of electrons in a gyrotron [39] occurs because the cyclotron frequency is inversely proportional to the relativistic electron mass. This further demonstrates that the electron frame is an inertial frame and that electron mass and time dilation occur. The special relativistic relationship in polar coordinates is derived. The result of the treatment of the electron motion relative to the laboratory frame is in excellent agreement with numerous experimental observables such as the electron g factor, the invariance of the electron magnetic moment of μ_B and angular momentum of $\hbar$, the fine structure of the hydrogen atom, and the relativistically corrected ionization energies of one and two electron

atoms found *infra.* and in the Excited States of the One-Electron Atom (Quantization) and The Two-Electron Atoms sections.

The relativistic correction to the ionization energies is determined by determining the corrected radius in Eq. (1.243) corresponding to a decrease in the electron wavelength and period due to relativistic length contraction and time dilation of the electron motion in the laboratory inertial frame[9]. Each infinitesimal point of the orbitsphere moves on a great circle as shown in the Orbitsphere Equation of Motion for $\ell = 0$ section. The electron motion is tangential to the radius; thus, r_n is Lorentzian invariant. A further consequence of the electron's motion always being perpendicular to its radius is that the electron's angular momentum of $\hbar$ is invariant as shown by Eq. (1.57). The electron's magnetic moment of a Bohr magneton μ_B given by Eq. (1.110) is also invariant as well as its angular momentum of $\hbar$. Furthermore, the electron is nonradiative due to its angular motion as shown in the Spacetime Fourier Transform of the Electron Function section, Appendix I, and the Stability of Atoms and Hydrinos section. The radiative instability of excited states is due to a radial dipole term in the function representative of the excited state due to the interaction of the photon and the excited state electron as shown in the Instability of Excited States section. The angular momentum of the photon given in the Equation of the Photon section is $\mathbf{m} = \int \frac{1}{8\pi c} \mathrm{Re}\left[\mathbf{r} \times (\mathbf{E} \times \mathbf{B}^*)\right] dx^4 = \hbar$. It is conserved for the solutions for the resonant photons and excited state electron functions given in the Excited States of the One-Electron Atom (Quantization) section and the Equation of the Photon section. The photons emitted during the formation of each one-electron atom are its excited state photons. Thus, the electrodynamic angular momentum and the inertial angular momentum are matched such that the correspondence principle holds. It follows from the principle of conservation of angular momentum of $\hbar$ that $\frac{e}{m_e}$ of Eq. (1.110) is invariant (See the Determination of Orbitsphere Radii section). Since charge is invariant according to special relativity, the electron mass of the orbitsphere must also be invariant. But, as shown in the Spacetime Fourier Transform of the Electron Function section, the tangential distance along a great circle is $2\pi r_n$ in the $v = c$ frame is r_n in the laboratory frame. Thus, the effect of special relativity is to increase the mass and charge densities identically such that $\frac{e}{m_e}$ is a constant invariant. In the present case, the electron mass density along each great circle can be considered to contract to a point with an increase of the relativistic mass density by a factor of 2π. The remarkable agreement

[9] Many problems arise in the case of applying special relativity to standard quantum mechanical solutions for one-electron atoms as discussed in the Quantum Theory Past and Future section, the Shortcomings of Quantum Theory section, and Appendix II: Quantum Electrodynamics is Purely Mathematical and Has No Basis in Reality. Spin was missed entirely by the Schrödinger equation, and it was forced by spin matrices in the Dirac equation. It does not arise from first principles, and it results in nonsensical consequences such as infinities and "a sea of virtual particles". These are not consistent with observation and paradoxically the virtual particles constitute an ether, the elimination of which was the basis of special relativity and is the supposed basis of the Dirac equation. In addition, the electron motion in the Schrödinger and Dirac equations is in all directions; consequently, the relativistic increase in electron mass results in an instability since the electron radius is inversely proportional to the electron mass. Since the electron mass in special relativity is not invariant, but the charge is, the electron magnetic moment of a Bohr magneton μ_B as well as its angular momentum of $\hbar$ cannot be invariant in contradiction with experimental observations known to 14 figure accuracy [28].

between the calculated and observed value of the fine structure of the hydrogen atom which depends on the conditions of the invariance of the electron's charge and charge-to-mass ratio $\frac{e}{m_e}$ as given in the Spin-Orbital Coupling section further confirms the validity of this result.

Each infinitesimal point of the orbitsphere moves on a great circle, and each point charge has the charge density $\frac{e}{4\pi r_n^2}$ and mass density $\frac{m_e}{4\pi r_n^2}$ as shown in the Orbitsphere Equation of Motion for $\ell = 0$ section. Consider a charge-density element (and correspondingly a mass-density element) of a great circle current loop of the electron orbitsphere in the y'z'-plane as shown in Figure 1.4. The distance on a great circle is given by

$$\int_0^{2\pi} r_n d\theta = r_n \theta \Big|_0^{2\pi} = 2\pi r_n \tag{1.244}$$

Due to relative motion, the distance along the great circle must contract and the time must dilate due to special relativity. The special relativistic length contraction relationship observed for a laboratory frame relative to an inertial frame moving at constant velocity v in the direction of velocity v is

$$l = l_o \sqrt{1 - \left(\frac{v}{c}\right)^2} \tag{1.245}$$

For Figure 1.4, the relationship between polar and Cartesian coordinates of special relativity (the Cartesian coordinate system as compared to general coordinates is special with regard to special relativity as discussed in the Relativity section) is given by Eq. (1.68)

$$x_1' = 0 \qquad y_1' = -r_n \sin(\omega_n t) \qquad z_1' = r_n \cos(\omega_n t) \tag{1.246}$$

where ω_n is given by Eq. (1.55), r_n is from Eq. (1.236) and

$$\phi = \omega_n t \tag{1.247}$$

Due to relativity, a contracted wavelength arises. The distance on the great circle undergoes length contraction only in the $\hat{\phi}$ direction as $v \to c$. Thus, as $v \to c$ the distance on a great circle approaches its radius which is the relativistically contracted electron wavelength since the relationship between the radius and the wavelength given by Eq. (1.43) is

$$2\pi r_n = \lambda_n \tag{1.248}$$

With $v = c$,

$$r^* = \lambda \tag{1.249}$$

where * indicates the relativistically corrected parameter. Thus,

$$r^* = \frac{r_n}{2\pi} \tag{1.250}$$

The relativistically corrected mass m^* follows from Eq. (1.250) with maintenance of the invariance of the electron angular momentum of $\hbar$ given by Eqs. (1.56) and (1.57).

$$m\mathbf{r} \times \mathbf{v} = m_e r \frac{\hbar}{m_e r} \tag{1.251}$$

With Eq. (1.250), the relativistically corrected mass m^* corresponding to an increase in its

density only is[10]

$$m^* = 2\pi m_e \tag{1.252}$$

The charge (mass) motion may be visualized. At light speed, there can be no motion transverse to the radius. The radial projection of the time harmonic motion of a point charge of a great circle becomes equivalent to a time harmonic oscillator moving along an axis of distance $2r_n$ in the direction of r. In spherical coordinates, the lab frame is at rest at the origin. Relativistic invariance of charge requires that all of the charge of a current loop be projected onto a line in the radial direction. For $n=1$, $\ell=0$, the charge is uniformly distributed. Consider, the radial projection of a point charge on a great circle at $\phi = 0$ and a point charge at $\phi = \pi$. Both points move from opposite ends of a line of length $2r_n$ ($-r_n \le r \le +r_n$) and are at the origin in a quarter of a period which is time $t = \frac{r_n}{2c}$. The points then cross. (The crossing is equivalent to elastic scattering at the origin which results in a momentum reversal for both points.) The points

---

[10] The scalar sum of the magnitude of the angular momentum of each infinitesimal point of the orbitsphere $\mathbf{L}_i$ of mass m_i must be constant. The constant is $\hbar$.

$$\sum |\mathbf{L}_i| = \sum \left|\mathbf{r} \times m_i \mathbf{v}\right| = m_e r_n \frac{\hbar}{m_e r_n} = \hbar \tag{1}$$

where the velocity is given by Eq. (1.47). In the limit, the sum is replaced by a continuous integral over the surface wherein the point element masses and angular momenta are replaced by the corresponding densities. The integral of the magnitude of the angular momentum of the electron is $\hbar$ in any inertial frame and is *relativistically invariant*.

According to special relativity, the electron's relative motion with respect to the laboratory frame causes the distance along the great circle to contract and the time to dilate such that a contracted radius arises as given by Eq. (1.259). As $v \to c$ the relativistically corrected radius in the laboratory frame r^* is given by

$$r^* = \frac{r_n}{2\pi} \tag{2}$$

where r_n is the radius in the electron frame. Eq. (1.240) applies for both the mass and charge densities which are interchangeable by the ratio $\frac{e}{m_e}$. Thus, the ratio is invariant.

However, a relativistically corrected mass m^* can be defined from Eq. (1.250) with maintenance of the invariance of the electron angular momentum of $\hbar$ given by Eqs. (1.56) and (1.57). Due to spherical symmetry, the correction is the same along each great circle of the orbitsphere. Thus, the motion of the mass density of the electron along a great circle may be considered. Then,

$$m\mathbf{r} \times \mathbf{v} = m_e r \frac{\hbar}{m_e r} \tag{3}$$

With Eq. (1.250), the relativistically corrected mass m^* corresponding to an increase in its density only is

$$m^* = 2\pi m_e \tag{4}$$

In other words, the correction of the radius gives an effective relativistic mass as follows:

$$m\mathbf{r} \times \mathbf{v} = m_e \frac{r}{2\pi} \frac{\hbar}{m_e \frac{r}{2\pi}} = 2\pi m_e \frac{r}{2\pi} \frac{\hbar}{m_e r} = m^* \frac{r}{2\pi} \frac{\hbar}{m_e r} = m^* r^* v = \hbar \tag{5}$$

where v is the electron velocity in its frame given by Eq. (1.47).

interchange roles and travel to the opposite starting points in a half of a period which is time $t = \frac{2r_n}{2c}$. So, with respect to each position, a point left and a point reappeared in $t = \frac{2r_n}{2c}$. Since $T = \frac{2\pi}{\omega} = \frac{\lambda}{c}$, the wavelength is r_n. This situation applies for any ϕ.

Thus, the effect of the relativistic contraction of the distance along a great circle loop is to change the angle of constant motion in Eq. (1.246) with a corresponding decrease in the electron wavelength. The relativistically corrected wavelength that follows from Eqs. (1.244-1.248) is given by the sum of the relativistic electron motion along the great circle (y' direction for point 1 of Figure 1.4) and that projected along the radial axis (z' direction for point 1 of Figure 1.4):

$$\lambda_n = r^*_{n,y'} \sin\phi^* \int_0^{2\pi} d\phi + \cos\phi^* \int_0^{r^*_{n,z'}} dr \tag{1.253}$$

where the * indices corresponds to the relativistically corrected parameters in the y' and z' directions. The length contraction is only in the direction of motion which is orthogonal to the radius and constant as a function of angle. Thus, Eq. (1.247) is given by

$$\lambda_n = 2\pi r_n' \sqrt{1-\left(\frac{v}{c}\right)^2} \sin\phi^* + r_n' \cos\phi^* \tag{1.254}$$

The projection of the angular motion onto the radial axis is determined by determining the relativistic angle ϕ^* corresponding to a decrease in the electron wavelength and period due to relativistic length contraction and time dilation of the electron motion in the laboratory inertial frame. Substitution of Eq. (1.55) into Eq. (1.247) gives

$$\phi = \omega_n t = \frac{\hbar}{m_e r_n^2} t \tag{1.255}$$

The correction for the time dilation and length contraction due to electron motion gives the relativistic angle ϕ^* as

$$\phi^* = \omega_n t = \frac{\hbar}{m_e \left(\frac{r_n}{\sqrt{1-\left(\frac{v}{c}\right)^2}}\right)^2} t\sqrt{1-\left(\frac{v}{c}\right)^2} = \frac{\hbar}{m_e r_n^2} t\left(1-\left(\frac{v}{c}\right)^2\right)^{3/2} \tag{1.256}$$

The period for a wavelength due to electron motion is

$$T = \frac{2\pi}{\omega} = \frac{\lambda}{v} \tag{1.257}$$

Only the elements of the second y'z'-quadrant need be considered due to symmetry and continuity of the motion. Thus, using Eqs. (1.255-1.256) for a quarter period of time, Eq. (1.254) becomes

$$\lambda_n = 2\pi r_n' \sqrt{1-\left(\frac{v}{c}\right)^2} \sin\left[\frac{\pi}{2}\left(1-\left(\frac{v}{c}\right)^2\right)^{3/2}\right] + r_n' \cos\left[\frac{\pi}{2}\left(1-\left(\frac{v}{c}\right)^2\right)^{3/2}\right] \tag{1.258}$$

The relativistic correction to the ionization energies is determined by using the corrected radius in Eq. (1.243). Using a phase matching condition, the wavelengths of the electron (Eq. (1.248)) and laboratory (Eq. (1.258)) inertial frames are equated, and the corrected radius is given by

$$r_n = r_n' \left[\sqrt{1-\left(\frac{v}{c}\right)^2}\, \sin\left[\frac{\pi}{2}\left(1-\left(\frac{v}{c}\right)^2\right)^{3/2}\right] + \frac{1}{2\pi}\cos\left[\frac{\pi}{2}\left(1-\left(\frac{v}{c}\right)^2\right)^{3/2}\right]\right] \tag{1.259}$$

From Eqs. (1.233) and (1.249) the ionization energies are corrected by a factor γ^* of

$$\gamma^* = \frac{2\pi}{2\pi\sqrt{1-\left(\frac{v}{c}\right)^2}\, \sin\left[\frac{\pi}{2}\left(1-\left(\frac{v}{c}\right)^2\right)^{3/2}\right] + \cos\left[\frac{\pi}{2}\left(1-\left(\frac{v}{c}\right)^2\right)^{3/2}\right]} \tag{1.260}$$

where the velocity is given by Eq. (1.56) with the radius given by Eq. (1.233). In Eq. (1.233), the reduced mass is that of the corresponding nucleus. Plots of ratio of the radii from Eq. (1.259) and the correction to the ionization energy γ^* (Eq. (1.260)) as a function of the electron velocity v relative to the speed of light c are given in Figures 1.21 and 1.22, respectively.

As the electron velocity goes to the speed of light ($v \to c$) the electron radius in the laboratory frame goes to a factor of $\frac{1}{2\pi}$ that in the electron frame ($\frac{r_n}{r_n'} = \frac{1}{2\pi}$). One model to interpret this result is to consider that with $v = c$ the electron motion looks like a line for all angles which corresponds to a orbitsphere of radius $\frac{1}{2\pi}$ that of the radius in the electron frame. Also, for all directions, the angle ϕ in polar coordinates is corrected in going from the electron to the laboratory frame as given in Eq. (1.256) to make the transformation to an orbitsphere of reduced radius.

Figure 1.21. The normalized radius as a function of v/c due to relativistic contraction.

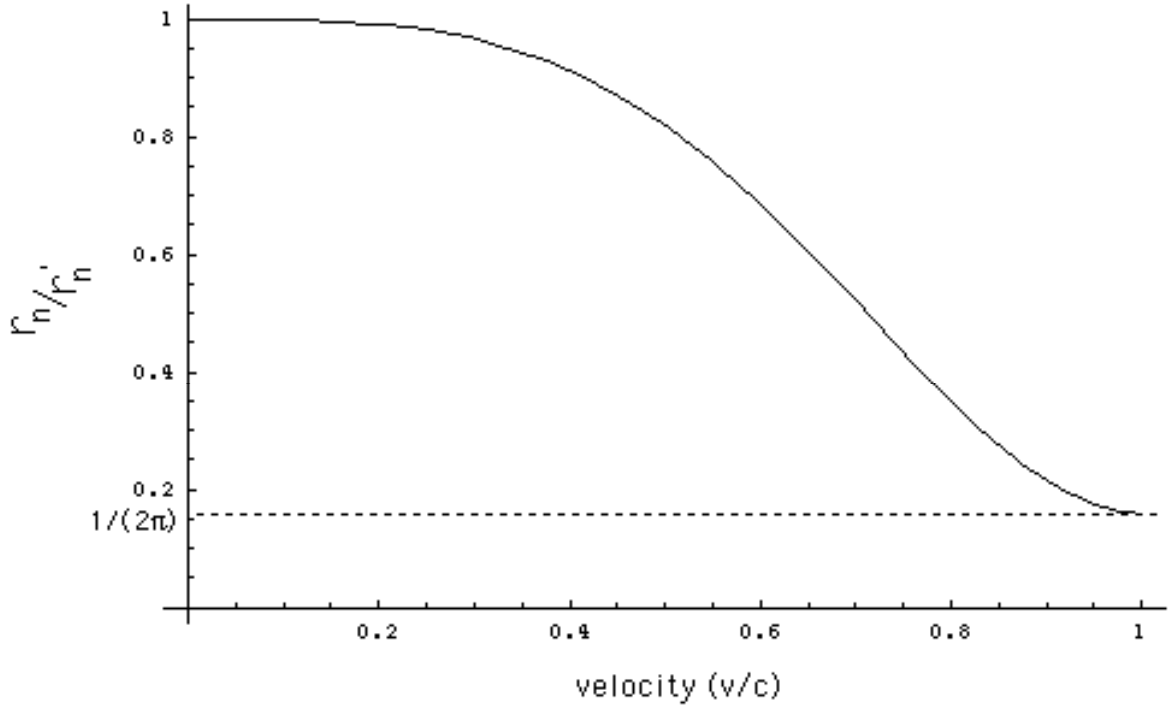

Figure 1.22. The relativistic correction to the one-atom-electron ionization energies as a function of v/c due to relativistic contraction.

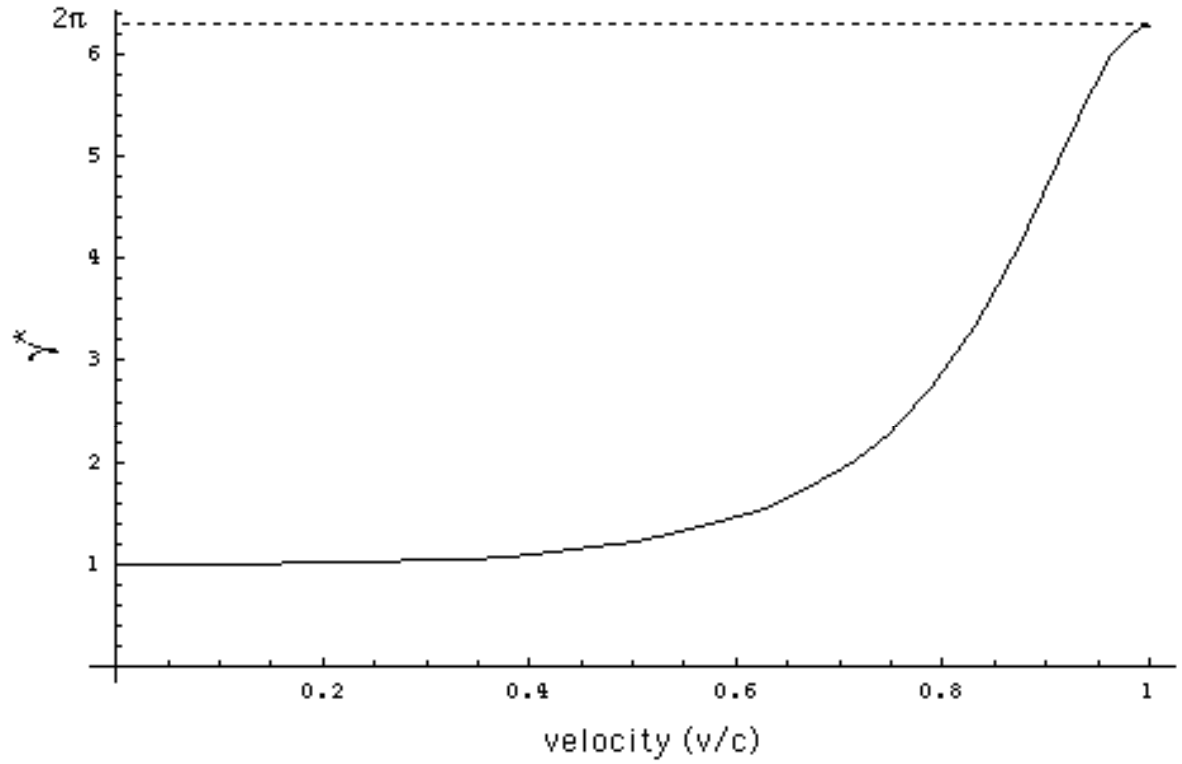

The electron possesses an invariant angular momentum and magnetic moment of $\hbar$ and a Bohr magneton, respectively. *This invariance feature provides for the stability of multielectron*

atoms and the existence of excited states wherein electrons magnetically interact as shown in the Two-Electron Atoms section, the Three- Through Twenty-Electron Atoms section, and the Excited States of Helium section. The electron's motion corresponds to a current which gives rise to a magnetic field with a field strength that is inversely proportional to its radius cubed wherein the magnetic field is a relativistic effect of the electric field as shown by Jackson [40]. As there is *no electrostatic self-energy* as shown in the Determination of Orbitsphere Radii section and Appendix IV, there is also *no magnetic self-energy* for the bound electron since the magnetic moment is invariant for all states and the surface current is the source of the discontinuous field that does not exist inside of the electron as given by Eq. (1.115), $\mathbf{n}\ X\ (\mathbf{H}_a - \mathbf{H}_b) = \mathbf{K}$. No energy term is associated with the magnetic field unless another source of magnetic field is present. In general, the corresponding relativistic correction can be calculated from the effect of the electron's magnetic field on the force balance and energies of other electrons and the nucleus which also produce magnetic fields. In the case of one-electron atoms, the nuclear-electron magnetic interaction is the only factor. Thus, for example, the effect of the proton was included in the derivation of Eq. (1.239) for the hydrogen atom. The relativistically corrected one electron ionization energies given by the product of Eqs. (1.243) and (1.260) is

$$E_{ele} = -\gamma^* \frac{Z^2 e^2}{8\pi\varepsilon_o a_0}\frac{\mu}{m_e} = -\gamma^* \frac{\mu}{m_e} Z^2\ X\ 2.1799\ X\ 10^{-18}\ J = -\gamma^* \frac{\mu}{m_e} Z^2\ X\ 13.606\ eV \qquad (1.261)$$

where the reduced mass term μ_e corresponds to the electron-nucleus relativistic correction and is only given by Eq. (1.234) for the hydrogen atom where $Z = 1$. These energies are plotted in Figure 1.23 and are given in Table 1.5.

`Figure 1.23.` The relativistically corrected one-electron-atom ionization energies as a function of the nuclear charge Z.

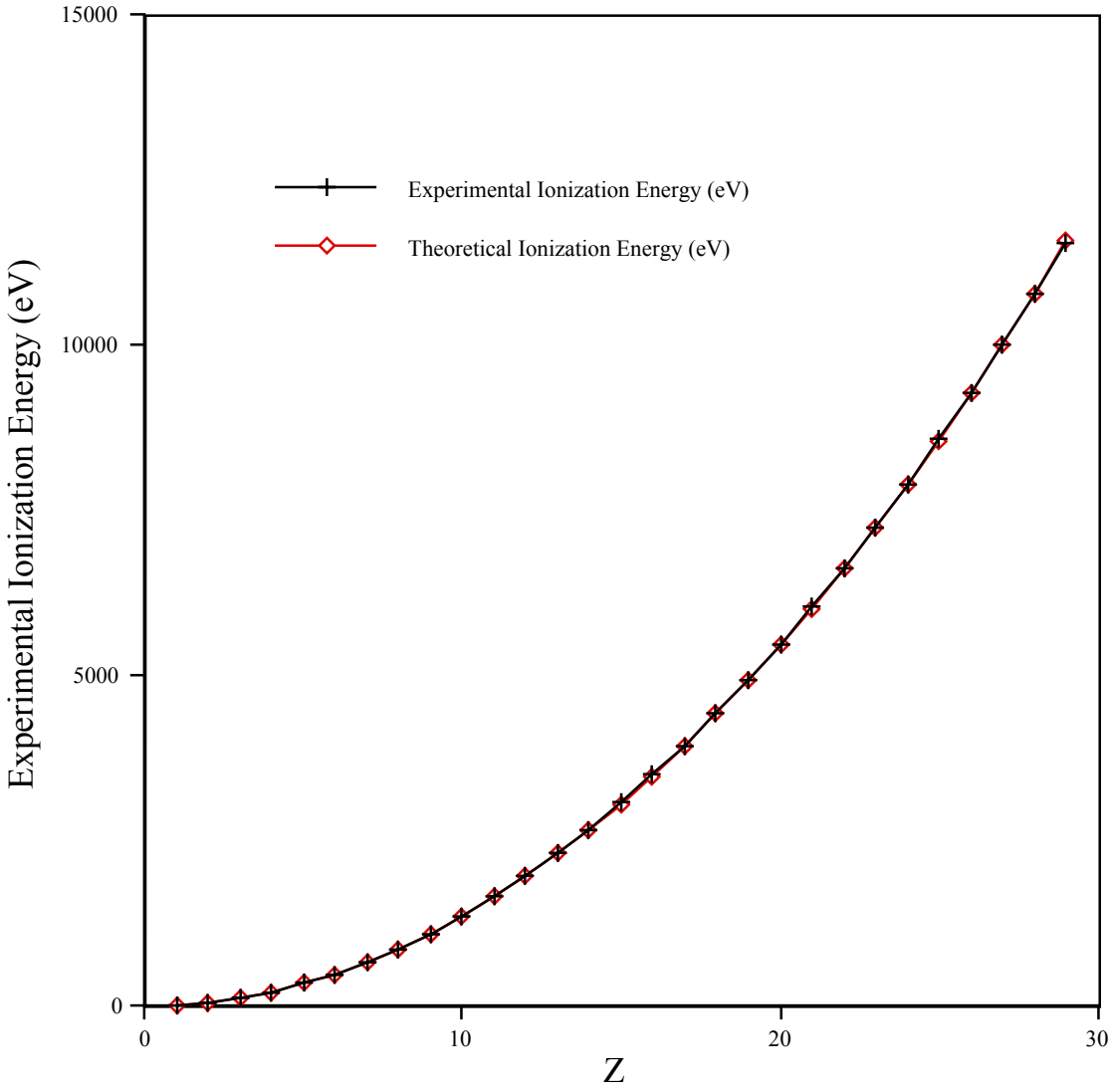

Table 1.5. Relativistically corrected ionization energies for some one-electron atoms.

One e Atom	Z	γ^* (from Eq. (1.250))	Theoretical Ionization Energies (eV) (from Eq. (1.251))	Experimental Ionization Energies (eV) [a]	Relative Difference between Experimental and Calculated [b]
H	1	1.000007	13.59838	13.59844	0.00000
He^{+}	2	1.000027	54.40941	54.41778	0.00015
Li^{2+}	3	1.000061	122.43642	122.45429	0.00015
Be^{3+}	4	1.000109	217.68510	217.71865	0.00015
B^{4+}	5	1.000172	340.16367	340.2258	0.00018
C^{5+}	6	1.000251	489.88324	489.99334	0.00022
N^{6+}	7	1.000347	666.85813	667.046	0.00028
O^{7+}	8	1.000461	871.10635	871.4101	0.00035
F^{8+}	9	1.000595	1102.65013	1103.1176	0.00042
Ne^{9+}	10	1.000751	1361.51654	1362.1995	0.00050
Na^{10+}	11	1.000930	1647.73821	1648.702	0.00058
Mg^{11+}	12	1.001135	1961.35405	1962.665	0.00067
Al^{12+}	13	1.001368	2302.41017	2304.141	0.00075
Si^{13+}	14	1.001631	2670.96078	2673.182	0.00083
P^{14+}	15	1.001927	3067.06918	3069.842	0.00090
S^{15+}	16	1.002260	3490.80890	3494.1892	0.00097
Cl^{16+}	17	1.002631	3942.26481	3946.296	0.00102
Ar^{17+}	18	1.003045	4421.53438	4426.2296	0.00106
K^{18+}	19	1.003505	4928.72898	4934.046	0.00108
Ca^{19+}	20	1.004014	5463.97524	5469.864	0.00108
Sc^{20+}	21	1.004577	6027.41657	6033.712	0.00104
Ti^{21+}	22	1.005197	6619.21462	6625.82	0.00100
V^{22+}	23	1.005879	7239.55091	7246.12	0.00091
Cr^{23+}	24	1.006626	7888.62855	7894.81	0.00078
Mn^{24+}	25	1.007444	8566.67392	8571.94	0.00061
Fe^{25+}	26	1.008338	9273.93857	9277.69	0.00040
Co^{26+}	27	1.009311	10010.70111	10012.12	0.00014
Ni^{27+}	28	1.010370	10777.26918	10775.4	-0.00017
Cu^{28+}	29	1.011520	11573.98161	11567.617	-0.00055

[a] From theoretical calculations, interpolation of H isoelectronic and Rydberg series, and experimental data [41-42].
[b] (Experimental-theoretical)/experimental.

The agreement between the experimental and calculated values of Table 1.5 is well within the experimental capability of the spectroscopic determinations including the values at large Z which relies on X-ray spectroscopy. In this case, the experimental capability is three to four significant figures which is consistent with the last column. The hydrogen atom isoelectronic series is given in Table 1.5 [41-42] to much higher precision than the capability of X-ray spectroscopy, but these values are based on theoretical and interpolation techniques rather than data alone. Ionization energies are difficult to determine since the cut-off of the Rydberg series of lines at the ionization energy is often not observed, and the ionization energy must be determined from theoretical calculations, interpolation of H isoelectronic and Rydberg series, as well as direct

REFERENCES

1. H. A. Haus, "On the radiation from point charges", American Journal of Physics, 54, (1986), pp. 1126-1129.
2. J. D. Jackson, *Classical Electrodynamics*, Second Edition, John Wiley & Sons, New York, (1975), p. 111.
3. R. N. Bracewell, *The Fourier Transform and Its Applications*, McGraw-Hill Book Company, New York, (1978), pp. 252-253.
4. W. McC. Siebert, *Circuits, Signals, and Systems*, The MIT Press, Cambridge, Massachusetts, (1986), p. 415.
5. Y. L. Luke, *Integrals of Bessel Functions*, McGraw-Hill, New York, (1962), p.22.
6. M. Abramowitz, I. Stegun (3rd Printing 1965), p. 366, eq. 9.1.10, and p. 255, eq. 6.1.6.
7. Y. L. Luke, *Integrals of Bessel Functions*, McGraw-Hill, New York, (1962), p.30.
8. H. Bateman, *Tables of Integral Transforms*, Vol. III, McGraw-Hill, New York, (1954), p. 33.
9. H. Bateman, *Tables of Integral Transforms*, Vol. III, McGraw-Hill, New York, (1954), p. 5.
10. G. O. Reynolds, J. B. DeVelis, G. B. Parrent, B. J. Thompson, *The New Physical Optics Notebook,* SPIE Optical Engineering Press, (1990).
11. T. A. Abbott, D. J. Griffiths, Am. J. Phys., Vol. 53, No. 12, (1985), pp. 1203-1211.
12. D. A. McQuarrie, *Quantum Chemistry*, University Science Books, Mill Valley, CA, (1983), pp. 206-221.
13. J. D. Jackson, *Classical Electrodynamics*, Second Edition, John Wiley & Sons, New York, (1975), p. 99.
14. H. A. Haus, J. R. Melcher, "Electromagnetic Fields and Energy", Department of Electrical engineering and Computer Science, Massachusetts Institute of Technology, (1985), Sec. 8.6.
15. Mathematica modeling of R. Mills' theory by B. Holverstott in "Modeling the Orbitsphere Current-Vector Field (cvf)", posted at www.blacklightpower.com.
16. E. M. Purcell, *Electricity and Magnetism*, McGraw-Hill, New York, (1965), pp. 370-375, 447.
17. P. Pearle, Foundations of Physics, "Absence of radiationless motions of relativistically rigid classical electron", Vol. 7, Nos. 11/12, (1977), pp. 931-945.
18. G. R. Fowles, *Analytical Mechanics*, Third Edition, Holt, Rinehart, and Winston, New York, (1977), p. 196.
19. L. Pauling, E. B. Wilson, *Introduction to Quantum Mechanics with Applications to Chemistry*, McGraw-Hill Book Company, New York, (1935), pp. 118-121.
20. D. A. McQuarrie, *Quantum Chemistry*, University Science Books, Mill Valley, CA, (1983), pp. 238-241.

21. J. D. Jackson, *Classical Electrodynamics*, Second Edition, John Wiley & Sons, New York, (1975), p. 178.
22. J. D. Jackson, *Classical Electrodynamics*, Second Edition, John Wiley & Sons, New York, (1975), pp. 194-197.
23. C. E. Gough, M. S. Colclough, E. M. Forgan, R. G. Jordan, M. Keene, C. M. Muirhead, A. I. M. Rae, N. Thomas, J. S. Abell, S. Sutton, Nature, Vol. 326, (1987), p. 855.
24. S. Das Sarma, R. E. Prange, Science, Vol. 256, (1992), pp. 1284-1285.
25. J. D. Jackson, *Classical Electrodynamics*, Second Edition, John Wiley & Sons, New York, (1975), pp. 582-584.
26. J. D. Jackson, *Classical Electrodynamics*, Second Edition, John Wiley & Sons, New York, (1975), pp. 758-763.
27. R. C. Weast, *CRC Handbook of Chemistry and Physics*, 68th Edition, CRC Press, Boca Raton, Florida, (1987-88), p. F-186 to p. F-187.
28. R. S. Van Dyck, Jr., P. Schwinberg, H. Dehmelt, "New high precision comparison of electron and positron g factors", Phys. Rev. Lett., Vol. 59, (1987), p. 26-29.
29. P. J. Mohr, B. N. Taylor, "CODATA recommended values of the fundamental physical constants: 1998", Reviews of Modern Physics, Vol. 72, No. 2, April, (2000), pp. 351-495.
30. G. P. Lepage, "Theoretical advances in quantum electrodynamics, International Conference on Atomic Physics, Atomic Physics; Proceedings, Singapore, World Scientific, Vol. 7, (1981), pp. 297-311.
31. E. R. Williams and P. T. Olsen, Phys. Rev. Lett. Vol. 42, (1979), p. 1575.
32. K. V. Klitzing et al., Phys. Rev. Lett. Vol. 45, (1980), p. 494.
33. R. M. Carey et al., Muon (g-2) Collaboration, "New measurement of the anomalous magnetic moment of the positive muon", Phys. Rev. Lett., Vol. 82, (1999), pp. 1632-1635.
34. J. D. Jackson, *Classical Electrodynamics*, Second Edition, John Wiley & Sons, New York, (1975), pp. 556-560.
35. H. N. Brown et al., Muon (g-2) Collaboration, "Precise measurement of the positive muon anomalous magnetic moment", Phys. Rev. D62, 091101 (2000).
36. F. Bueche, *Introduction to Physics for Scientists and Engineers*, McGraw-Hill, (1975), pp. 352-353.
37. J. D. Jackson, *Classical Electrodynamics*, Second Edition, John Wiley & Sons, New York, (1975), pp. 236-240, 601-608, 786-790.
38. E. M. Purcell, *Electricity and Magnetism*, McGraw-Hill, New York, (1985), Second Edition, pp. 451-458.
39. P. Sprangle, A. T. Drobot, "The linear and self-consistent nonlinear theory of the electron cyclotron maser instability", IEEE Transactions on Microwave Theory and Techniques, Vol. MTT-25, No. 6, June, (1977), pp. 528-544.
40. J. D. Jackson, *Classical Electrodynamics*, Second Edition, John Wiley & Sons, New York, (1975), pp. 503-561.
41. C. E. Moore, "Ionization Potentials and Ionization Limits Derived from the Analyses of Optical Spectra, Nat. Stand. Ref. Data Ser.-Nat. Bur. Stand. (U.S.), No. 34, 1970.
42. D. R. Lide, *CRC Handbook of Chemistry and Physics*, 79th Edition, CRC Press, Boca Raton, Florida, (1998-9), p. 10-175 to p. 10-177.